Practical Strategies of Wind Energy Utilization for Uninhabited Aerial Vehicles in Loiter Flights

A DISSERTATION

SUBMITTED TO THE FACULTY OF THE GRADUATE SCHOOL

OF THE UNIVERSITY OF MINNESOTA

BY

Hong Yang Singhania

IN PARTIAL FULFILLMENT OF THE REQUIREMENTS

FOR THE DEGREE OF

DOCTOR OF PHILOSOPHY

Yiyuan Joseph Zhao, Advisor

December 2008

Acknowledgements

A simple "thank you" cannot express how grateful I am to my advisor, Professor Yiyuan Zhao. I would not have come this far in my education without his guidance, support, and patience in every step of my professional and personal growth. His confidence in me has empowered me with great courage and aspiration to take on challenges and strive for success in life.

I would like to thank all the faculty who had given me a fascinating learning experience in the graduate school. Special thanks to my committee members, Professor Demoz Gebre-Egziabher, Professor William Garrard, and Professor Rajesh Rajamani, for their advice and support in my research. I am also very thankful to the Department of Aerospace Engineering and Mechanics at the University of Minnesota for providing the administrative and financial assistance during my graduate studies.

I would like to express my gratitude to my managers at Eaton Corporation, Steve Zielinski and Ron Tonn, who encouraged and supported me to complete this dissertation and to pursue professional development.

I thank my friends in graduate school, especially my former officemates in AkerH 3: Ying Qi, Vibhor Bageshwar, and Yunfeng Shao. Their friendship had made this part of my life very colorful and enjoyable.

I am forever indebted to my mother, Guiqing Ma, for her unconditional

and selfless love. I would like to thank my father, Xiaoli Yang, for being the first teacher in my life. I am very grateful to my in-laws, Laxmi Prakash and Sandhya, for their love, enthusiasm, and support during this journey. Finally, I thank my husband, Vivek, for making me smile even during the most difficult times. His love, patience, encouragement, and understanding has given me the greatest strength. Without my beloved family, this work would not have been possible.

To My Parents

And To Vivek

Abstract

Uninhabited Aerial Vehicle (UAV) is becoming increasingly attractive in missions where human presence is undesirable or impossible. Agile maneuvers and long endurance are among the most desired advantages of UAVs over aircraft that have human pilots onboard. Past studies suggest that the performance of UAVs may be considerably improved by utilizing natural resources, especially wind energy, during flights. The key challenge of exploiting wind energy in practical UAV operations lies in the availability of reliable and timely wind field information in the operational region.

This thesis presents a practical onboard strategy that attempts to overcome this challenge, to enable UAVs in utilizing wind energy effectively during flights, and therefore to enhance performance. We propose and explore a strategy that combines wind measurement and optimal trajectory planning onboard UAVs. During a cycle of a loiter flight, a UAV can take measurements of wind velocity components over the flight region, use these measurements to estimate the local wind field through a model-based approach, and then compute a flight trajectory for the next flight cycle with the objective of optimizing fuel. As the UAV follows the planned trajectory, it continues to measure the wind components and repeats the process of updating the wind model with new estimations and planning optimal trajectories for the next flight cycle. Besides

presenting an onboard trajectory planning strategy of wind energy exploration, estimation, and utilization, this research also develops a semi-analytical linearized solution to the formulated nonlinear optimal control problem.

Simulations and numerical results indicate that the fuel savings of trajectories generated using the proposed scheme depend on wind speed, wind estimation errors, rates of change in wind speed, and the wind model structures. For a given wind field, the magnitude of potential fuel savings is also contingent upon UAVs' performance capabilities.

Contents

List of Tables

List of Figures

Nomenclature and Acronyms

C_{D_0}	Parasite drag coefficient
C_D	Drag coefficient
C_L	Lift coefficient
$\mathbf{f}$	UAV dynamic equations
g	Gravitational acceleration
h	Inertial altitude
H_0	Transition altitude for wind gradient
I	Cost functional in an optimal control problem
m	Aircraft mass; Dimension of the control vector
n	Dimension of the state vector
N	Number of nodes in the discretization of time interval
q	Dimension of the terminal constraint vector
$\mathbf{r}$	Position vector
S	Aircraft reference area
T	Engine thrust
t	Time
$\mathbf{u}$	Control vector
V	True airspeed
$\mathbf{W}$	Wind velocity vector

(W_x, W_y, W_h)	Real wind components in (East, North, Up)
$(\hat{W}_x, \hat{W}_y, \hat{W}_h)$	Measured wind components in (East, North, Up)
$(\dot{W}_V, \dot{W}_\Psi, \dot{W}_\gamma)$	Real wind acceleration components
$\mathbf{x}$	State vector
(x, y)	(East, North) position
β	Wind gradient slope
γ	Air-relative flight path angle
μ	Bank angle
ψ	Air-relative velocity heading measured from the North
ψ_w	Wind velocity heading
ρ	Air density
τ	Normalized final time variant
$\bar{(\ )}$	Normalized variable
$(\ )^o$	Nominal variable
$(\ )'$	Derivative with respect to normalized time
$(\ )_{\min}$	Minimum value
$(\ )_{\max}$	Maximum value
$(\ )_0$	Initial value
$(\ )_f$	Final value
UAV	Uninhabited Aerial Vehicle

Chapter 1

Introduction

Uninhabited Aerial Vehicles (UAVs) are aircraft with no pilot onboard. Either remotely controlled or autonomously operated, UAVs are becoming increasingly attractive in missions where human presence is undesirable, because of their abilities to perform dull, dirty, and dangerous tasks. Long endurance, long range capability, and responsiveness are important UAV qualities. While proper designs of engines and aerodynamic frames are essential for achieving good UAV performances, it is highly beneficial to take advantage of all natural energy sources to enhance UAV mission capabilities. In particular, wind is a ubiquitous energy source in nature. Wind energies may be used to significantly increase UAV flight performances.

Indeed, the atmospheric wind can have a strong effect on the flight performances of air vehicles. Jet streams are being routinely used in planning efficient flight routes for transport aircraft. Sailplane pilots have been using wind gradients and/or vertical thermals for sustained powerless flights[1]. By taking advantage of thermals, for example, an average sailplane can achieve altitudes that are not possible for an average single engine aircraft.

UAVs differ from both transport aircraft and sailplanes in important ways, and these differences may enable them to better exploit the wind energy. UAVs are in general lighter in weight than transport aircraft. As a result, wind energies are potentially more beneficial for UAV flights. Because there are no humans onboard UAVs, they can perform more drastic maneuvers and fly more flexible trajectories than habited aircraft in taking advantage of wind energies. Compared with gliders, engine powers onboard UAVs can enable them to pass through regions of less favorable winds in search for a more favorable wind field.

In Zhao's work[2], Minimum-fuel UAV flight trajectories through known wind gradients are studied. The utilization of wind gradient energy can significantly decrease the fuel consumptions of periodic UAV flights thus improve the endurance capabilities. Furthermore, patterns and benefits of optimal UAV flights through thermals are studied[3].

There is a unique challenge to wind energy utilization in UAV operations. In order to utilize wind energies, wind velocities over the region of operation must be determined. However, the flexible nature of some UAV missions makes it difficult to rely exclusively on ground-based infrastructures for wind measurements. The absence of human pilots onboard UAVs also deprives them of human experiences in recognizing favorable weather patterns. In addition, complex variations of wind magnitude and direction especially in the lower atmosphere make it difficult to effectively incorporate wind information in pre-

flight mission planning. As a result, a major issue in the effective utilization of wind energy for practical UAV operations is the need to accurately and timely determine wind fields over operational areas.

This research presents the strategy of onboard real-time wind field determination and utilization that employs the UAV as *insitu* wind sensors. In this strategy, wind components are first measured along the current UAV flight trajectory. A model of the wind field is then extracted from these measurements. Optimal flight trajectories from now to some future time are next planned based on the established wind field model. After the UAV follows the optimal trajectories for a certain period of time, this process is repeated.

In loiter missions, a UAV can measure the wind field during its flight. If the temporal variations of wind components are small relative to the cycle time of periodic UAV motions, the wind field information determined during one cycle of the UAV flight can be used to improve its flight efficiency in the next cycle. As a result, the UAV can continually modify its flight trajectories in real time to improve its mission performances.

In the rest of this thesis, the problem of wind energy utilization and proposed solution strategies are presented in Chapter 2. Chapter 3 discusses the wind field modeling and parameter estimation. In Chapter 4, a set of point-mass equations of motion for a generic UAV is presented. The problem of adaptive trajectory optimization with wind energy exploration and estimation is formulated as nonlinear optimal control problem in Chapter 5. The problem

is then linearized to obtain incremental trajectory updates. Flight constraints on states and controls are enforced indirectly through the choices of proper trajectory update stepsizes. Chapter 6 obtains semi-analytical solutions to the linearized optimization problem based on the state transition method. Chapter 7 discusses the simulation scenarios of the UAV flights and proposes an evaluation criteria that is used to quantify the efficiency and benefits of the proposed cyclic trajectory improvement strategy. Chapter 8 presents the numerical examples with different wind conditions and simulation results. Finally, Chapter 9 draws the conclusions of this research and suggests potential future work on this topic.

This research proposes a practical strategy for onboard trajectory planning and optimization utilizing wind energy and also demonstrates a linearized solution framework for the formulated nonlinear optimal control problem.

Chapter 2

Problem Statement and Solution Strategy

2.1 UAV Loiter Flight

Loiter flights may be used for surveillance or data gathering. As illustrated by Figure 2.1 below, in a typical loiter flight, a UAV circles around some specified geographical point and performs periodic motion. It may change altitude during each cycle.

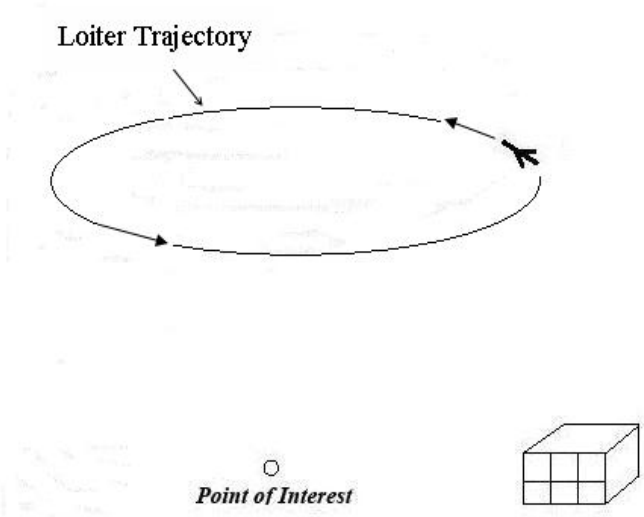

Figure 2.1 An Illustration of UAV Loiter Flight

In general, the wind field of the local area over which the UAV performs a

loiter mission may change over time. If this temporal change of the wind field is sufficiently slow, the wind field may be assumed constant for each cycle of the loiter flight.

2.2 Problem Statement

This research studies the problem of utilizing wind energies to generate fuel-efficient trajectories and thus enhance the flight performance for a UAV in loiter missions.

In order for UAVs to take advantage of wind energies, wind velocity profiles in the region of UAV operations, hereby called wind field information, need to be accurately and timely determined. For flexible UAV operations, airborne strategies of wind measurements are in general required. This is because UAVs can operate in remote areas where ground-based wind measurements may not be available or may be too coarse for operational needs. In particular, local wind fields especially close to the ground can vary randomly over short distances or times, and are thus very difficult to determine in advance. Accurate measurement of local wind fields using ground-based equipment would not work well for UAVs that need to operate in changing areas.

2.3 Trajectory Improvement Strategy

A key idea proposed in this research is that UAVs can serve as wind sensors for airborne wind measurement. The premise of the proposed strategy is

that a UAV can derive wind velocities at points on its flight path. For example, direct wind measurements onboard air vehicles may be accomplished through *insitu* sensors and/or forward-looking sensors if available. Alternatively, local wind velocities can also be estimated reliably onboard UAVs based on vector differences between inertial flight velocities and air velocities, where inertial positions and velocities can be measured using Global Positioning System (GPS) receivers and/or Inertial Measuring Units (IMUs), and air-relative quantities can be obtained from air data sensors.

In a loiter mission, a UAV will need to circle around a given area repeatedly (Figure 2.1). In this case, a UAV can measure the wind profile on its flight path during one cycle of the loiter flight, and then use this information to improve its flight efficiency for the next cycle. It can be assumed that measurements of the local field along a periodic UAV trajectory are representative of the local wind field.

Because wind measurements and/or estimations are confined to points along the original trajectory, the obtained wind information is only valid in a small neighborhood around the first trajectory. As a result, only small trajectory improvement changes should be made. On the other hand, the UAV can apply the idea of trajectory improvement repeatedly. This gradual trajectory improvement strategy, as illustrated in Figure 2.2, is also desirable for UAV flights in a changing wind field.

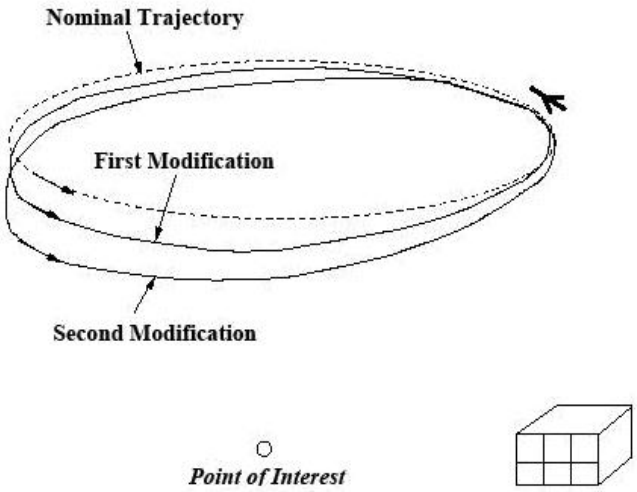

Figure 2.2 Gradual Trajectory Improvement

Let us assume that a UAV is following a certain nominal trajectory circling around a specified area in a loiter mission. The proposed strategy consists of the following steps.

1. Measure the wind components at a series of points along the trajectory;
2. Fit these wind component measurements into a certain model of the local wind field by estimating the model parameters;
3. Plan optimal fuel-efficient trajectories for the UAV from the current time to some future time based on the local wind field model established above;
4. Follow the optimal planned trajectories for a certain period of time;
5. Repeat the process by going to Step 1.

Figure 2.3 below further describes the proposed solution framework for

gradual trajectory improvement.

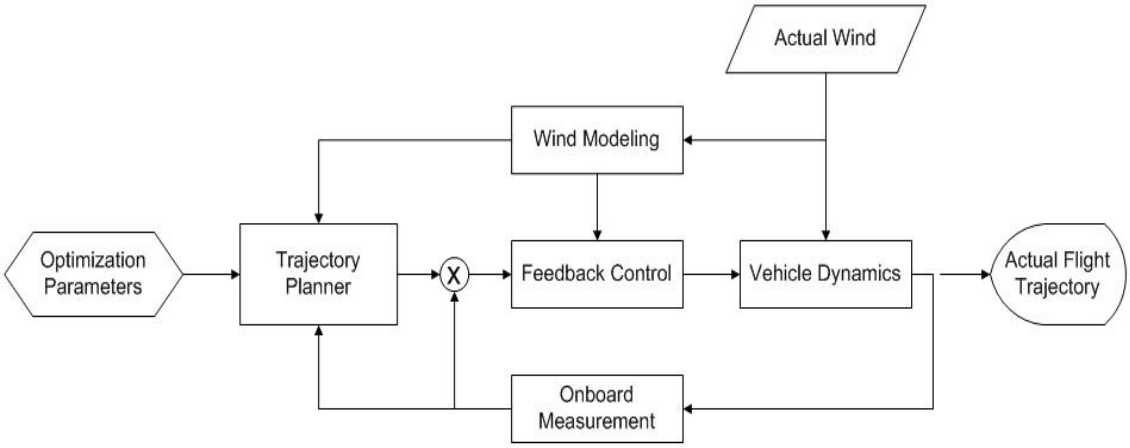

Figure 2.3 Solution Strategy Framework

In order for the proposed strategy to work well, the wind model structure should be representative of the actual local wind field. Preferably, the wind model structure should be simple enough for the convenience and efficiency of onboard trajectory planning. In addition, solution methods for the onboard trajectory planning must be reliable and fast for real-time applications. They should be modest in their memory requirements and should produce feasible, albeit sub-optimal solutions at each solution cycle.

In this research, a wind gradient model is used in which the wind magnitude changes over altitude. This is reasonable for low altitude loiter missions. To obtain reliable and fast solutions, a successive linearization of the nonlinear optimal control problem for trajectory planning is employed. At each step of the solution, this requires the solution of a linear quadratic optimal control problem for which semi-analytical, non-iterative solutions are available using

a state transition approach. The non-iterative nature can greatly help the reliability of the solution method.

2.4 A Comment on the Proposed Solution Strategy

The proposed solution strategy and the corresponding algorithms can only determine locally optimal solutions. In fact, because they use an assumed model structure for the local wind field, the resulting trajectories may not even be optimal for the actual wind if it is significantly different from the assumed wind model.

On the other hand, the proposed solution strategy does not rely on an explicit model of the wind field to work. Because of its repetitive improvement nature, it can adapt to slow changes in the wind field. If the assumed wind model is close in structure to the actual wind field, the proposed strategy represents an effective, intelligent method to plan optimal flight trajectories in real-time applications.

Chapter 3

Wind Field Modeling and Estimation

In this chapter, generic nonlinear and linear wind gradient models are used to approximate a real wind field. The algorithm of using wind velocity measurements to estimate wind model parameters is also presented.

3.1 Review of Atmosphere and Wind Properties

Wind is essentially moving air, horizontally and/or vertically. Before discussing wind modeling, it is useful to briefly review the atmosphere properties for the possibilities and variabilities of using wind as a source of energy.

Solar radiation energizes the wind on earth. The power of solar radiation reaching the earth's surface decreases from the equator to the poles; causing latitudinal temperature gradient. Correspondingly, the atmosphere develops a pressure gradient somewhat matching the temperature gradient, with high pressures around the tropics and low pressures in the polar regions. Pressure gradients produce winds.

Because of the earth's rotation, however, any wind is deflected from its course unless it happens to be blowing parallel with the equator and directly

above it. In the Northern Hemisphere, the wind is always deflected to the right (as one stands with one's back to it), and in the Southern Hemisphere, always to the left. This deflection is known as the *Coriolis effect*. As a result, what were south winds in the Northern Hemisphere have become west winds or "westerlies" and what were north winds have become east winds or "easterlies", and vice versa in the Southern Hemisphere. These winds, known as geostrophic winds, are the dominant winds of the general atmospheric circulation. In general at high altitudes far above the influence of friction with the ground surface, the tendency of the wind to blow down the pressure gradient and its tendency to turn right because of the Coriolis effect come into balance, resulting in the wind blowing directly across the pressure gradient. The fastest winds in the Northern Hemisphere tend to be at the level of the tropopause in two widely separated latitude belts; forming the so-called *jet streams*. Both of these jet streams are westerlies. The wind speed at the center of a jet stream is typically about 200 km/h, occasionally rising to over 450 km/h. Jet streams are usually strongest in winter, because the temperature contrast between the tropics and the polar regions is greatest.

At lower elevations, where frictional drag is appreciable, the average wind pattern is governed by three factors: the pressure gradient, the Coriolis effect, and drag. Drag reduces the Coriolis effect; causing the wind to be deflected through an angle of less than 90^o from the direction of the pressure gradient. In addition to the frictional drag, other factors also influence both the magni-

tude and direction of winds at low elevations than at high ones. As a result, atmospheric conditions near the surface are much more variable both spatially and temporally, and thus more complicated, than those higher up.

Vertical motion of the air within the atmosphere occurs on a number of scales. Large scale ascent and descent of the atmosphere are often associated with major weather systems. Significant changes to daily weather are generally caused by large or synoptic scale weather systems such as the areas of high and low pressure. Embedded within these large scale weather systems, are mesoscale, or smaller scale weather events. Mesoscale systems include thermal updrafts resulting from heating of the earth's surface, the wind regime over hills and small mountain ranges, valley and mountain winds, and thunderstorms to name just a few. Thermals are usually scattered. The rising thermals flow up as separate small air streams through a mass of slowly descending air.

3.2 A Nonlinear Wind Gradient Model Near Ground

As discussed above, the actual wind field and atmosphere is very complicated. However, when considering wind in a UAV's flight, it is meaningful to examine the essence of wind properties while ignoring some insignificant variations of wind. UAV loiter missions often occur close to the ground, where the vertical wind component is small or negligible.

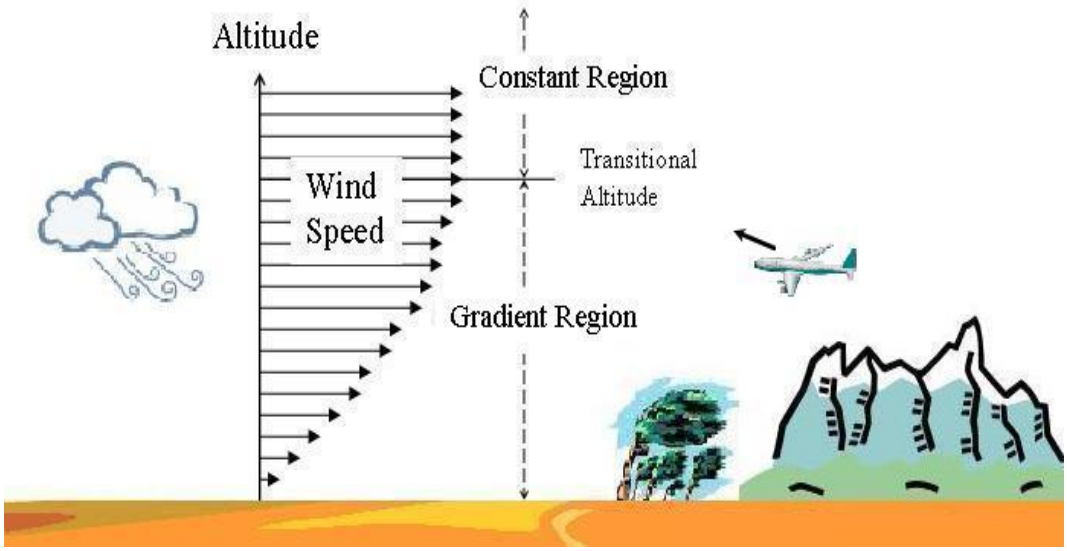

Figure 3.1 An Illustration of Wind Speed Profile Near Ground

In this research, it is assumed that there is no vertical wind in the wind gradient model, and the horizontal wind speed is a function of altitude and does not change over time, i.e. the steady wind moves only horizontally along the Earth's surface, and the wind speed increases along with the altitude.

$$W_x = W(h)\sin\psi_w \tag{3.1}$$

$$W_y = W(h)\cos\psi_w \tag{3.2}$$

$$W_h = 0 \tag{3.3}$$

where $W(h)$ is the horizontal wind speed expressed as a function of altitude, and ψ_w is a constant that gives the direction of the wind, which is measured clockwise from the North.

Consider a nonlinear wind gradient model for W:

$$W(h) = W_0 \left[A_w \frac{h}{H_0} + (1 - A_w) \left(\frac{h}{H_0} \right)^2 \right], \quad 0 < A_w < 2 \tag{3.4}$$

where H_0 is the transition altitude above which the horizontal wind speed remains constant with respect to altitude and W_0 is the maximum horizontal wind speed. The parameter A_w represents the nonlinear effect of the wind gradient profile. Specifically, $A_w = 1$ corresponds to a linear wind profile, $0 < A_w < 1$ reflects a more exponential wind magnitude profile, and $1 < A_w < 2$ reflects a more logarithmic wind magnitude profile.

The following figure shows the modeled wind speed profile with respect to altitude for different values of A_w. In particular, H_0 is set to 2500 ft and W_0 is set to 100 ft/s.

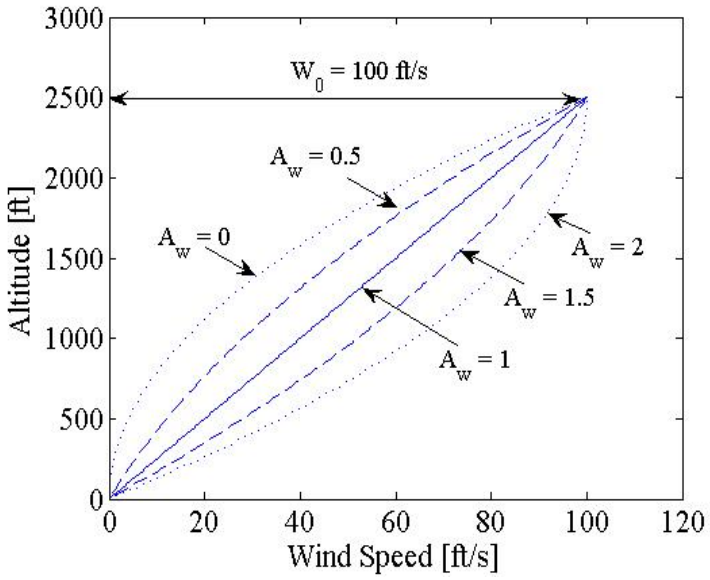

Figure 3.2 Modeled Wind Speed Profile vs. Altitude

3.3 Parameter Estimation For Nonlinear Wind Gradient Model

In practical flights, coefficients of the above nonlinear wind gradient model can be estimated from measurements of wind components along a trajectory. Specifically, the problem can be stated as

$$\min_{W_0,\,\psi_w,\,A_w} I = \sum_{k=1}^{N} \left\{ \left[W_x(h_k) - \hat{W}_{x_k} \right]^2 + \left[W_y(h_k) - \hat{W}_{y_k} \right]^2 \right\} \tag{3.5}$$

where $\hat{W}_{x_k}$ and $\hat{W}_{y_k}$ are the wind velocity components measured at position (x_k, y_k, h_k), $k = 1, 2, ..., N$, i.e.

$$\hat{W}_{x_k} \triangleq \hat{W}_x(x_k, y_k, h_k) \tag{3.6}$$

$$\hat{W}_{y_k} \triangleq \hat{W}_y(x_k, y_k, h_k) \tag{3.7}$$

and

$$W_x(h_k) = \left(\frac{W_0}{H_0} \sin\psi_w \right) \frac{h_k^2}{H_0} + A_w \left(\frac{W_0}{H_0} \sin\psi_w \right) \left(h_k - \frac{h_k^2}{H_0} \right) \tag{3.8}$$

$$W_y(h_k) = \left(\frac{W_0}{H_0} \cos\psi_w \right) \frac{h_k^2}{H_0} + A_w \left(\frac{W_0}{H_0} \cos\psi_w \right) \left(h_k - \frac{h_k^2}{H_0} \right) \tag{3.9}$$

Define

$$p_1 \triangleq \frac{W_0}{H_0} \sin\psi_w, \quad p_2 \triangleq \frac{W_0}{H_0} \cos\psi_w \tag{3.10}$$

$$z_0(h) \triangleq \frac{h^2}{H_0}, \quad z_1(h) \triangleq h - \frac{h^2}{H_0} \tag{3.11}$$

then

$$W_x(h_k) = p_1 z_0(h_k) + A_w p_1 z_1(h_k) \tag{3.12}$$

$$W_y(h_k) = p_2 z_0(h_k) + A_w p_2 z_1(h_k) \tag{3.13}$$

and

$$W_0 = H_0\sqrt{p_1^2 + p_2^2} \tag{3.14}$$

$$\tan\psi_w = \frac{p_1}{p_2}, \quad 0 \le \psi_w < 2\pi \tag{3.15}$$

Replacing $W_x(h_k)$ and $W_y(h_k)$ in (3.5) by (3.12) and (3.13), we convert the problem into the following format:

$$\begin{aligned}\min_{p_1,\, p_2,\, A_w} \; I = &\sum_{k=1}^{N} \left[p_1 z_0(h_k) + A_w p_1 z_1(h_k) - \hat{W}_{x_k}\right]^2 + \\ &+ \sum_{k=1}^{N} \left[p_2 z_0(h_k) + A_w p_2 z_1(h_k) - \hat{W}_{y_k}\right]^2\end{aligned} \tag{3.16}$$

This is a nonlinear least square fit problem. Solution details are presented in Appendix A. Based on the solutions, the procedure of estimating the parameters of the nonlinear wind model is summarized below.

1. Obtain wind velocity measurements at N locations (x_k, y_k, h_k) for $k = 1, 2, ..., N$ along the trajectory. Denote the measurements as $(\hat{W}_{x_k}, \hat{W}_{y_k})$, for $k = 1, 2, ..., N$. Define measurement vectors $\hat{\mathbf{W}}_\mathbf{x}$ and $\hat{\mathbf{W}}_\mathbf{y}$ as

$$\hat{\mathbf{W}}_\mathbf{x} \triangleq [\hat{W}_{x_1}, \hat{W}_{x_2}, ..., \hat{W}_{x_N}]^T \tag{3.17}$$

$$\hat{\mathbf{W}}_\mathbf{y} \triangleq [\hat{W}_{y_1}, \hat{W}_{y_2}, ..., \hat{W}_{y_N}]^T \tag{3.18}$$

2. Compute the following intermediate variables

$$z_{0_k} = \frac{h_k^2}{H_0}, \quad z_{1_k} = h_k - z_{0_k}, \quad \text{for } k = 1, 2, ..., N \tag{3.19}$$

Define coefficient vectors as

$$\mathbf{z_0} \triangleq [z_{0_1}, z_{0_2}, ..., z_{0_N}]^T \tag{3.20}$$

$$\mathbf{z_1} \triangleq [z_{1_1}, z_{1_2}, ..., z_{1_N}]^T \tag{3.21}$$

3. Compute the following coefficients:

$$a_0 = \mathbf{z_0}^T \mathbf{z_0}, \quad a_1 = 2\mathbf{z_0}^T \mathbf{z_1}, \quad a_2 = \mathbf{z_1}^T \mathbf{z_1} \tag{3.22}$$

$$b_{0_x} = \hat{\mathbf{W}}_\mathbf{x}^T \mathbf{z_0}, \quad b_{0_y} = \hat{\mathbf{W}}_\mathbf{y}^T \mathbf{z_0}, \quad b_{1_x} = \hat{\mathbf{W}}_\mathbf{x}^T \mathbf{z_1}, \quad b_{1_y} = \hat{\mathbf{W}}_\mathbf{y}^T \mathbf{z_1} \tag{3.23}$$

$$c_0 = \mathbf{z_0}^T \hat{W} \mathbf{z_0}, \quad c_1 = 2\mathbf{z_0}^T \hat{W} \mathbf{z_1}, \quad c_2 = \mathbf{z_1}^T \hat{W} \mathbf{z_1} \tag{3.24}$$

where

$$\hat{W} \triangleq \hat{\mathbf{W}}_x \hat{\mathbf{W}}_\mathbf{x}^T + \hat{\mathbf{W}}_\mathbf{y} \hat{\mathbf{W}}_\mathbf{y}^T \tag{3.25}$$

4. Calculate A_w as follows:

$$A_w = \begin{cases} \dfrac{-B_1 + \sqrt{B_1^2 - B_0 B_2}}{B_2} & \text{if } B2 > 0,\ -4(B_1 + B_2) \le B_0 \le 0 \\ \dfrac{-B_1 - \sqrt{B_1^2 - B_0 B_2}}{B_2} & \text{if } B2 < 0,\ 0 \le B_0 \le -4(B_1 + B_2) \\ \dfrac{-B_0}{2B_1} & \text{if } B2 = 0,\ -4 \le \frac{B_0}{B_1} \le 0 \end{cases} \tag{3.26}$$

where

$$B_0 = c_1 a_0 - c_0 a_1 \tag{3.27}$$

$$B_1 = c_2 a_0 - c_0 a_2 \tag{3.28}$$

$$B_2 = c_2 a_1 - c_1 a_2 \tag{3.29}$$

5. Calculate W_0 as follows:

$$W_0 = H_0 \frac{\sqrt{c_0 + c_1 A_w + c_2 A_w^2}}{a_0 + a_1 A_w + a_2 A_w^2} \tag{3.30}$$

6. Calculate p_1 and p_2 as follows:

$$p_1 = \frac{b_{0_x} + b_{1_x} A_w}{a_0 + a_1 A_w + a_2 A_w^2} \tag{3.31}$$

$$p_2 = \frac{b_{0_y} + b_{1_y} A_w}{a_0 + a_1 A_w + a_2 A_w^2} \tag{3.32}$$

Define

$$\psi_0 = \tan^{-1} \frac{p_1}{p_2}, \quad -\frac{\pi}{2} < \psi_0 < \frac{\pi}{2} \tag{3.33}$$

then

$$\psi_w = \begin{cases} \psi_0 & \text{if } p_1 > 0,\ p_2 > 0 \\ \psi_0 + \pi & \text{if } p_1 > 0,\ p_2 < 0 \\ \psi_0 + 2\pi & \text{if } p_1 < 0,\ p_2 > 0 \\ \psi_0 + \pi & \text{if } p_1 < 0,\ p_2 < 0 \\ 0 & \text{if } p_1 = 0,\ p_2 > 0 \\ \frac{\pi}{2} & \text{if } p_1 > 0,\ p_2 = 0 \\ \pi & \text{if } p_1 = 0,\ p_2 < 0 \\ \frac{3\pi}{2} & \text{if } p_1 < 0,\ p_2 = 0 \end{cases} \tag{3.34}$$

Once the wind model parameters are obtained, the estimated wind model is given by (3.1) - (3.4).

3.4 A Linear Wind Gradient Model Near Ground

A linear gradient wind model is a simplified version of the above nonlinear wind model presented in the previous section. In (3.8) and (3.9), if we set $A_w = 1$, then the simplified wind model is

$$W_x = \frac{W_0}{H_0} h \sin \psi_w \tag{3.35}$$

$$W_y = \frac{W_0}{H_0} h \cos\psi_w \tag{3.36}$$

$$W_h = 0 \tag{3.37}$$

where W_0, H_0, and ψ_w are defined the same as in Section 3.2.

3.5 Parameter Estimation for Linear Wind Gradient Model

The procedure of estimating the parameters in the linear gradient wind model can be derived from the procedure presented in Section 3.3 by setting the following conditions:

$$A_w = 1, \quad z_0(h_k) = 0, \quad z_1(h_k) = h_k \quad \text{for } k = 1, 2, ..., N \tag{3.38}$$

The procedure is summarized as follows:

1. Obtain horizontal wind velocity measurements at N locations (x_k, y_k, h_k) for $k = 1, 2, ..., N$ along the trajectory. Denote the measurements as $(\hat{W}_{x_k}, \hat{W}_{y_k})$, for $k = 1, 2, ..., N$. Define measurement vectors $\hat{\mathbf{W}}_\mathbf{x}$ and $\hat{\mathbf{W}}_\mathbf{y}$ as

$$\hat{\mathbf{W}}_\mathbf{x} \stackrel{\triangle}{=} [\hat{W}_{x_1}, \hat{W}_{x_2}, ..., \hat{W}_{x_N}]^T \tag{3.39}$$

$$\hat{\mathbf{W}}_\mathbf{y} \stackrel{\triangle}{=} [\hat{W}_{y_1}, \hat{W}_{y_2}, ..., \hat{W}_{y_N}]^T \tag{3.40}$$

Define altitude measurement vector $\mathbf{h}$ as

$$\mathbf{h} \stackrel{\triangle}{=} [h_1, h_2, ..., h_N]^T \tag{3.41}$$

2. Compute p_1 and p_2 in

$$p_1 = \frac{\hat{\mathbf{W}}_{\mathbf{x}}^T \mathbf{h}}{\mathbf{h}^T \mathbf{h}} \tag{3.42}$$

$$p_2 = \frac{\hat{\mathbf{W}}_{\mathbf{y}}^T \mathbf{h}}{\mathbf{h}^T \mathbf{h}} \tag{3.43}$$

3. Solve for W_0 and ψ_w using the following equations:

$$W_0 = H_0 \sqrt{p_1^2 + p_2^2} \tag{3.44}$$

$$\tan \psi_w = \frac{p_1}{p_2} \tag{3.45}$$

Define

$$\psi_0 = \tan^{-1} \frac{p_1}{p_2}, \quad -\frac{\pi}{2} < \psi_0 < \frac{\pi}{2} \tag{3.46}$$

then

$$\psi_w = \begin{cases} \psi_0 & \text{if } p_1 > 0,\ p_2 > 0 \\ \psi_0 + \pi & \text{if } p_1 > 0,\ p_2 < 0 \\ \psi_0 + 2\pi & \text{if } p_1 < 0,\ p_2 > 0 \\ \psi_0 + \pi & \text{if } p_1 < 0,\ p_2 < 0 \\ 0 & \text{if } p_1 = 0,\ p_2 > 0 \\ \frac{\pi}{2} & \text{if } p_1 > 0,\ p_2 = 0 \\ \pi & \text{if } p_1 = 0,\ p_2 < 0 \\ \frac{3\pi}{2} & \text{if } p_1 < 0,\ p_2 = 0 \end{cases} \tag{3.47}$$

4. The estimated wind model is given by Eq. (3.35) to (3.37)

3.6 Preventing Degeneracy in Wind Model Parameter Estimation

There are two scenarios in which the parameters of the wind model may not be reliably estimated. The corresponding mechanisms to prevent these scenarios are discussed below.

1. Insufficient Data

In the nonlinear wind gradient model, 3 parameters need to be estimated. Theoretically, we need 3 sets of linearly independent data to be able to estimate the 3 parameters. If the measured wind components represent less than 3 sets of linearly independent data, then the parameters cannot be estimated.

2. Inconsistent Data

If the wind model does not capture the feature of the real wind field, using measured wind data in the estimation procedure might produce erroneous parameters.

Mathematically, for the nonlinear gradient wind model, (3.26) indicates that if any of the following conditions is true, A_w cannot be estimated based on the given data sets:

$$B_1^2 - B_0 B_2 < 0 \tag{3.48}$$

$$B_0 = 0 \quad \text{and} \quad B_1 B_2 > 0 \tag{3.49}$$

$$B_1 = 0 \quad \text{and} \quad B_0 B_2 > 0 \tag{3.50}$$

$$B_2 = 0 \quad \text{and} \quad B_0 B_1 > 0 \tag{3.51}$$

$$B_2 = 0 \quad \text{and} \quad B_1 = 0 \tag{3.52}$$

When using a linear gradient wind model, p_1 and p_2 may not be estimated if $\mathbf{h}^T\mathbf{h} = 0$, which means if all the wind data are measured at $h = 0$, then the data are not sufficient to estimate the linear gradient wind model parameters.

The sufficient condition of the data can be stated as

$$h_k \neq 0 \quad \text{for } k = 1, 2, ..., N \tag{3.53}$$

Overall, an adequate number of independent wind measurement data must be made and they must satisfy the above equation.

3.7 Other Possible Wind Models

In general, a more general form of the wind model may be stated as

$$W_x = W_H(t, x, y, h) \sin \psi_w(t, x, y, h) \tag{3.54}$$

$$W_y = W_H(t, x, y, h) \cos \psi_w(t, x, y, h) \tag{3.55}$$

$$W_h = W_h(t, x, y, h) \tag{3.56}$$

where $W_H(t, x, y, h)$ is the horizontal wind speed, $\psi_w(t, x, y, h)$ is the wind direction, and $W_h(t, x, y, h)$ is the vertical wind speed. All three variables are functions of time t and position (x, y, h). Equation (3.54), (3.55), and (3.56) together represent a non-stationary wind field where wind velocity components and direction vary with respect to time and geographic locations.

If we assume the changes in wind velocity components are sufficiently slow, then we can use a stationary wind model instead:

$$W_x = W_H(x, y, h) \sin \psi_w(x, y, h) \tag{3.57}$$

$$W_y = W_H(x, y, h) \cos \psi_w(x, y, h) \tag{3.58}$$

$$W_h = W_h(x, y, h) \tag{3.59}$$

If we further assume the vertical wind speed only depends on altitude, then

$$W_x = W_H(x, y, h) \sin \psi_w(x, y, h) \tag{3.60}$$

$$W_y = W_H(x, y, h) \cos \psi_w(x, y, h) \tag{3.61}$$

$$W_h = W_h(h) \tag{3.62}$$

A special case is when the vertical wind speed changes with the altitude exponentially,

$$W_h = W_{h0} \left(\frac{h}{h_0} \right)^{\alpha} \tag{3.63}$$

where W_{h0} is the vertical wind speed at altitude h_0.

In this research, only the nonlinear wind gradient model is used to illustrate the proposed onboard wind energy utilization strategy. Other wind models can be used if they can better represent the actual wind field encountered in practical operations. Use of more complicated models may potentially improve the fuel-saving performances of the proposed strategy at the expense of increased computational efforts, but it does not fundamentally change the structure and flow of the proposed concept.

Chapter 4

UAV Modeling and Equations of Motion

In this chapter, equations of motion of a point-mass model for a generic conventional UAV are presented. The equations are further normalized using characteristic UAV airspeed for computational efficiency.

4.1 3-D Point-Mass Equations of Motion

A point-mass model is generally adequate for aircraft trajectory planning and analysis. In addition, the following assumptions are made in the current research:

1. Flat earth
2. UAV performs coordinated turns. For the time interval of interest, the bank angle and lift coefficient can be changed instantaneously.
3. During a cycle of trajectory planning, the UAV mass is assumed constant

The resulting three dimensional point-mass equations of motion for a generic unmanned aerial vehicle are listed below.

$$m\ \dot{V} = T - D - mg\sin\gamma - m\dot{W}_V \tag{4.1}$$

$$mV\cos\gamma\ \dot{\psi} = L\sin\mu - m\dot{W}_\psi \tag{4.2}$$

$$mV\ \dot{\gamma} = L\cos\mu - mg\cos\gamma + m\dot{W}_\gamma \tag{4.3}$$

$$\dot{x} = V\cos\gamma\sin\psi + W_x \tag{4.4}$$

$$\dot{y} = V\cos\gamma\cos\psi + W_y \tag{4.5}$$

$$\dot{h} = V\sin\gamma + W_h \tag{4.6}$$

where the lift and drag are given by

$$L = \frac{1}{2}\rho V^2 S C_L, \quad D = \frac{1}{2}\rho V^2 S C_D \tag{4.7}$$

The drag coefficient is modeled by

$$C_D = C_{D_0} + K C_L^2 \tag{4.8}$$

where the induced drag factor K can be conveniently expressed as a function of the parasitic drag coefficient and the best lift-to-drag ratio $E_{\max}$ as

$$K = \frac{1}{4E_{\max}^2 C_{D_0}} \tag{4.9}$$

where

$$E_{\max} = \left(\frac{C_L}{C_D}\right)_{\max} = \left(\frac{C_L}{C_{D_0} + K C_L^2}\right)_{\max} \tag{4.10}$$

The time rate of the wind components along velocity, heading angle, and flight path angle rate directions are given by

$$\dot{W}_V = \cos\gamma\sin\psi\dot{W}_x + \cos\gamma\cos\psi\dot{W}_y + \sin\gamma\dot{W}_h \tag{4.11}$$

$$\dot{W}_\psi = \cos\psi\dot{W}_x - \sin\psi\dot{W}_y \tag{4.12}$$

$$\dot{W}_\gamma = \sin\gamma\sin\psi\dot{W}_x + \sin\gamma\cos\psi\dot{W}_y - \cos\gamma\dot{W}_h \tag{4.13}$$

Define a transformation matrix

$$R = \begin{bmatrix} \cos\gamma\sin\psi & \cos\gamma\cos\psi & \sin\gamma \\ \cos\psi & -\sin\psi & 0 \\ \sin\gamma\sin\psi & \sin\gamma\cos\psi & -\cos\gamma \end{bmatrix} \tag{4.14}$$

Then

$$\begin{bmatrix} \dot{W}_V \\ \dot{W}_\psi \\ \dot{W}_\gamma \end{bmatrix} = R \begin{bmatrix} \dot{W}_x \\ \dot{W}_y \\ \dot{W}_h \end{bmatrix} \tag{4.15}$$

The time rate of the wind components along x-, y-, and h- directions can be calculated using the wind gradient and the time rate of the aircraft position.

$$\dot{W}_x = \frac{\partial W_x}{\partial t} + \frac{\partial W_x}{\partial x}\dot{x} + \frac{\partial W_x}{\partial y}\dot{y} + \frac{\partial W_x}{\partial h}\dot{h} \tag{4.16}$$

$$\dot{W}_y = \frac{\partial W_y}{\partial t} + \frac{\partial W_y}{\partial x}\dot{x} + \frac{\partial W_y}{\partial y}\dot{y} + \frac{\partial W_y}{\partial h}\dot{h} \tag{4.17}$$

$$\dot{W}_h = \frac{\partial W_h}{\partial t} + \frac{\partial W_h}{\partial x}\dot{x} + \frac{\partial W_h}{\partial y}\dot{y} + \frac{\partial W_h}{\partial h}\dot{h} \tag{4.18}$$

Define

$$M = \begin{bmatrix} \frac{\partial W_x}{\partial t} & \frac{\partial W_x}{\partial x} & \frac{\partial W_x}{\partial y} & \frac{\partial W_x}{\partial h} \\ \frac{\partial W_y}{\partial t} & \frac{\partial W_y}{\partial x} & \frac{\partial W_y}{\partial y} & \frac{\partial W_y}{\partial h} \\ \frac{\partial W_h}{\partial t} & \frac{\partial W_h}{\partial x} & \frac{\partial W_h}{\partial y} & \frac{\partial W_h}{\partial h} \end{bmatrix} \tag{4.19}$$

then

$$\begin{bmatrix} \dot{W}_x \\ \dot{W}_y \\ \dot{W}_h \end{bmatrix} = M \begin{bmatrix} 1 \\ \dot{x} \\ \dot{y} \\ \dot{h} \end{bmatrix} \tag{4.20}$$

In (4.1) - (4.6), the state, control, position, and wind velocity vectors are defined as

$$\mathbf{x} = \begin{bmatrix} V \\ \Psi \\ \gamma \\ x \\ y \\ h \end{bmatrix} \quad \mathbf{u} = \begin{bmatrix} T \\ C_L \\ \mu \end{bmatrix} \quad \mathbf{r} = \begin{bmatrix} x \\ y \\ h \end{bmatrix} \quad \mathbf{W} = \begin{bmatrix} W_x \\ W_y \\ W_h \end{bmatrix} \tag{4.21}$$

Symbolically, the general equations of motion for a point-mass UAV model can be stated as

$$\dot{\mathbf{x}} = \mathbf{f}(\mathbf{x}, \mathbf{u}, \mathbf{W}(\mathbf{x}, t), t) \tag{4.22}$$

where the necessary flight constraints are expressed as

$$\mathbf{u} \in \mathbf{U}, \quad \mathbf{x} \in \mathbf{X} \tag{4.23}$$

4.2 Normalized Equations of Motion

To enhance the efficiency of numerical solutions, the equations of motion given in (4.1) through (4.6) are normalized as follows. Choose a characteristic speed V_C and a characteristic air density ρ_C and define

$$d_C \triangleq \frac{V_C^2}{g}, \quad t_C \triangleq \frac{V_C}{g} \tag{4.24}$$

Also define

$$\bar{V} \triangleq \frac{V}{V_C}, \quad \bar{t} \triangleq \frac{t}{t_C} \tag{4.25}$$

$$(\bar{x}, \bar{y}, \bar{h}) \triangleq (\frac{x}{d_C}, \frac{y}{d_C}, \frac{h}{d_C}), \quad (\bar{W}_x, \bar{W}_y, \bar{W}_h) \triangleq (\frac{W_x}{V_C}, \frac{W_y}{V_C}, \frac{W_h}{V_C}) \tag{4.26}$$

and

$$\bar{\rho} \triangleq \frac{\rho}{\rho_C} \tag{4.27}$$

$$\bar{T} \triangleq \frac{T}{mg} \tag{4.28}$$

then we can obtain

$$(\,)' \triangleq \frac{d(\,)}{d\bar{t}} = t_C \frac{d(\,)}{dt} = t_C \dot{(\,)} \tag{4.29}$$

After some derivations, the normalized equations of motion are obtained as

$$\bar{V}' = \bar{T} - k_a \bar{\rho} \bar{V}^2 (C_{D_0} + K C_L^2) - \sin\gamma - \bar{W}_V' \tag{4.30}$$

$$\psi' = k_a \bar{\rho} \bar{V} C_L \frac{\sin\mu}{\cos\gamma} - \frac{1}{\bar{V}\cos\gamma} \bar{W}_\psi' \tag{4.31}$$

$$\gamma' = k_a \bar{\rho} \bar{V} C_L \cos\mu - \frac{1}{\bar{V}} \cos\gamma + \frac{1}{\bar{V}} \bar{W}_\gamma' \tag{4.32}$$

$$\bar{x}' = \bar{V} \cos\gamma \sin\psi + \bar{W}_x \tag{4.33}$$

$$\bar{y}' = \bar{V} \cos\gamma \cos\psi + \bar{W}_y \tag{4.34}$$

$$\bar{h}' = \bar{V} \sin\gamma + \bar{W}_h \tag{4.35}$$

where

$$k_a \triangleq \frac{\rho_C V_C^2}{2(mg/S)} \tag{4.36}$$

The normalized time rate of wind components along velocity, heading angle, and flight path angle rate directions are given by

$$\begin{bmatrix} \bar{W}_V' \\ \bar{W}_\psi' \\ \bar{W}_\gamma' \end{bmatrix} = R \begin{bmatrix} \bar{W}_x' \\ \bar{W}_y' \\ \bar{W}_h' \end{bmatrix} \tag{4.37}$$

where R is given by (4.14).

The normalized time rate of wind components along $\bar{x}$-, $\bar{y}$-, and $\bar{h}$-directions are given by

$$\begin{bmatrix} \bar{W}_x' \\ \bar{W}_y' \\ \bar{W}_h' \end{bmatrix} = \bar{M} \begin{bmatrix} 1 \\ \bar{x}' \\ \bar{y}' \\ \bar{h}' \end{bmatrix} \tag{4.38}$$

where $\bar{M}$ is given by

$$\bar{M} = \begin{bmatrix} \frac{\partial \bar{W}_x}{\partial \bar{t}} & \frac{\partial \bar{W}_x}{\partial \bar{x}} & \frac{\partial \bar{W}_x}{\partial \bar{y}} & \frac{\partial \bar{W}_x}{\partial \bar{h}} \\ \frac{\partial \bar{W}_y}{\partial \bar{t}} & \frac{\partial \bar{W}_y}{\partial \bar{x}} & \frac{\partial \bar{W}_y}{\partial \bar{y}} & \frac{\partial \bar{W}_y}{\partial \bar{h}} \\ \frac{\partial \bar{W}_h}{\partial \bar{t}} & \frac{\partial \bar{W}_h}{\partial \bar{x}} & \frac{\partial \bar{W}_h}{\partial \bar{y}} & \frac{\partial \bar{W}_h}{\partial \bar{h}} \end{bmatrix} \tag{4.39}$$

The normalized state, control, position, and wind velocity vectors are defined as

$$\bar{\mathbf{x}} = \begin{bmatrix} \bar{V} \\ \Psi \\ \gamma \\ \bar{x} \\ \bar{y} \\ \bar{h} \end{bmatrix} \quad \bar{\mathbf{u}} = \begin{bmatrix} \bar{T} \\ C_L \\ \mu \end{bmatrix} \quad \bar{\mathbf{r}} = \begin{bmatrix} \bar{x} \\ \bar{y} \\ \bar{h} \end{bmatrix} \quad \bar{\mathbf{W}} = \begin{bmatrix} \bar{W}_x \\ \bar{W}_y \\ \bar{W}_h \end{bmatrix} \tag{4.40}$$

The normalized equations of motion for a 3-D point mass UAV model can be expressed as

$$\bar{\mathbf{x}}' = \mathbf{f}(\bar{\mathbf{x}}, \bar{\mathbf{u}}, \bar{\mathbf{W}}(\bar{\mathbf{x}}, \bar{t}), \bar{t}) \tag{4.41}$$

4.3 Normalized Equations of Motion with Wind Gradient Model

Assume in the normalized equations of motion (4.30) through (4.35), the wind components can be modeled by the generic nonlinear model developed in Chapter 3, i.e.

$$W_x = W_0 \left[A_w \frac{h}{H_0} + (1 - A_w) \left(\frac{h}{H_0} \right)^2 \right] \sin \psi_w \tag{4.42}$$

$$W_y = W_0 \left[A_w \frac{h}{H_0} + (1 - A_w) \left(\frac{h}{H_0} \right)^2 \right] \cos \psi_w \tag{4.43}$$

$$W_h = 0 \tag{4.44}$$

Define

$$\bar{W}_0 = \frac{W_0}{V_C}, \quad \bar{H}_0 = \frac{H_0}{d_C} \tag{4.45}$$

and recall

$$\bar{h} = \frac{h}{d_C} \tag{4.46}$$

then

$$\bar{W}_x = \bar{W}_0 \left[A_w \frac{\bar{h}}{\bar{H}_0} + (1 - A_w) \left(\frac{\bar{h}}{\bar{H}_0} \right)^2 \right] \sin \psi_w \tag{4.47}$$

$$\bar{W}_y = \bar{W}_0 \left[A_w \frac{\bar{h}}{\bar{H}_0} + (1 - A_w) \left(\frac{\bar{h}}{\bar{H}_0} \right)^2 \right] \cos \psi_w \tag{4.48}$$

$$\bar{W}_h = 0 \tag{4.49}$$

Define

$$\bar{\beta}_w = \frac{\bar{W}_0}{\bar{H}_0}, \quad \bar{B}_w = \frac{1 - A_w}{\bar{H}_0} \tag{4.50}$$

then the wind model can be expressed as

$$\bar{W}_x = \bar{\beta}_w (A_w \bar{h} + \bar{B}_w \bar{h}^2) \sin \psi_w \tag{4.51}$$

$$\bar{W}_y = \bar{\beta}_w (A_w \bar{h} + \bar{B}_w \bar{h}^2) \cos \psi_w \tag{4.52}$$

$$\bar{W}_h = 0 \tag{4.53}$$

also

$$\bar{W}'_x = \bar{\beta}_w (A_w + 2\bar{B}_w \bar{h}) \sin \psi_w \bar{V} \sin \gamma \tag{4.54}$$

$$\bar{W}'_y = \bar{\beta}_w (A_w + 2\bar{B}_w \bar{h}) \cos \psi_w \bar{V} \sin \gamma \tag{4.55}$$

$$\bar{W}'_h = 0 \tag{4.56}$$

Substituting (4.54), (4.55), and (4.56) into (4.37), we get

$$\bar{W}'_V = \frac{1}{2}\bar{V}\bar{\beta}_w(A_w + 2\bar{B}_w\bar{h})\sin 2\gamma\cos(\psi - \psi_w) \tag{4.57}$$

$$\bar{W}'_\psi = -\bar{V}\sin\gamma\bar{\beta}_w(A_w + 2\bar{B}_w\bar{h})\sin(\psi - \psi_w) \tag{4.58}$$

$$\bar{W}'_\gamma = \bar{V}(\sin\gamma)^2\bar{\beta}_w(A_w + 2\bar{B}_w\bar{h})\cos(\psi - \psi_w) \tag{4.59}$$

Substituting the normalized wind model (4.51) to (4.53) and (4.57) to (4.59) into the normalized equations of motion (4.30) through (4.35), we obtain

$$\begin{aligned}\bar{V}' = \bar{T} - k_a\bar{\rho}\bar{V}^2(C_{D_0} + KC_L^2) - \sin\gamma - \\ - \frac{1}{2}\bar{V}\bar{\beta}_w(A_w + 2\bar{B}_w\bar{h})\sin 2\gamma\cos(\psi - \psi_w)\end{aligned} \tag{4.60}$$

$$\psi' = k_a\bar{\rho}\bar{V}C_L\frac{\sin\mu}{\cos\gamma} + \tan\gamma\bar{\beta}_w(A_w + 2\bar{B}_w\bar{h})\sin(\psi - \psi_w) \tag{4.61}$$

$$\begin{aligned}\gamma' = k_a\bar{\rho}\bar{V}C_L\cos\mu - \frac{1}{\bar{V}}\cos\gamma + \\ + (\sin\gamma)^2\bar{\beta}_w(A_w + 2\bar{B}_w\bar{h})\cos(\psi - \psi_w)\end{aligned} \tag{4.62}$$

$$\bar{x}' = \bar{V}\cos\gamma\sin\psi + \bar{\beta}_w(A_w\bar{h} + \bar{B}_w\bar{h}^2)\sin\psi_w \tag{4.63}$$

$$\bar{y}' = \bar{V}\cos\gamma\cos\psi + \bar{\beta}_w(A_w\bar{h} + \bar{B}_w\bar{h}^2)\cos\psi_w \tag{4.64}$$

$$\bar{h}' = \bar{V}\sin\gamma \tag{4.65}$$

Chapter 5

Optimal UAV Loiter Flight Utilizing Wind Energy

This chapter formulates the optimal control problem for a UAV in a loitering mission and presents the solution method.

5.1 Problem Formulation

The problem of trajectory optimization for a UAV in a loitering mission is formulated as follows:

$$\min_{\mathbf{u}(t),t_f} \quad I = \Phi(\mathbf{x}(t_f), t_f) + \frac{1}{t_f}\int_{t_0}^{t_f} L(\mathbf{x}, \mathbf{u}, t)\, dt \tag{5.1}$$

subject to

$$\dot{\mathbf{x}} = \mathbf{f}(\mathbf{x}, \mathbf{u}, \mathbf{W}(\mathbf{x}, t), t) \tag{5.2}$$

$$\mathbf{x}(t_0) = \mathbf{x_0} \quad \text{given} \tag{5.3}$$

$$C_f\mathbf{x}(t_f) \rightarrow \mathbf{y_s} \quad \text{given} \tag{5.4}$$

$$C_f \in R^{q\times n}, \quad \mathbf{x_0} \in R^n, \quad \mathbf{y_s} \in R^q \tag{5.5}$$

In (5.1), I is the optimization objective function, which includes a final cost $\Phi(\mathbf{x}(t_f), t_f)$ and an integral cost $\frac{1}{t_f}\int_{t_0}^{t_f} L dt$. t_f is the flight time of a loitering cycle. The aircraft vehicle dynamics is governed by the equations of motion

(5.2). Equation (5.3) represents the given initial condition of the state. In (5.4), $\rightarrow$ can be interpreted as "desired to be" because this constraint may not be satisfied strictly or immediately. C_f is a configurable transformation matrix that is applied on the final state so that a subset of the final state $\mathbf{x}(t_f)$ approaches the terminal conditions specified by $\mathbf{y_S}$. Specifically, in a loitering mission, $\mathbf{y_S}$ may be set to $\mathbf{x_0}$ and $q = n$ so that the state at the end of a flight cycle is sufficiently close to the state at the beginning of the cycle, which ensures the flight is periodic.

In this thesis, we consider the energy performance index as the integral cost to be optimized. In UAV missions, long operational endurance is achieved by low fuel consumptions. Therefore, optimal control problems can be formulated to minimize the fuel consumption per cycle of a periodic flight by taking advantage of wind energies.

For a UAV with jet engine, the minimum fuel consumption corresponds to the minimum thrust required. In this case, the cost function in (5.1) can be expressed as

$$\min_{\mathbf{u}(t),t_f} \quad I = \Phi(\mathbf{x}(t_f), t_f) + \frac{1}{t_f}\int_{t_0}^{t_f} T dt \tag{5.6}$$

where T represents the thrust.

For a propeller-driven UAV, the minimum fuel consumption corresponds to the minimum power required. Thus, the cost function in (5.1) can be

expressed as

$$\min_{\mathbf{u}(t),t_f} \quad I = \Phi(\mathbf{x}(t_f), t_f) + \frac{1}{t_f}\int_{t_0}^{t_f} TV dt \tag{5.7}$$

where T is the thrust and V is the speed.

5.2 Solution Requirements and Potential Solution Strategies

A restriction is first placed on the above optimal UAV flight problem. For practical UAV operations, it is assumed that **no information** is available on the wind field. The UAV can only rely on measurements of the wind components by its own sensors to estimate the wind field.

Furthermore in order to be used for real-time onboard applications, any potential solution method of the above problem needs to satisfy some or all of the following properties.

1. It must always produce physically meaningful and feasible solutions in a reliable manner.
2. It must be able to produce feasible solutions fast.
3. Intermediate solutions should be feasible so the improvement can be stopped at any number of iterations thought it may be sub-optimal.
4. Optimal solutions are desirable whenever possible. Particularly, the solution scheme should be able to produce optimal solutions if a sufficient number of repeats are used.

There are different solution frameworks to the above problem, including the following:

1. Nonlinear continuous-time optimal control, solved using a variational approach;
2. Nonlinear continuous-time optimal control solved through conversion into a parameter optimization method;
3. Nonlinear discrete-time optimal control problem through the time discretization of the original problem;
4. Successive linearization of the original problem either in continuous-time or discrete-time format, solved using linear quadratic optimal control methods.

Solutions of the nonlinear optimal control problem can truly optimize the performance. However, there is in general no guarantee on the convergence or convergence time of these solutions. These problems are often solved numerically via iterative schemes that may or may not produce feasible intermediate solutions.

In this research, a successive linearization approach is used in a continuous-time form. The resulting linearized problem can be solved using a state transition method result in semi-analytical solutions that do not require numerical iterations. When used as a solution scheme for each cycle of trajectory improvement, it produces feasible intermediate solutions. Such

a solution scheme can be carried out to any number of repetitions depending on the available planning time. When appropriately formated, the linear quadratic optimal control problem at each sub step can always lead to reliable solutions.

5.3 Linearization of the Original Optimal Control Problem

We choose a nominal trajectory $(\mathbf{x}^o, \mathbf{u}^o, t_f^o)$ and consider very small trajectory changes in order to determine directions of trajectory improvement updates. The equations of motion, constraints, and the cost function are linearized around the nominal trajectory as follows:

Equations of Motion

$$\begin{aligned}\delta\dot{\mathbf{x}} &= \mathbf{f}(\mathbf{x}^o + \delta\mathbf{x}, \mathbf{u}^o + \delta\mathbf{u}, \mathbf{W}(\mathbf{x}^o + \delta\mathbf{x}, t), t) - \mathbf{f}(\mathbf{x}^o, \mathbf{u}^o, \mathbf{W}(\mathbf{x}^o, t), t) \\ &= A\delta\mathbf{x} + B\delta\mathbf{u} \end{aligned} \tag{5.8}$$

where

$$A \triangleq \left(\frac{\partial \mathbf{f}}{\partial \mathbf{x}} + \frac{\partial \mathbf{f}}{\partial \mathbf{W}}\frac{\partial \mathbf{W}}{\partial \mathbf{x}}\right)_{\mathbf{x}^o, \mathbf{u}^o} \quad B \triangleq \left(\frac{\partial \mathbf{f}}{\partial \mathbf{u}}\right)_{\mathbf{x}^o, \mathbf{u}^o} \tag{5.9}$$

and

$$A \in R^{n\times n}, \quad B \in R^{n\times m} \tag{5.10}$$

Initial Condition

$$\delta\mathbf{x}(t_0) = 0 \tag{5.11}$$

Terminal Constraints

Since

$$\mathbf{x}(t_f) \approx \mathbf{x}(t_f^o) + \dot{\mathbf{x}}(t_f^o)dt_f = \mathbf{x}^o(t_f^o) + \delta\mathbf{x}(t_f^o) + \dot{\mathbf{x}}(t_f^o)dt_f \tag{5.12}$$

(5.4) can be linearized as

$$C_f\delta\mathbf{x}(t_f^o) + \mathbf{d_f}dt_f \rightarrow -\Delta\mathbf{y_s^o} \tag{5.13}$$

where

$$\mathbf{d_f} \stackrel{\triangle}{=} C_f\dot{\mathbf{x}}(t_f^o), \quad \mathbf{d_f} \in R^q \tag{5.14}$$

$$\Delta\mathbf{y_s^o} \stackrel{\triangle}{=} C_f\mathbf{x}^o(t_f^o) - \mathbf{y_s} \tag{5.15}$$

Because it may only be feasible to achieve (5.4) iteratively, a desirable linearized form of (5.4) may be stated as

$$C_f\delta\mathbf{x}(t_f^o) + \mathbf{d_f}dt_f = -\alpha_T\Delta\mathbf{y_s^o} \tag{5.16}$$

where $0 \leq \alpha_T \leq 1$ is a computational parameter that controls the step-size of the terminal constraint improvement. The smaller the value of α_T is, the faster the improved trajectory approaches satisfying the terminal constraint.

Cost Function

1 . Terminal Cost is given by

The first order variation of the terminal cost Φ is

$$\delta\Phi = \left[\frac{\partial\Phi}{\partial\mathbf{x}(t_f)}\dot{\mathbf{x}}(t) + \frac{\partial\Phi}{\partial t_f}\right]_{\mathbf{x}^o, t_f^o} dt_f \tag{5.17}$$

2 . Integral Cost is given by

Define

$$\hat{L} \triangleq \frac{1}{t_f} \int_{t_0}^{t_f} L(\mathbf{x}, \mathbf{u}, t)\ dt \tag{5.18}$$

Then the first order variation of the integral cost $\hat{L}$ is

$$\delta\hat{L} = \frac{1}{t_f^o + dt_f} \int_{t_0}^{t_f^o + dt_f} L(\mathbf{x}^o + \delta\mathbf{x}, \mathbf{u}^o + \delta\mathbf{u}, t)\ dt - \frac{1}{t_f^o} \int_{t_0}^{t_f^o} L(\mathbf{x}^o, \mathbf{u}^o, t)\ dt \tag{5.19}$$

and

$$\begin{aligned}\delta\hat{L} = {} & \frac{1}{(t_f^o + dt_f)t_f^o} \cdot \\ & \cdot \left[t_f^o \int_{t_0}^{t_f^o + dt_f} L(\mathbf{x}^o + \delta\mathbf{x}, \mathbf{u}^o + \delta\mathbf{u}, t)\ dt - (t_f^o + dt_f) \int_{t_0}^{t_f^o} L(\mathbf{x}^o, \mathbf{u}^o, t)\ dt \right]\end{aligned} \tag{5.20}$$

Since

$$\int_0^{t_f^o + dt_f} = \int_0^{t_f^o} + \int_{t_f^o}^{t_f^o + dt_f} \tag{5.21}$$

Re-arranging terms in (5.20), we obtain

$$\begin{aligned}\delta\hat{L} = {} & \frac{1}{(t_f^o + dt_f)} \int_{t_0}^{t_f^o} \left[L(\mathbf{x}^o + \delta\mathbf{x}, \mathbf{u}^o + \delta\mathbf{u}, t) - L(\mathbf{x}^o, \mathbf{u}^o, t) \right]\ dt + \\ & + \frac{1}{(t_f^o + dt_f)t_f^o} \left[t_f^o \int_{t_f^o}^{t_f^o + dt_f} L(\mathbf{x}^o + \delta\mathbf{x}, \mathbf{u}^o + \delta\mathbf{u}, t)\ dt - \left(\int_{t_0}^{t_f^o} L(\mathbf{x}^o, \mathbf{u}^o, t)\ dt \right) dt_f \right] \\ = {} & \frac{1}{t_f^o + dt_f} \int_{t_0}^{t_f^o} \left[\left(\frac{\partial L}{\partial \mathbf{x}} \right)_{\mathbf{x}^o, \mathbf{u}^o} \delta\mathbf{x} + \left(\frac{\partial L}{\partial \mathbf{u}} \right)_{\mathbf{x}^o, \mathbf{u}^o} \delta\mathbf{u} \right]\ dt + \\ & + \frac{1}{(t_f^o)^2 + t_f^o dt_f} \left[t_f^o L(\mathbf{x}^o, \mathbf{u}^o, t)|_{t_f^o} - \int_{t_0}^{t_f^o} L(\mathbf{x}^o, \mathbf{u}^o, t)\ dt \right] dt_f\end{aligned} \tag{5.22}$$

Ignore the dt_f term in the denominators. Define

$$L^o \triangleq L(\mathbf{x}^o, \mathbf{u}^o, t) \tag{5.23}$$

$$\delta L \triangleq \left(\frac{\partial L}{\partial \mathbf{x}}\right)_{\mathbf{x}^o,\mathbf{u}^o} \delta\mathbf{x} + \left(\frac{\partial L}{\partial \mathbf{u}}\right)_{\mathbf{x}^o,\mathbf{u}^o} \delta\mathbf{u} \tag{5.24}$$

then the first order variation of the integral cost $\hat{L}$ is

$$\delta\hat{L} = \frac{1}{t_f^o}\int_{t_0}^{t_f^o} \delta L \; dt + \frac{1}{(t_f^o)^2}\left[t_f^o \; L^o|_{t_f^o} - \int_{t_0}^{t_f^o} L^o \; dt\right] dt_f \tag{5.25}$$

Combining (5.17) and (5.25), we get the first order variation of the optimization cost function

$$\begin{aligned}\delta I = &\left[\left(\frac{\partial \Phi}{\partial \mathbf{x}(t_f)}\dot{\mathbf{x}}(t) + \frac{\partial \Phi}{\partial t_f}\right)_{\mathbf{x}^o,t_f^o} + \frac{1}{(t_f^o)^2}\left(t_f^o \; L^o|_{t_f^o} - \int_{t_0}^{t_f^o} L^o \; dt\right)\right] dt_f + \\ &+ \frac{1}{t_f^o}\int_{t_0}^{t_f^o} \delta L \; dt\end{aligned} \tag{5.26}$$

For a jet-engined UAV,

$$\delta L = \delta T \tag{5.27}$$

$$L^o = T^o \tag{5.28}$$

For a propeller-driven UAV,

$$\delta L = V\delta T + T\delta V \tag{5.29}$$

$$L^o = T^o V^o \tag{5.30}$$

In summary, the linearized periodic trajectory improvement problem can be stated as follows:

$$\begin{aligned}\min_{\delta\mathbf{u},dt_f} \quad \delta I = &\, p_f dt_f + \frac{1}{2}q_f(dt_f)^2 + \\ &+ \int_{t_0}^{t_f^o}\left(\mathbf{e}^T\delta\mathbf{x} + \mathbf{c}^T\delta\mathbf{u} + \frac{1}{2}\delta\mathbf{x}^T Q^{-1}\delta\mathbf{x} + \frac{1}{2}\delta\mathbf{u}^T R^{-1}\delta\mathbf{u}\right) dt\end{aligned} \tag{5.31}$$

subject to (5.8), (5.11), and (5.16). The quadratic terms in (5.31) are included to control the magnitude of trajectory improvements, where q_f is a positive scalar, $Q \in R^{n\times n}$ and $R \in R^{m\times m}$ are non-singular diagonal matrices. With R being non-singular and diagonal, we may apply upper bound and lower bound on each component in the computed control vector in computation without losing optimality. Also, p_f is scalar, $\mathbf{e} \in R^n$, and $\mathbf{c} \in R^m$.

To simplify the notations, we define

$$\mathbf{z} \triangleq \delta\mathbf{x}, \quad \mathbf{w} \triangleq \delta\mathbf{u}, \quad \tau_f \triangleq dt_f, \quad J \triangleq \delta I \tag{5.32}$$

then the linearized problem can be stated as follows:

$$\begin{aligned}\min_{\mathbf{w},\tau_f} \quad & J = p_f\tau_f + \frac{1}{2}q_f\tau_f^2 + \\ & + \int_{t_0}^{t_f^o}\left(\mathbf{e}^T\mathbf{z} + \mathbf{c}^T\mathbf{w} + \frac{1}{2}\mathbf{z}^TQ^{-1}\mathbf{z} + \frac{1}{2}\mathbf{w}^TR^{-1}\mathbf{w}\right)d\tau \end{aligned} \tag{5.33}$$

subject to

$$\dot{\mathbf{z}} = A(t)\mathbf{z} + B(t)\mathbf{w} \tag{5.34}$$

$$\mathbf{z}(t_0) = 0 \tag{5.35}$$

$$C_f\mathbf{z}(t_f^o) + \mathbf{d_f}\tau_f + \alpha_T\Delta\mathbf{y_s^o} = 0 \tag{5.36}$$

For a jet-engined UAV,

$$p_f = \left[\frac{\partial\Phi}{\partial\mathbf{x}(t_f)}\dot{\mathbf{x}}(t) + \frac{\partial\Phi}{\partial t_f}\right]_{\mathbf{x}^o,t_f^o} + \frac{1}{(t_f^o)^2}\left(t_f^o\ T^o|_{t_f^o} - \int_{t_0}^{t_f^o}T^o\ dt\right) \tag{5.37}$$

$$\mathbf{e} = [\,0 \quad 0 \quad 0 \quad 0 \quad 0 \quad 0\,]^T \tag{5.38}$$

$$\mathbf{c} = \left[\,\frac{1}{t_f^o} \quad 0 \quad 0\,\right]^T \tag{5.39}$$

For a propeller-driven UAV,

$$p_f = \left[\frac{\partial \Phi}{\partial \mathbf{x}(t_f)}\dot{\mathbf{x}}(t) + \frac{\partial \Phi}{\partial t_f}\right]_{\mathbf{x}^o, t_f^o} + \frac{1}{(t_f^o)^2}\left(t_f^o\ T^o V^o|_{t_f^o} - \int_{t_0}^{t_f^o} T^o V^o\ dt\right) \tag{5.40}$$

$$\mathbf{e} = \begin{bmatrix} \frac{T^o}{t_f^o} & 0 & 0 & 0 & 0 & 0 \end{bmatrix}^T \tag{5.41}$$

$$\mathbf{c} = \begin{bmatrix} \frac{V^o}{t_f^o} & 0 & 0 \end{bmatrix}^T \tag{5.42}$$

This thesis considers the specific problem of minimizing the combination of final time and average power for a propeller-driven UAV, i.e.

$$\Phi = t_f \tag{5.43}$$

$$L = TV \tag{5.44}$$

thus

$$p_f = 1 + \frac{1}{(t_f^o)^2}\left(t_f^o\ T^o V^o|_{t_f^o} - \int_{t_0}^{t_f^o} T^o V^o\ dt\right) \tag{5.45}$$

$$\mathbf{e} = \begin{bmatrix} \frac{T^o}{t_f^o} & 0 & 0 & 0 & 0 & 0 \end{bmatrix}^T \tag{5.46}$$

$$\mathbf{c} = \begin{bmatrix} \frac{V^o}{t_f^o} & 0 & 0 \end{bmatrix}^T \tag{5.47}$$

5.4 Trajectory Optimization with Fixed Final Time

In the periodic trajectory improvement for a UAV, if the final time is fixed, the problem becomes simpler. Specifically, the problem formulation can be modified as follows:

$$\min_{\mathbf{u}(t), t_f} \quad I = \frac{1}{t_{f_s}} \int_0^{t_{f_s}} L(\mathbf{x}, \mathbf{u}, t)\ dt \tag{5.48}$$

subject to

$$\dot{\mathbf{x}} = \mathbf{f}(\mathbf{x}, \mathbf{u}, \mathbf{W}(\mathbf{x}, t), t) \tag{5.49}$$

$$\mathbf{x}(0) = \mathbf{x_0} \quad \text{given} \tag{5.50}$$

where t_{f_s} is the fixed final time.

Following similar derivations used in solving the open final time problem, we can linearize the problem of fixed final time as

$$\min_{\mathbf{w}(t)} \quad J = \int_0^{t_{f_s}} \left(\mathbf{e}^T \mathbf{z} + \mathbf{c}^T \mathbf{w} + \frac{1}{2} \mathbf{z}^T Q^{-1} \mathbf{z} + \frac{1}{2} \mathbf{w}^T R^{-1} \mathbf{w} \right) dt \tag{5.51}$$

subject to

$$\dot{\mathbf{z}} = A(t)\mathbf{z} + B(t)\mathbf{w} \tag{5.52}$$

$$\mathbf{z}(0) = 0 \tag{5.53}$$

Chapter 6

Solution to the Linearized Problems

This chapter presents the solution method to the linearized trajectory improvement problem utilizing estimated wind velocity.

6.1 The Linearized Problem Formulation

The linearized problem can be formulated as follows:

$$\min_{\mathbf{w},\tau_f} \quad J = p_f\tau_f + \frac{1}{2}q_f\tau_f^2 + \\ + \int_{t_0}^{t_f^o} \left(\mathbf{e}^T\mathbf{z} + \mathbf{c}^T\mathbf{w} + \frac{1}{2}\mathbf{z}^T Q^{-1}\mathbf{z} + \frac{1}{2}\mathbf{w}^T R^{-1}\mathbf{w}\right) d\tau \tag{6.1}$$

subject to

$$\dot{\mathbf{z}} = A(t)\mathbf{z} + B(t)\mathbf{w} \tag{6.2}$$

$$\mathbf{z}(t_0) = 0 \tag{6.3}$$

$$C_f\mathbf{z}(t_f^o) + \mathbf{d_f}\tau_f + \alpha_T\Delta\mathbf{y_s^o} = 0 \tag{6.4}$$

6.2 Derivation of Solution Algorithms

For the problem defined in equations (6.1) through (6.4), define the Hamiltonian function as

$$H = \mathbf{e}^T\mathbf{z} + \mathbf{c}^T\mathbf{w} + \frac{1}{2}\mathbf{z}^T Q^{-1}\mathbf{z} + \frac{1}{2}\mathbf{w}^T R^{-1}\mathbf{w} + \lambda^T(A\mathbf{z} + B\mathbf{w}) \tag{6.5}$$

where $\lambda(t) \in R^n$.

Define the terminal cost as

$$\phi = p_f \tau_f + \frac{1}{2} q_f \tau_f^2 \tag{6.6}$$

and the terminal constraint as

$$\mathbf{\Psi} = C_f \mathbf{z}(t_f^o) + \mathbf{d_f} \tau_f + \alpha_T \Delta \mathbf{y_s^o} = 0 \tag{6.7}$$

Then the adjoint cost function is given by

$$\bar{J} = \phi(\tau_f) + \nu^T \mathbf{\Psi} + \int_0^{t_f^o} (H - \lambda^T \dot{\mathbf{z}})\, dt \tag{6.8}$$

where $\nu \in R^q$.

The Euler-Lagrange equations become

$$\dot{\lambda} = -H_{\mathbf{z}}^T = -A^T \lambda - Q^{-1} \mathbf{z} - \mathbf{e}, \quad \lambda(t_f^o) = C_f^T \nu \tag{6.9}$$

$$0 = H_{\mathbf{w}}^T = R^{-1} \mathbf{w} + B^T \lambda + \mathbf{c} \tag{6.10}$$

which leads to

$$\mathbf{w} = -R[B^T \lambda + \mathbf{c}] \tag{6.11}$$

and

$$0 = \frac{d\phi}{d\tau_f} + \nu^T \frac{d\mathbf{\Psi}}{d\tau_f} = p_f + q_f \tau_f + \nu^T \mathbf{d_f} \tag{6.12}$$

Solving for τ_f in terms of ν in the above equation, we get

$$\tau_f = -\frac{1}{q_f}(p_f + \nu^T \mathbf{d_f}) \tag{6.13}$$

Substituting (6.13) into (6.7), we have

$$\mathbf{\Psi} = C_f \mathbf{z}(t_f^o) - \frac{1}{q_f}\mathbf{d_f}\mathbf{d_f}^T\nu - \frac{p_f}{q_f}\mathbf{d_f} + \alpha_T \Delta \mathbf{y_s^o} \tag{6.14}$$

Substituting (6.11) into (6.2) and combining with (6.3), we obtain the following differential equation and initial condition for $\mathbf{z}$:

$$\dot{\mathbf{z}} = A\mathbf{z} - BRB^T\lambda - BR\mathbf{c}, \quad \mathbf{z}(t_0) = 0 \tag{6.15}$$

(6.9) and (6.15) constitute a two-point boundary value problem, which can be solved through the Riccati Equations. Define

$$\lambda(t) = S(t)\mathbf{z}(t) + G(t)\nu + \lambda_B(t) \tag{6.16}$$

where $S \in R^{n\times n}$, $G \in R^{n\times q}$, and $\lambda_B \in R^n$. Substituting (6.16) into (6.15), we obtain

$$\begin{aligned}\dot{\mathbf{z}} &= A\mathbf{z} - BRB^T(S\mathbf{z} + G\nu + \lambda_B) - BR\mathbf{c} \\ &= (A - BRB^TS)\mathbf{z} - BRB^TG\nu - BRB^T\lambda_B - BR\mathbf{c}\end{aligned} \tag{6.17}$$

Differentiating (6.16), we obtain

$$\dot{\lambda} = \dot{S}\mathbf{z} + S\dot{\mathbf{z}} + \dot{G}\nu + \dot{\lambda}_B \tag{6.18}$$

Substituting (6.17) into (6.18), we get

$$\dot{\lambda} = (\dot{S} + SA - SBRB^TS)\mathbf{z} - (SBRB^TG - \dot{G})\nu - SBRB^T\lambda_B - SBR\mathbf{c} + \dot{\lambda}_B \tag{6.19}$$

Combining (6.19) with (6.9), after some algebra, we get

$$\dot{S} = -A^T S - SA + SBRB^T S - Q^{-1}, \quad S(t_f^o) = 0 \tag{6.20}$$

$$\dot{\lambda}_{\mathbf{B}} = (SBRB^T - A^T)\lambda_B + SBR\mathbf{c} - \mathbf{e}, \quad \lambda_{\mathbf{B}}(t_f^o) = 0 \tag{6.21}$$

$$\dot{G} = (SBRB^T - A^T)G, \quad G(t_f^o) = C_f^T \tag{6.22}$$

Substituting (6.16) into (6.11), we get

$$\mathbf{w} = -RB^T S\mathbf{z} - RB^T G\nu - RB^T\lambda_B - R\mathbf{c} \tag{6.23}$$

Assume $\mathbf{\Psi}$ has the following form:

$$\mathbf{\Psi} = U\mathbf{z} + V\nu + \psi_B \tag{6.24}$$

where $U \in R^{q\times n}$, $V \in R^{q\times q}$, and $\psi_B \in R^q$. Then (6.14) gives the final condition for U, V, and ψ_B as

$$U(t_f^o) = C_f, \quad V(t_f^o) = -\frac{1}{q_f}\mathbf{d_f}\mathbf{d_f}^T, \quad \psi_B(t_f^o) = -\frac{p_f}{q_f}\mathbf{d_f} + \alpha_T\Delta\mathbf{y_s^o} \tag{6.25}$$

Differentiating (6.24), we get

$$\dot{\mathbf{\Psi}} = \dot{U}\mathbf{z} + U\dot{\mathbf{z}} + \dot{V}\nu + \dot{\psi}_B \tag{6.26}$$

Substituting (6.17) into (6.26), we get

$$\dot{\mathbf{\Psi}} = [\dot{U} + U(A - BRB^T S)]\mathbf{z} + (\dot{V} - UBRB^T G)\nu + \dot{\psi}_B - UBRB^T\lambda_B - UBR\mathbf{c} \tag{6.27}$$

Since $\dot{\mathbf{\Psi}} = 0$ for all $\mathbf{z}(t)$, ν, and $\lambda_B(t)$, we have

$$\dot{U} = U(BRB^T S - A) \tag{6.28}$$

$$\dot{V} = UBRB^T G \tag{6.29}$$

$$\dot{\psi}_B = UBRB^T\lambda_B + UBR\mathbf{c} \tag{6.30}$$

The final conditions are given by

$$U(t_f^o) = C_f \tag{6.31}$$

$$V(t_f^o) = -\frac{1}{q_f}\mathbf{d_f}\mathbf{d_f}^T \tag{6.32}$$

$$\psi_B(t_f^o) = -\frac{p_f}{q_f}\mathbf{d_f} + \alpha_T \Delta \mathbf{y_s^o} \tag{6.33}$$

Compare (6.22) and (6.28), we get

$$U = G^T \tag{6.34}$$

then (6.29) and (6.30) become

$$\dot{V} = G^T B R B^T G \tag{6.35}$$

$$\dot{\psi}_B = G^T B R B^T \lambda_B + G^T B R \mathbf{c} \tag{6.36}$$

In (6.24), set $t = t_0$, we get

$$0 = U(t_0)\mathbf{z}(t_0) + V(t_0)\nu + \psi_B(t_0) \tag{6.37}$$

Since $\mathbf{z}(t_0) = 0$, we can solve for ν in (6.37) and get

$$\nu = -V^{-1}(t_0)\psi_B(t_0) \tag{6.38}$$

6.3 Inequality Constraints

In the current solution algorithms, it is assumed that the nominal solution is feasible: it satisfies all constraints. In the subsequent successive

improvements, any bounds on the controls are directly applied after an improved trajectory solution is obtained. The trajectory improvement step size is limited so that all the state inequality constraints are satisfied.

It would be highly desirable if algorithms for the linear quadratic problem can directly incorporate any linear state and/or control inequality constraints. No significant progress was made in this endeavor during the time period of this research. Therefore, the development of such algorithms is recommended for future research.

6.4 Solution Procedure for the Problem with Open Final Time

Below are the computation steps to determine $\mathbf{w}(t)$ and τ_f that optimize the augmented cost function given in (6.1).

1 . Solve the following differential equations simultaneously by backward integration

$$\dot{S} = -A^T S - SA + SBRB^T S - Q^{-1}, \quad S(t_f^o) = 0 \tag{6.39}$$

$$\dot{\lambda}_B = (SBRB^T - A^T)\lambda_B + SBR\mathbf{c} - \mathbf{e}, \quad \lambda_B(t_f^o) = 0 \tag{6.40}$$

$$\dot{G} = (SBRB^T - A^T)G, \quad G(t_f^o) = C_f^T \tag{6.41}$$

$$\dot{V} = G^T BRB^T G, \quad V(t_f^o) = -\frac{1}{q_f}\mathbf{d_f}\mathbf{d_f}^T \tag{6.42}$$

$$\dot{\psi}_B = G^T BRB^T \lambda_B + G^T BR\mathbf{c}, \quad \psi_B(t_f^o) = -\frac{p_f}{q_f}\mathbf{d_f} + \alpha_T \Delta \mathbf{y_s^o} \tag{6.43}$$

where

$$\Delta \mathbf{y_s^o} = C_f \mathbf{x}^o(t_f^o) - \mathbf{y_s} \tag{6.44}$$

At each integration time step t_k, calculate the following matrices: K_d, N_d, and $\mathbf{w_f}$

$$K_d(t_k) = R(t_k)B(t_k)^T S(t_k) \tag{6.45}$$

$$N_d(t_k) = R(t_k)B(t_k)^T G(t_k) \tag{6.46}$$

$$\mathbf{w_f}(t_k) = R(t_k)B(t_k)^T \lambda_B(t_k) + R(t_k)\mathbf{c}(t_k) \tag{6.47}$$

2 . Calculate ν

$$\nu = -V^{-1}(t_0)\psi_B(t_0) \tag{6.48}$$

3 . Solve the following differential equation by forward integration to obtain $\mathbf{z}(t)$ and calculate $\mathbf{w}$

$$\dot{\mathbf{z}} = (A - BK_d)\mathbf{z} - BN_d\nu - B\mathbf{w_f}, \quad \mathbf{z}(t_0) = 0 \tag{6.49}$$

$$\mathbf{w} = -K_d\mathbf{z} - N_d\nu - \mathbf{w_f} \tag{6.50}$$

4 . Calculate τ_f

$$\tau_f = -\frac{1}{q_f}(p_f + \nu^T \mathbf{d_f}) \tag{6.51}$$

6.5 Solution Procedure for the Problem with Fixed Final Time

Similarly, the linearized version of the problem with fixed final time can be solved as follows. These steps compute the control update $\mathbf{w}(t)$ that optimizes the augmented cost function given in (5.51).

1 . Solve the following differential equations simultaneously by backward integration

$$\dot{S} = -A^T S - SA + SBRB^T S - Q^{-1}, \quad S(t_{f_s}) = 0 \tag{6.52}$$

$$\dot{\lambda}_B = (SBRB^T - A^T)\lambda_B + SBR\mathbf{c} - \mathbf{e}, \quad \lambda_B(t_{f_s}) = 0 \tag{6.53}$$

At each integration time step t_k, calculate the following matrices: K_d and $\mathbf{w_f}$

$$K_d(t_k) = R(t_k)B(t_k)^T S(t_k) \tag{6.54}$$

$$\mathbf{w_f}(t_k) = R(t_k)B(t_k)^T \lambda_B(t_k) + R(t_k)\mathbf{c}(t_k) \tag{6.55}$$

2 . Solve the following differential equation by forward integration to obtain $\mathbf{z}(t)$ and calculate $\mathbf{w}$

$$\dot{\mathbf{z}} = (A - BK_d)\mathbf{z} - B\mathbf{w_f}, \quad \mathbf{z}(0) = 0 \tag{6.56}$$

$$\mathbf{w} = -K_d\mathbf{z} - \mathbf{w_f} \tag{6.57}$$

Chapter 7

Simulation Procedure and Solution Evaluations

In this chapter, a numerical simulation environment is established that can be used to evaluate the proposed strategy for planning UAV fuel-efficient flight trajectories in practical operations. In particular, an evaluation criterion is proposed that represents the improvement of efficiency brought about by the proposed strategy.

7.1 Simulation Environment

A simulation environment is developed based on the solution framework presented in Chapter 2. In practical operations, real wind velocity components can be measured onboard, but in simulations, the wind field can only be simulated using various models, including linear and nonlinear models depending on the scenarios being studied. On the other hand, the wind model that is used to approximate and estimate the simulated 'real' wind is fixed when setting up the simulation environment. As a preparation step, atmospheric constants, such as air density, air density gradients, and transition altitude, UAV dynamics specifications and performance limitations, such as wing loading, maximum lift-to-drag ratio, profile drag coefficient, maximum

speed, maximum thrust, etc., are specified in the beginning of the simulation, as well as algorithm parameters. Furthermore, an initial nominal trajectory is chosen as a start point of the successive trajectory improvement procedure. The flowchart below describes the simulation environment and procedure used in this research:

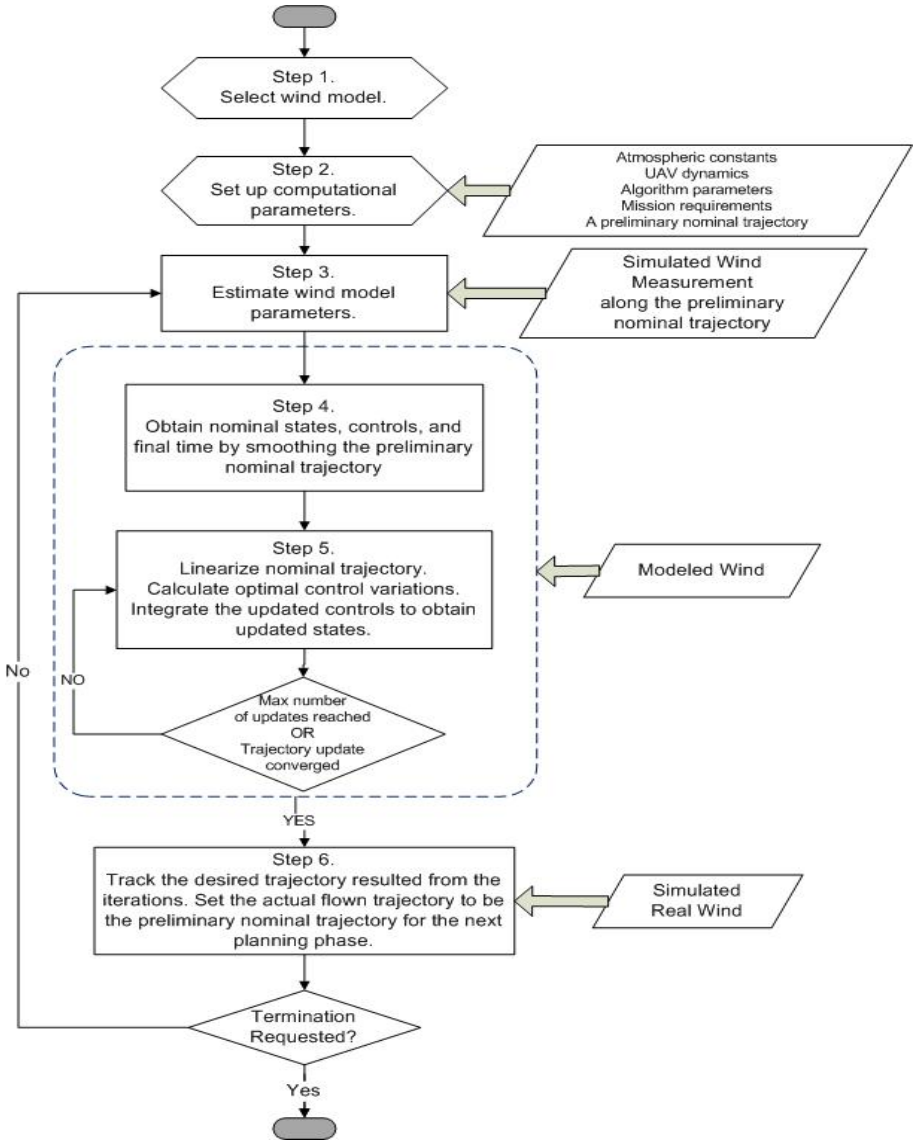

Figure 7.1 Simulation Flowchart

Once a preliminary nominal trajectory is specified, wind measurements are collected along the trajectory as the first step in the successive trajectory improvement algorithm. The parameters of wind model are estimated using the wind measurements. Nominal states, controls, and final time of the trajectory are obtained by smoothing the nominal trajectory.

The nominal trajectory, states, and controls, are then linearized and optimal control variations are calculated based on the optimization objective of minimizing fuel. After a specified number of calculations, the controls are updated with the resultant control variations, and a desired optimal trajectory is obtained by integrating the updated controls. By tracking the desired trajectory in the simulated real wind field, a new set of controls are generated and the actual flown trajectory is set to be the nominal trajectory for the next optimization cycle. The wind measurement process repeats along the new nominal trajectory, as well as the successive trajectory optimization procedure. This procedure may continue unless an external termination request is received.

7.2 Detailed Simulation Procedure

This section describes the detailed step-by-step simulation procedure.

Step 1. Select wind model

Specify the wind model format. For example, the following equations define a stationary linear gradient wind model with the assumption of zero

vertical wind.

$$W_x = \frac{W_0}{H_0} h \sin\psi_w \tag{7.1}$$

$$W_y = \frac{W_0}{H_0} h \cos\psi_w \tag{7.2}$$

$$W_h = 0 \tag{7.3}$$

Step 2. Set up computational parameters

• Specify characteristic variables used in normalization

$$V_C, T_C, D_C, \rho_C$$

• Specify normalized atmospheric parameters, UAV performance limitations, and UAV vehicle dynamics parameters

$$H_0, g, \bar{\rho}(\bar{h}), \frac{d\bar{\rho}}{d\bar{h}}(\bar{h})$$

$$C_{D_0}, E_{\max}, mg/S, k_a, k_l$$

$$\bar{V}_{\max}, \bar{V}_{\min}, \gamma_{\max}, \gamma_{\min}$$

$$\mathbf{U}_{\max} = [\bar{T}_{\max}, C_{L_{\max}}, \mu_{\max}]^T$$

$$\mathbf{U}_{\min} = [\bar{T}_{\min}, C_{L_{\min}}, \mu_{\min}]^T$$

• Specify mission requirement parameters that define the initial and terminal constraints

$$\bar{t}_0, \bar{\mathbf{x}}_0, \bar{\mathbf{y}}_\mathbf{s}, C_f$$

$$\bar{t}_{f,\max}, \quad \bar{t}_{f,\min}$$

- Specify algorithm parameters

  $q_f > 0$ Weighting on the quadratic term of τ_f

  $Q \succ 0$ Weighting matrix on the quadratic term of $\mathbf{z}$

  $R \succ 0$ Weighting matrix on the quadratic term of $\mathbf{w}$

  N_t The number of trajectory time steps

  N_w The number of wind measurements along the trajectory

  ϵ_τ The convergence criteria for τ_f

  $\epsilon_{\mathbf{z}}$ The convergence criteria for $\mathbf{z}$

  $\epsilon_{\mathbf{w}}$ The convergence criteria for $\mathbf{w}$

  α_{term} The deviation coefficient for the terminal constraint

  η_t The maximum percent update on t_f in each iteration

  $\eta_{\mathbf{u}}$ The maximum percent update on $\mathbf{u}$ in each iteration

  $\alpha_{t,\max}$ The maximum step-size on τ_f

  $\alpha_{u,\max}$ The maximum step-size on $\mathbf{w}$

  $N_{i,\max}$ The maximum number of iterations

- Specify the format of the coefficient matrices on the performance index

$$p_f, \mathbf{e}(\bar{t}), \mathbf{c}(\bar{t}), A(\bar{t}), B(\bar{t})$$

- Specify an initial nominal trajectory

For $0 \leq \bar{t} \leq \bar{t}_{f_s}$,

$$\bar{x}_s(\bar{t}), \bar{y}_s(\bar{t}), \bar{h}_s(\bar{t}); \quad \bar{x}'_s(\bar{t}), \bar{y}'_s(\bar{t}), \bar{h}'_s(\bar{t}); \quad \bar{x}''_s(\bar{t}), \bar{y}''_s(\bar{t}), \bar{h}''_s(\bar{t})$$

• Obtain measurements of wind velocity components along the desired trajectory

For $k = 1, 2, ..., N_w$,

$$\hat{W}_{\bar{x}_k} = \hat{W}_x(\bar{t}_k, \bar{x}_k, \bar{y}_k, \bar{h}_k) = \bar{W}_x(\bar{t}_k, \bar{x}_k, \bar{y}_k, \bar{h}_k) + e_{x_k} \tag{7.4}$$

$$\hat{W}_{\bar{y}_k} = \hat{W}_y(\bar{t}_k, \bar{x}_k, \bar{y}_k, \bar{h}_k) = \bar{W}_y(\bar{t}_k, \bar{x}_k, \bar{y}_k, \bar{h}_k) + e_{y_k} \tag{7.5}$$

$$\hat{W}_{\bar{h}_k} = \hat{W}_h(\bar{t}_k, \bar{x}_k, \bar{y}_k, \bar{h}_k) = \bar{W}_h(\bar{t}_k, \bar{x}_k, \bar{y}_k, \bar{h}_k) + e_{h_k} \tag{7.6}$$

where e_{x_k}, e_{y_k}, e_{h_k} are wind estimation errors and

$$\bar{x}_k = \bar{x}_s(\bar{t}_k), \quad \bar{y}_k = \bar{y}_s(\bar{t}_k), \quad \bar{h}_k = \bar{h}_s(\bar{t}_k) \tag{7.7}$$

Step 3. Estimate wind model parameters

Use the measured wind velocity components $(\hat{W}_{\bar{x}_k}, \hat{W}_{\bar{y}_k}, \hat{W}_{\bar{h}_k})$, $k = 1, 2, ..., N_w$ to estimate the parameters of wind gradient model:

$$W_0 = H_0\sqrt{p_1^2 + p_2^2} \tag{7.8}$$

$$\tan\psi_w = \frac{p_1}{p_2} \tag{7.9}$$

where $\psi_w \in [0, 2\pi]$ and

$$p_1 = \frac{\hat{\mathbf{W}}_\mathbf{x}^T\mathbf{h}}{\mathbf{h}^T\mathbf{h}}; \quad p_2 = \frac{\hat{\mathbf{W}}_\mathbf{y}^T\mathbf{h}}{\mathbf{h}^T\mathbf{h}} \tag{7.10}$$

Step 4. Generate nominal controls to track the desired trajectory

A method for generating feasible controls to track a reference trajectory is discussed in another section. Mathematically, the generated reference states

and controls can be expressed as

$$\bar{t}_f^o, \quad [\bar{\mathbf{x}}^o(\bar{t}), \bar{\mathbf{u}}^o(\bar{t})] \quad \text{for} \quad \bar{t} \in [\bar{t}_0, \bar{t}_f^o]$$

Step 5. Improve the reference trajectory successively

5.1) Initialize the iteration counter $i = 1$.

5.2) Calculate control and final time improvement $[\mathbf{w}(\bar{t}), \tau_f]$

5.2.a) Obtain coefficient matrices for the linearized system:

$$A(\bar{t}) \in R^{n\times n}, B(\bar{t}) \in R^{n\times m}, \mathbf{e}(\bar{t}) \in R^n, \mathbf{c}(\bar{t}) \in R^m \quad \text{for} \quad \bar{t}_0 \le \bar{t} \le \bar{t}_f^o$$

$$\Delta\mathbf{y_s^o} = C_f\mathbf{x}^o(t_f^o) - \bar{\mathbf{y}}_\mathbf{s} \tag{7.11}$$

$$\mathbf{d}_f = C_f\dot{\bar{\mathbf{x}}}^o(\bar{t}_f^o) = C_f\mathbf{f}(\bar{\mathbf{x}}^o(\bar{t}_f^o), \bar{\mathbf{u}}^o(\bar{t}_f^o), t_f^o, \bar{\mathbf{W}}_{model}) \tag{7.12}$$

5.2.b) Solve for the following informational matrices through backward integration

$$S(\bar{t}) \in R^{n\times n}, \lambda_B(\bar{t}) \in R^n, G(\bar{t}) \in R^{n\times q}, V(\bar{t}) \in R^{q\times q}, \psi_B(\bar{t}) \in R^q$$

$$\dot{S} = -A^TS - SA + SBRB^TS - Q^{-1}, \quad S(t_f^o) = 0 \tag{7.13}$$

$$\dot{\lambda}_B = (SBRB^T - A^T)\lambda_B + SBR\mathbf{c} - \mathbf{e}, \quad \lambda_B(t_f^o) = 0 \tag{7.14}$$

$$\dot{G} = (SBRB^T - A^T)G, \quad G(t_f^o) = C_f^T \tag{7.15}$$

$$\dot{V} = G^TBRB^TG, \quad V(t_f^o) = -\frac{1}{q_f}\mathbf{d_f}\mathbf{d_f}^T \tag{7.16}$$

$$\dot{\psi}_B = G^TBRB^T\lambda_B + G^TBR\mathbf{c}, \quad \psi_B(t_f^o) = -\frac{p_f}{q_f}\mathbf{d_f} + \alpha_T\Delta\mathbf{y_s^o} \tag{7.17}$$

5.2.c) Compute the following coefficient matrices that are used in calculating control improvement

$$K_d(\bar{t}) \in R^{m\times n}, N_d(\bar{t}) \in R^{n\times q}, \mathbf{w_f} \in R^n$$

$$K_d(\bar{t}) = R(\bar{t})B(\bar{t})^T S(\bar{t}) \tag{7.18}$$

$$N_d(\bar{t}) = R(\bar{t})B(\bar{t})^T G(\bar{t}) \tag{7.19}$$

$$\mathbf{w_f}(\bar{t}) = R(\bar{t})B(\bar{t})^T \lambda_B(\bar{t}) + R(\bar{t})\mathbf{c}(\bar{t}) \tag{7.20}$$

5.2.d) Solve for ν

$$\nu = -V^{-1}(\bar{t}_0)\psi_B(\bar{t}_0) \tag{7.21}$$

5.2.e) Solve for τ_f

$$\tau_f = -\frac{1}{q_f}(p_f + \nu^T \mathbf{d_f}) \tag{7.22}$$

5.2.f) Solve for $\mathbf{z}(\bar{t})$ by forward integration

$$\dot{\mathbf{z}} = (A - BK_d)\mathbf{z} - BN_d\nu - B\mathbf{w_f}, \quad \mathbf{z}(\bar{t}_0) = 0 \tag{7.23}$$

5.2.g) Solve for $\mathbf{w}(\bar{t})$

$$\mathbf{w} = -K_d\mathbf{z} - N_d\nu - \mathbf{w_f} \tag{7.24}$$

5.3) Check for convergence

Define

$$||\mathbf{z}|| \triangleq \sqrt{\int_{\bar{t}_0}^{\bar{t}_f^o} \mathbf{z}(\bar{t})^T\mathbf{z}(\bar{t})dt} \tag{7.25}$$

$$||\mathbf{w}|| \triangleq \sqrt{\int_{\bar{t}_0}^{\bar{t}_f^o} \mathbf{w}(\bar{t})^T\mathbf{w}(\bar{t})dt} \tag{7.26}$$

If all of the following conditions are satisfied, proceed to Step 5.9). Otherwise, continue to Step 5.4.

$$|\tau_f| \leq \epsilon_\tau, \quad ||\mathbf{z}|| \leq \epsilon_{\mathbf{z}}, \quad ||\mathbf{w}|| \leq \epsilon_{\mathbf{w}} \tag{7.27}$$

5.4) Define the maximum step-size for this cycle.

Calculate $||\bar{\mathbf{u}}^o||$,

$$||\bar{\mathbf{u}}^o|| \triangleq \sqrt{\int_{\bar{t}_0}^{\bar{t}_f^o} \bar{\mathbf{u}}^o(\bar{t})^T \bar{\mathbf{u}}^o(\bar{t}) dt} \tag{7.28}$$

The maximum step-size in the final time update is determined from

$$\alpha_{tm} = \min\left(\frac{\eta_t \bar{t}_f^o}{|\tau_f|}, \ \alpha_{t,\max}\right) \tag{7.29}$$

The maximum step-size in the control update is determined from

$$\alpha_{um} = \min\left(\frac{\eta_u ||\bar{\mathbf{u}}^o||}{||\mathbf{w}||}, \ \alpha_{u,\max}\right) \tag{7.30}$$

5.5) Record the current reference final time and current reference control

$$\bar{t}_{f_{old}} = \bar{t}_f^o, \quad \bar{\mathbf{u}}_{old} = \bar{\mathbf{u}}^o \tag{7.31}$$

5.6) Update final time

Obtain the new reference final time

$$\bar{t}_f^o = \bar{t}_{f_{old}} + \alpha_{tm}\tau_f \tag{7.32}$$

Check the updated $\bar{t}_f^o$. If $\bar{t}_f^o > \bar{t}_{f,\max}$ or $\bar{t}_f^o < \bar{t}_{f,\min}$, reduce α_{tm} by half and repeat calculating $\bar{t}_f^o$ until final time constraints are satisfied, i.e. $\bar{t}_{f,\min} \leq \bar{t}_f^o \leq \bar{t}_{f,\max}$.

5.7) Update control history

Obtain a temporary reference control as

$$\bar{\mathbf{u}}^{temp}(\bar{t}) = \bar{\mathbf{u}}_{old}(\bar{t}) + \alpha_{um}\mathbf{w}(\bar{t}) \tag{7.33}$$

If $\bar{t}_f^o <= \bar{t}_{f_{old}}$, then interpolate $\bar{\mathbf{u}}^{temp}(\bar{t})$ over the interval of $[\bar{t}_0, \bar{t}_f^o]$.

If $\bar{t}_f^o > \bar{t}_{f_{old}}$, extend the control history to the interval of $[\bar{t}_{f_{old}}, \bar{t}_f^o]$ by extrapolation of $\mathbf{u}^{temp}(\bar{t})$ using polynomials. A time step is defined as $\Delta\bar{t} \triangleq (\bar{t}_{f_{old}} - \bar{t}_0)/N_t$. If $\bar{t}_f^o - \bar{t}_{f_{old}} \leq \Delta\bar{t}$, use linear extrapolation. If $\Delta\bar{t} < \bar{t}_f^o - \bar{t}_{f_{old}} \leq 2\Delta\bar{t}$, use quadratic extrapolation. Otherwise, use a third-order polynomial extrapolation.

Limit the updated $\bar{\mathbf{u}}^{temp}(\bar{t})$ within the upper bound and lower bound of the control vector, thus

$$\bar{\mathbf{u}}^o(\bar{t}_k) = \begin{cases} \mathbf{U}_{\max} & \text{if} \quad \bar{\mathbf{u}}^{temp}(\bar{t}_k) > U_{\max} \\ \mathbf{U}_{\min} & \text{if} \quad \bar{\mathbf{u}}^{temp}(\bar{t}_k) < U_{\min} \\ \bar{\mathbf{u}}^{temp}(\bar{t}_k) & \text{else} \end{cases} \tag{7.34}$$

where $\bar{t}_k$ is any given time instance in $[\bar{t}_0, \bar{t}_f^o]$.

5.8) Further limit the final time and control by updating state history

Integrate the nonlinear systems equation using the updated controls and final time. For $\bar{t} \in [\bar{t}_0, \bar{t}_f^o]$, integrate

$$\dot{\bar{\mathbf{x}}}^{temp} = \mathbf{f}(\bar{\mathbf{x}}^{temp}, \bar{\mathbf{u}}^o, \bar{t}; \mathbf{W}_{model}), \quad \bar{\mathbf{x}}^{temp}(\bar{t}_0) = \bar{\mathbf{x}}_0 \tag{7.35}$$

If any path constraint is violated, reduce α_{um} by half and repeat the process by going back to (5.7).

Once $\bar{\mathbf{x}}^{temp}(\bar{t})$ satisfies all the path constraints for $\bar{t}_0 \leq \bar{t} \leq \bar{t}_f^o$, set

$$\bar{\mathbf{x}}^o(\bar{t}) = \bar{\mathbf{x}}^{temp}(\bar{t}) \tag{7.36}$$

.

5.9) Set $i = i + 1$.

If $i < N_{i,\max}$, go back to step (5.2) to continue improving the reference trajectory. Otherwise, proceed to Step 5.10).

5.10) Update state history

Set new initial state

$$\bar{\mathbf{x}}_0^{new} = \bar{\mathbf{x}}^o(\bar{t}_f^o) \tag{7.37}$$

Simulate the UAV flight by integrating the following equations for $\bar{t} \in [\bar{t}_0, \bar{t}_f^o]$

$$\dot{\bar{\mathbf{x}}} = \mathbf{f}(\bar{\mathbf{x}}, \bar{\mathbf{u}}^o, \bar{t}; \mathbf{W}_{model}), \quad \bar{\mathbf{x}}(\bar{t}_0) = \bar{\mathbf{x}}_0^{new} \tag{7.38}$$

Set the integration results of $\bar{\mathbf{x}}(\bar{t})$ as the new reference states

$$\bar{\mathbf{x}}^o(\bar{t}) = \bar{\mathbf{x}}(\bar{t}) \tag{7.39}$$

Step 6. Track the updated optimal trajectory in real wind field

Calculate controls to track the new reference states $\bar{\mathbf{x}}^o(\bar{t})$ based on the equations of motion below:

$$\dot{\bar{\mathbf{x}}} = \mathbf{f}(\bar{\mathbf{x}}, \bar{\mathbf{u}}, \bar{t}; \mathbf{W}_{real}), \quad \bar{\mathbf{x}}(\bar{t}_0) = \bar{\mathbf{x}}_0^{new} \tag{7.40}$$

Go to Step 3. Repeat the process.

7.3 A Model of UAV Trajectory Feedback Control

Recall the solution framework presented in Chapter 2, a feedback control module is required for a UAV to track the generated fuel-efficient trajectory for each flight cycle. In this thesis, feedback linearization method is used to generate feedback control. The relevant derivation is presented in Appendix C. Below is a detailed procedure of feedback control generation used in simulations.

1 . Specify normalized time steps $0 = t_1 < t_2 < ... < t_{N-1} < t_N = t_{f_d}$.

Denote $(\ \ )_k \triangleq (\ \ )(t_k)$ for $k = 1, 2, ..., N$.

At each time step t_k, specify parameters of the desired trajectory $[\bar{x}_{d,k}, \bar{y}_{d,k}, \bar{h}_{d,k}]^T$, $[\bar{x}'_{d,k}, \bar{y}'_{d,k}, \bar{h}'_{d,k}]^T$, and $[\bar{x}''_{d,k}, \bar{y}''_{d,k}, \bar{h}''_{d,k}]^T$.

2 . Get current state $\bar{V}_k$, ψ_k, γ_k, $\bar{x}_k$, $\bar{y}_k$, $\bar{h}_k$.

3 . Get wind velocity components

$$\bar{W}_{x,k} \triangleq \bar{W}_x(t_k, \bar{x}_k, \bar{y}_k, \bar{h}_k) \tag{7.41}$$

$$\bar{W}_{y,k} \triangleq \bar{W}_y(t_k, \bar{x}_k, \bar{y}_k, \bar{h}_k) \tag{7.42}$$

$$\bar{W}_{h,k} \triangleq \bar{W}_h(t_k, \bar{x}_k, \bar{y}_k, \bar{h}_k) \tag{7.43}$$

and wind derivatives

$$\bar{W}'_{x,k} = \frac{\partial \bar{W}_x}{\partial t_k} + \frac{\partial \bar{W}_x}{\partial \bar{x}_k}\bar{x}'_k + \frac{\partial \bar{W}_x}{\partial \bar{y}_k}\bar{y}'_k + \frac{\partial \bar{W}_x}{\partial \bar{h}_k}\bar{h}'_k \tag{7.44}$$

$$\bar{W}'_{y,k} = \frac{\partial \bar{W}_y}{\partial t_k} + \frac{\partial \bar{W}_y}{\partial \bar{x}_k}\bar{x}'_k + \frac{\partial \bar{W}_y}{\partial \bar{y}_k}\bar{y}'_k + \frac{\partial \bar{W}_y}{\partial \bar{h}_k}\bar{h}'_k \tag{7.45}$$

$$\bar{W}'_{h,k} = \frac{\partial \bar{W}_h}{\partial t_k} + \frac{\partial \bar{W}_h}{\partial \bar{x}_k}\bar{x}'_k + \frac{\partial \bar{W}_h}{\partial \bar{y}_k}\bar{y}'_k + \frac{\partial \bar{W}_h}{\partial \bar{h}_k}\bar{h}'_k \tag{7.46}$$

$$\bar{W}'_{V,k} = \bar{W}'_{x,k}\cos\gamma_k \sin\psi_k + \bar{W}'_{y,k}\cos\gamma_k \cos\psi_k + \bar{W}'_{h,k}\sin\gamma_k \tag{7.47}$$

$$\bar{W}'_{\psi,k} = \bar{W}'_{x,k}\cos\psi_k - \bar{W}'_{y,k}\sin\psi_k \tag{7.48}$$

$$\bar{W}'_{\gamma,k} = \bar{W}'_{x,k}\sin\gamma_k \sin\psi_k + \bar{W}'_{y,k}\sin\gamma_k \cos\psi_k - \bar{W}'_{h,k}\cos\gamma_k \tag{7.49}$$

4 . Calculate

$$\bar{x}'_k = \bar{V}_k \cos\gamma_k \sin\psi_k + \bar{W}_{x,k} \tag{7.50}$$

$$\bar{y}'_k = \bar{V}_k \cos\gamma_k \cos\psi_k + \bar{W}_{y,k} \tag{7.51}$$

$$\bar{h}'_k = \bar{V}_k \sin\gamma_k + \bar{W}_{h,k} \tag{7.52}$$

5 . Define parameters of the tracking error dynamics ξ_x, ω_x, ξ_y, ω_y, ξ_h, and ω_h.

Calculate

$$\bar{x}''_k = \bar{x}''_{d,k} + 2\xi_x\omega_x(\bar{x}'_{d,k} - \bar{x}'_k) + \omega_x^2(\bar{x}_{d,k} - \bar{x}_k) \tag{7.53}$$

$$\bar{y}''_k = \bar{y}''_{d,k} + 2\xi_y\omega_y(\bar{y}'_{d,k} - \bar{y}'_k) + \omega_y^2(\bar{y}_{d,k} - \bar{y}_k) \tag{7.54}$$

$$\bar{h}''_k = \bar{h}''_{d,k} + 2\xi_h\omega_h(\bar{h}'_{d,k} - \bar{h}'_k) + \omega_h^2(\bar{h}_{d,k} - \bar{h}_k) \tag{7.55}$$

6 . Solve for $\bar{V}'_k$, ψ'_k, and γ'_k in the following equations:

$$\begin{bmatrix} \cos\gamma_k \sin\psi_k & \bar{V}_k \cos\gamma_k \cos\psi_k & -\bar{V}_k \sin\gamma_k \sin\psi_k \\ \cos\gamma_k \cos\psi_k & -\bar{V}_k \cos\gamma_k \sin\psi_k & -\bar{V}_k \sin\gamma_k \cos\psi_k \\ \sin\gamma_k & 0 & \bar{V}_k \cos\gamma_k \end{bmatrix} \begin{bmatrix} \bar{V}'_k \\ \psi'_k \\ \gamma'_k \end{bmatrix} =$$

$$= \begin{bmatrix} \bar{x}''_k - \bar{W}'_{x,k} \\ \bar{y}''_k - \bar{W}'_{y,k} \\ \bar{h}''_k - \bar{W}'_{h,k} \end{bmatrix} \tag{7.56}$$

7 . Calculate

$$a_{1,k} = -k_a \bar{\rho} \bar{V}_k^2 K \tag{7.57}$$

$$b_{1,k} = -k_a \bar{\rho} \bar{V}_k^2 C_{D_0} - \sin\gamma_k - \bar{W}'_{V,k} \tag{7.58}$$

$$a_{2,k} = k_a \bar{\rho} \bar{V}_k \frac{1}{\cos\gamma_k} \tag{7.59}$$

$$b_{2,k} = -\frac{1}{\bar{V}_k \cos\gamma_k} \bar{W}'_{\psi,k} \tag{7.60}$$

$$a_{3,k} = k_a \bar{\rho} \bar{V}_k \tag{7.61}$$

$$b_{3,k} = -\frac{1}{\bar{V}_k} \cos\gamma_k + \frac{1}{\bar{V}_k} \bar{W}'_{\gamma,k} \tag{7.62}$$

Then

$$\mu_k = \tan^{-1}\left(\frac{a_{3,k}(\psi'_k - b_{2,k})}{a_{2,k}(\gamma'_k - b_{3,k})}\right) \tag{7.63}$$

$$C_{L_k} = \sqrt{(\frac{\psi'_k - b_{2,k}}{a_{2,k}})^2 + (\frac{\gamma'_k - b_{3,k}}{a_{3,k}})^2} \tag{7.64}$$

$$\bar{T}_k = \bar{V}'_k - a_{1,k} C_{L_k}^2 - b_{1,k} \tag{7.65}$$

8 . Integrate the normalized equations of motion with wind measurements and calculated control over time interval $t \in [t_k, t_{k+1}]$ to get states at time t_{k+1}.

$$\bar{V}' = \bar{T}_k - k_a \bar{\rho} \bar{V}_k^2 (C_{D_0} + K C_{L_k}^2) - \sin\gamma_k - \bar{W}'_{V,k} \tag{7.66}$$

$$\psi' = k_a \bar{\rho} \bar{V}_k C_{L_k} \frac{\sin\mu_k}{\cos\gamma_k} - \frac{1}{\bar{V}_k \cos\gamma_k} \bar{W}'_{\psi,k} \tag{7.67}$$

$$\gamma' = k_a \bar{\rho} \bar{V}_k C_{L_k} \cos\mu_k - \frac{1}{\bar{V}_k} \cos\gamma_k + \frac{1}{\bar{V}_k} \bar{W}'_{\gamma,k} \tag{7.68}$$

$$\bar{x}' = \bar{V}_k \cos\gamma_k \sin\psi_k + \bar{W}_{x,k} \tag{7.69}$$

$$\bar{y}' = \bar{V}_k \cos\gamma_k \cos\psi_k + \bar{W}_{y,k} \tag{7.70}$$

$$\bar{h}' = \bar{V}_k \sin\gamma_k + \bar{W}_{h,k} \tag{7.71}$$

7.4 Evaluation Criteria

The benefit of the optimized trajectories may be measured by a Fuel Savings Index, defined as the percentage savings of approximate fuel consumption of the optimized trajectory compared with that of a regular trajectory without wind utilization.

For a jet-engined UAV, the fuel consumption can be approximated by the average thrust over a number of flight cycles.

$$I_{fuel} \triangleq \frac{1}{N} \sum_{i=1}^{N} \int_{t_{0_i}}^{t_{f_i}} T dt \tag{7.72}$$

where N is the number of flight cycles, T is the thrust.

For a propeller-driven UAV, the fuel consumption can be approximated by the average power over a number of flight cycles.

$$I_{fuel} \triangleq \frac{1}{N} \sum_{i=1}^{N} \int_{t_{0_i}}^{t_{f_i}} TV dt \tag{7.73}$$

where V is the true airspeed.

The fuel saving index is defined as follows:

$$Q \triangleq \frac{I^n_{fuel} - I^o_{fuel}}{I^n_{fuel}} \tag{7.74}$$

where I^n_{fuel} is the approximate fuel consumption of a regular trajectory without wind utilization and I^o_{fuel} is the approximate average fuel consumption of a number of optimized trajectories under the same wind condition.

Chapter 8

Results

8.1 UAV Model Parameters

This research studies the utilization of wind energy in trajectory planning for a generic UAV model, as illustrated by Figure 8.1 below.

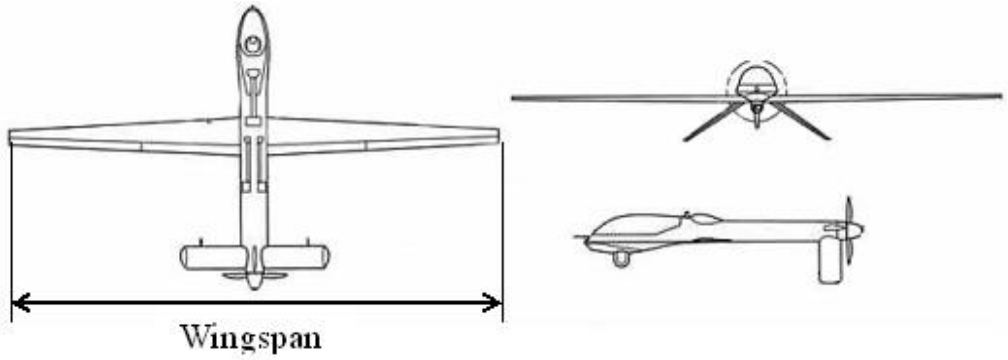

Figure 8.1 A UAV Model

Table 8.1 lists the dimensions, dynamics specifications, and performance capabilities of two UAV models: RQ-11B RavenB and ScanEagle. RQ-11B Raven is a remote-controlled miniature unmanned aerial vehicle used in military applications. ScanEagle is an economical, long endurance unmanned aircraft and can be an enabler of network centric warfare. ScanEagle is designed to track an object of interest for extended periods of time. It is ideal for

missions such as surveillance and reconnaissance, search and rescue, geomagnetic and atmospheric surveys, coastal patrol, terrain mapping, and weather forecasting.

	RQ-11B RavenB	ScanEagle
Length [ft]	3.6	3.9
Wing Span [ft]	4.25	10.2
Gross Weight [lb]	4.2	37.9
Cruise Speed [ft/s]	88	82

Table 8.1 Sample UAV Model Specifications and Performance Parameters

By synthesizing the varieties in UAV dimensions, performance capabilities, and dynamics parameters, we choose to study the significant parameters in the representative ranges as listed in the table below. Note that due to the difficulties of obtaining all the performance data, missing data are estimated based on photos and other available information. As a result, the parameters used in the studies are representative of the two UAV models discussed above, but may no have the exact values.

mg/S [lbf/ft^2]	2, 4, 6
C_{D0}	0.02, 0.025, 0.03
$E_{\max}$	20, 25, 30

Table 8.2 Ranges of UAV Model Parameters

8.2 Overview of Cases Studied

For all simulation cases in this thesis, a linear gradient model is used to

estimate the real wind field:

$$W_x = \frac{W_0}{H_0} h \sin \psi_w \tag{8.1}$$

$$W_y = \frac{W_0}{H_0} h \cos \psi_w \tag{8.2}$$

$$W_h = 0 \tag{8.3}$$

where $H_0 = 2000$ ft is assumed to be a constant atmospheric parameter. W_0 and ψ_w are the parameters to be estimated. The real wind field is simulated using various models as discussed further in the following sections.

Algorithm parameters are chosen as $Q = I_3$, $R = 10I_6$, $q_f = 1000$, $\alpha_{Term} = 0.8$, Max Update Iterations = 20, and Max Flight Intervals = 10.

Variations of the following parameters are considered:

1. UAV Specifications: wing loading mg/S, profile drag coefficient C_{D_0}, and maximum lift-to-drag ratio $E_{\max}$
2. Wind intensity: maximum wind speed at transition altitude W_0
3. Wind speed estimation error: e_w
4. Rate of change of wind speed: c_w
5. Rate of change of wind model gradient coefficient: A_1

By varying the above parameters, simulation cases are categorized into the following four groups:

1 . Potentials of fuel saving with perfect model structure where there are no estimation errors. Impacts on fuel savings from wind wind speed and UAV

dynamics specifications are also studied.

2 . Effects of measurement errors: perfect wind model structure with errors in wind speed estimations.

3 . Effects of actual wind changes over time.

4 . Effects of wind model structure errors.

8.3 A Nominal Case

This section demonstrates a nominal case of fuel efficient trajectory generated by the successive improvement solution strategy.

The actual wind field is simulated by a linear gradient wind model shown in Eq. (8.1)- (8.3) with $W_0 = 80$ ft/s and $\psi_w = 0$. The following dimension and performance specifications for a propeller-driven UAV are used:

$$mg/S = 4 \text{ lb/ft}^2, \quad C_{D_0} = 0.02, \quad E_{\max} = 20 \tag{8.4}$$

Figure 8.2 shows the initial nominal loiter trajectory before the successive improvement algorithm was applied.

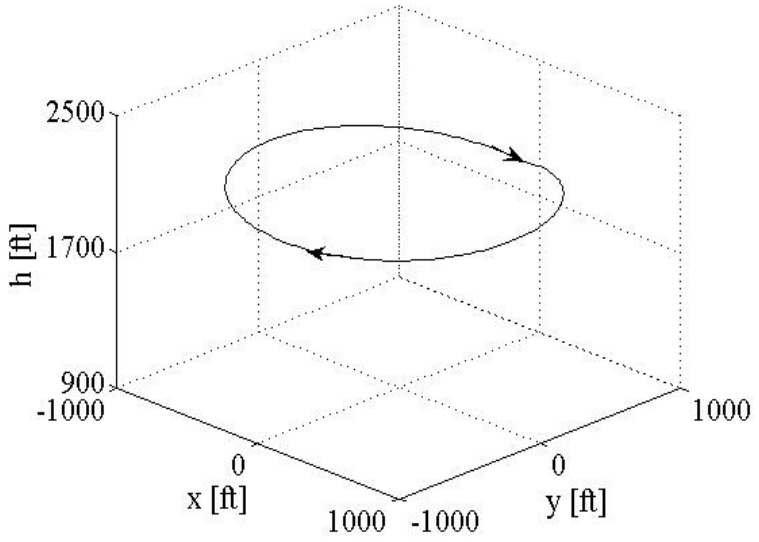

Figure 8.2 A Nominal Loiter Trajectory in 3-D, $W_0 = 80$ ft/s, $mg/S = 4$ lb/ft^2, $C_{D_0} = 0.02$, and $E_{\max} = 20$

Figure 8.3 - 8.5 demonstrate the state and control histories of the optimized trajectory compared to those of the initial nominal trajectory, as well as the three-dimensional trajectories in space.

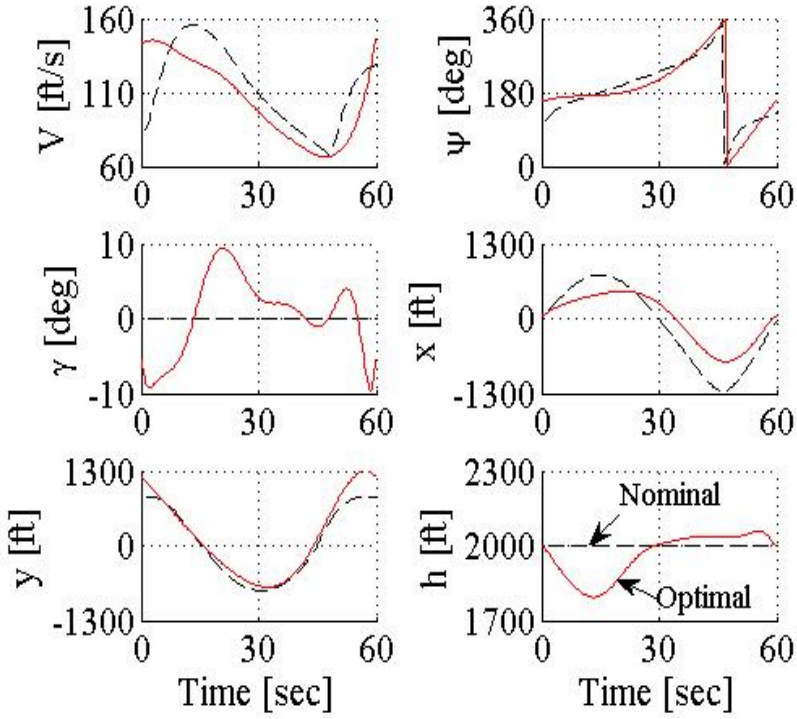

Figure 8.3 State Histories, $W_0 = 80$ ft/s, $mg/S = 4$ lb/ft^2, $C_{D_0} = 0.02$, and $E_{\max} = 20$

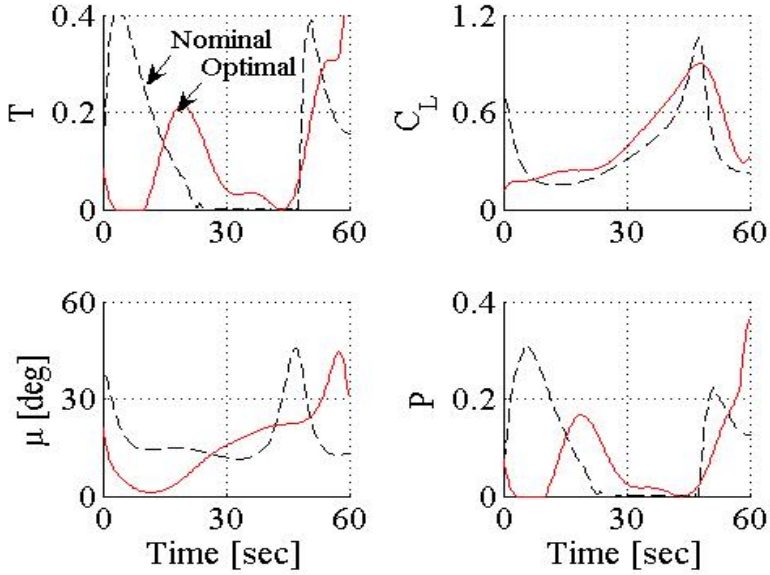

Figure 8.4 Control Histories, $W_0 = 80$ ft/s, $mg/S = 4$ lb/ft^2, $C_{D_0} = 0.02$, and $E_{\max} = 20$

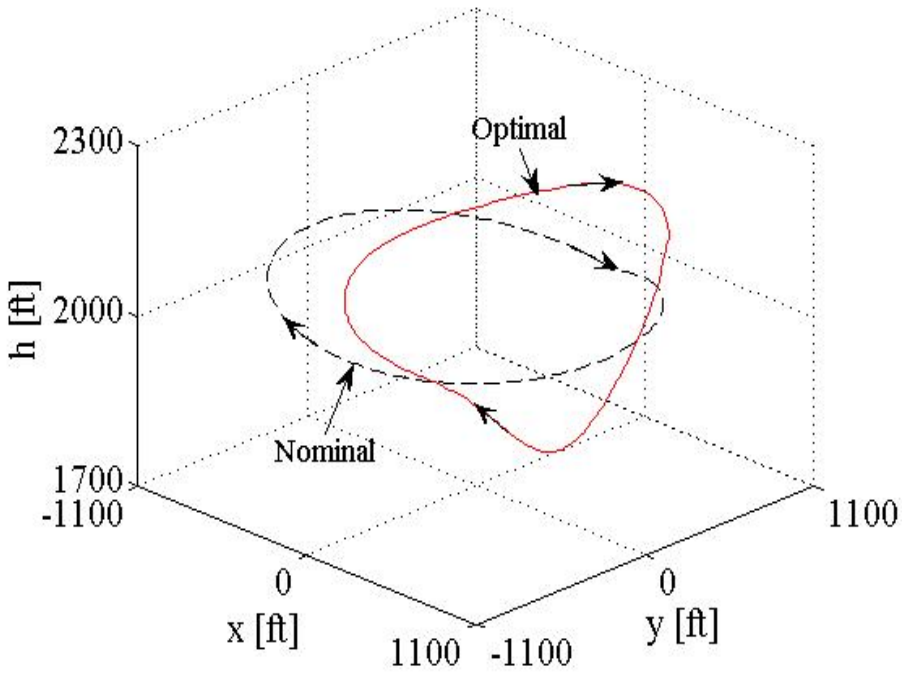

Figure 8.5 3-D Trajectories, $W_0 = 80$ ft/s, $mg/S = 4$ lb/ft^2, $C_{D_0} = 0.02$, and $E_{\max} = 20$

The estimated fuel savings of the improved trajectory compared to the initial nominal trajectory is 27%.

8.4 Effects of Wind Speed with Perfect Wind Model

It is first assumed that the selected wind model matches the actual wind field perfectly, with only model parameters to be determined in optimization cycles. The purpose of this study is to establish the potentials of fuel saving

of the proposed strategy.

The following dimension and performance specifications for a propeller-driven UAV are used:

$$mg/S = 4 \text{ lb/ft}^2, \quad C_{D_0} = 0.02, \quad E_{\max} = 20 \tag{8.5}$$

Figure 8.6 shows that as the fuel benefit of the optimized trajectories increases as wind speed increases.

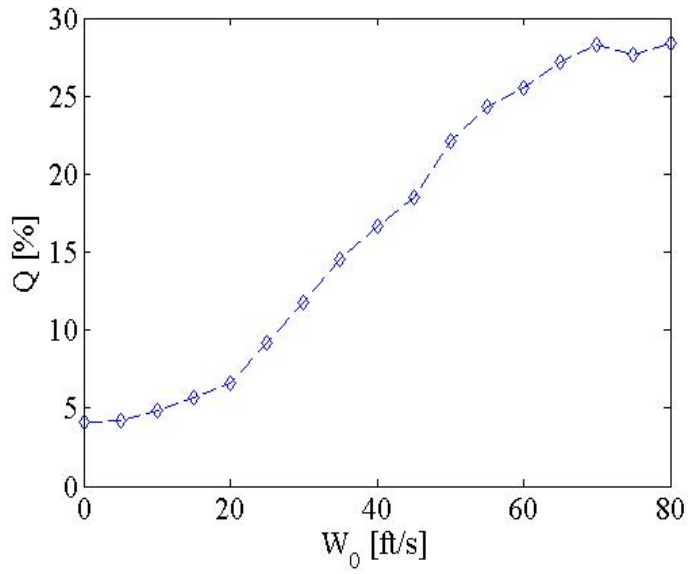

Figure 8.6 Fuel Improvement vs. Wind Speed

8.4.1 Fuel Savings vs. Wing Loading

This section examines the change in fuel savings with respect to the wing loading value of a UAV while other specifications are fixed: $C_{D_0} = 0.02$ and $E_{\max} = 20$. Two different values of wing loading are considered: $mg/S = 2$ lb/ft^2 and $mg/S = 4$ lb/ft^2. Results indicate that in the same wind field,

UAVs with lower wing loading values can achieve higher fuel savings.

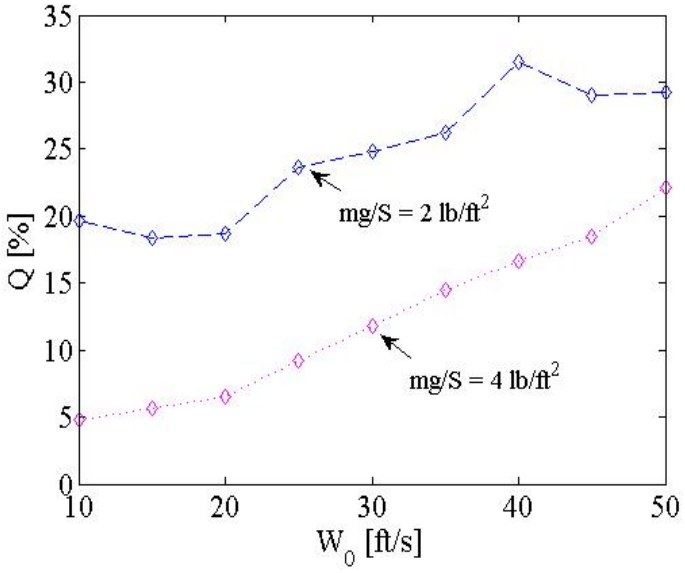

Figure 8.7 Fuel Improvement vs. Wing Loading

8.4.2 Fuel Savings vs. C_{D_0}

This section examines the change in fuel savings with respect to the profile drag coefficient values while other specifications are fixed: $mg/S = 4$ lb/ft^2 and $E_{\max} = 20$. Two different values of profile drag coefficient are considered: $C_{D_0} = 0.02$ and $C_{D_0} = 0.025$. The figure below shows that as in a given wind field, the profile drag coefficient increases, the fuel savings increases.

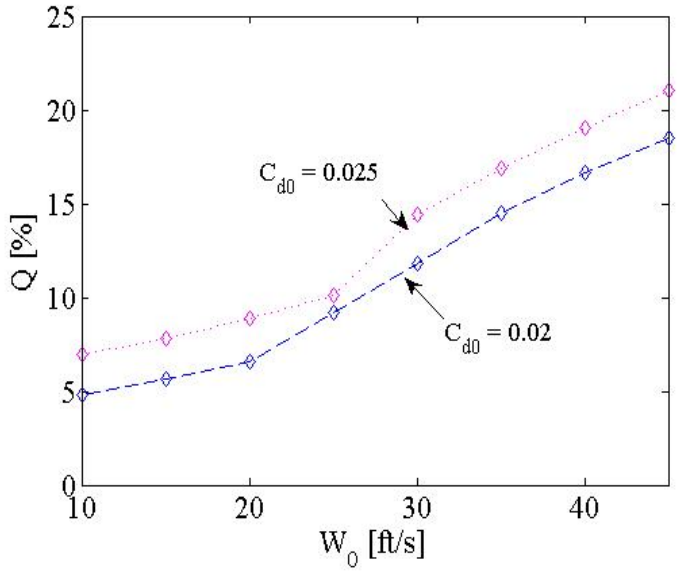

Figure 8.8 Fuel Improvement vs. Profile Drag Coefficient

8.4.3 Fuel Savings vs. $E_{\max}$

This section examines the change in fuel savings with respect to the maximum lift-to-drag ratios while other specifications are fixed: $mg/S = 4$ lb/ft^2 and $C_{D_0} = 0.02$. Three different values of maximum drag-to-lift ratio are considered: $E_{\max} = 20$, $E_{\max} = 25$, and $E_{\max} = 30$. Figure below illustrates the fuel saving differences for UAVs with different $E_{\max}$ values. Higher $E_{\max}$ yields higher fuel savings in generated fuel-efficient trajectories.

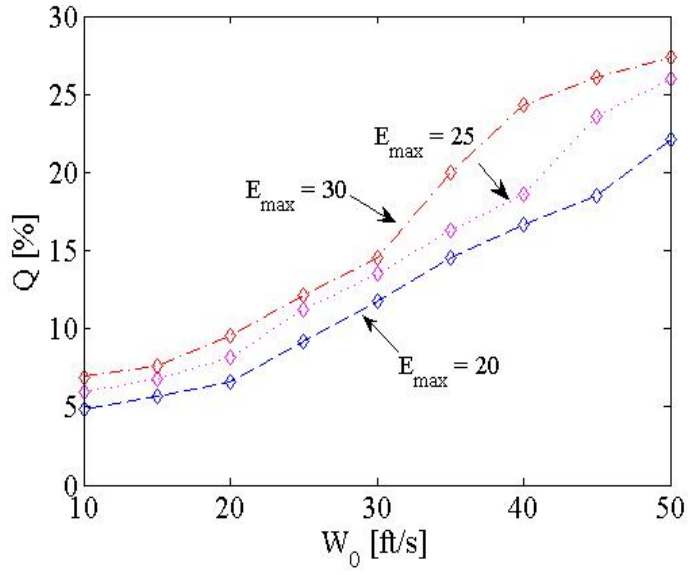

Figure 8.9 Fuel Improvement vs. Maximum Lift-to-Drag Ratio

8.5 Perfect Wind Model Structure with Parameters Errors

In this section, it is assumed that wind model used in trajectory planning captures the structure of the real wind field, but there are discrepancies between the estimated wind speed with that of the real wind field. The purpose of this study is to examine the effects of wind estimation error on fuel savings.

The following reference values of UAV specifications are used

$$mg/S = 4, \quad C_{D_0} = 0.02, \quad E_{\max} = 20 \tag{8.6}$$

8.5.1 Constant Parameter Errors

Simulate the real wind field using a linear model below:

$$W_x = \frac{\hat{W}_0}{H_0} h \sin \psi_w \tag{8.7}$$

$$W_y = \frac{\hat{W}_0}{H_0} h \cos \psi_w \tag{8.8}$$

$$W_h = 0 \tag{8.9}$$

where

$$\hat{W}_0 = W_0 + e_w \tag{8.10}$$

W_0 and ψ_w are the parameters of the wind model used in generating fuel-efficient trajectories. e_w represents the constant error in wind speed estimation compared to the real wind speed.

Figure below depicts the change in fuel saving Q with respect to wind speed with different wind speed estimation error e_w. At the same wind speed, larger wind speed estimation error gives less fuel savings.

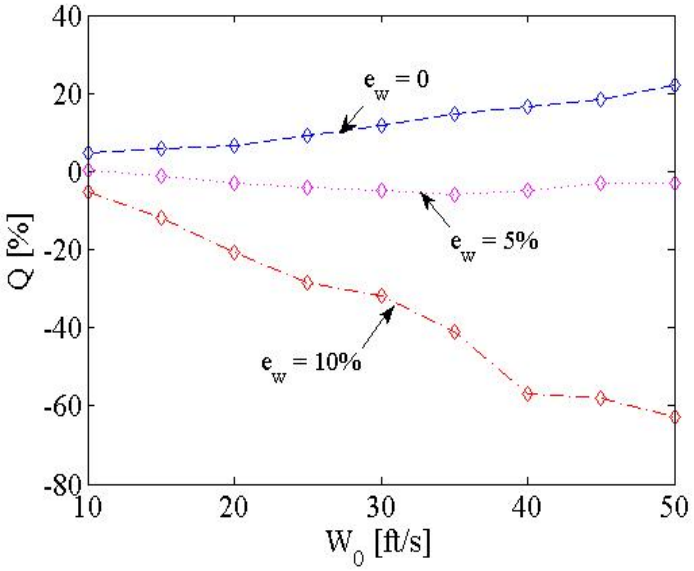

Figure 8.10 Fuel Improvement vs. Wind Speed Estimation Error

8.5.2 Time-Varying Parameter Errors

Time-varying errors between the estimated wind speed with the real wind speed is assumed. In other words, stationary wind model is used to approximate a time-varying real wind field:

$$\hat{W}_0 = W_0 + c_w t \tag{8.11}$$

where W_0 is the real wind speed and $\hat{W}_0$ is the wind speed estimation. The coefficient c_w depicts how fast the real wind field may change in intensity.

The flight cycle time of the nominal trajectory studied in this simulation is $t_f = 60$ seconds and the real wind speed is $W_0 = 50$ ft/s, thus the range of the rate of change c_w is selected to be $[0,\ 0.2]$ so that

$$0 \leq \frac{c_w t_f}{W_0} < 20\% \tag{8.12}$$

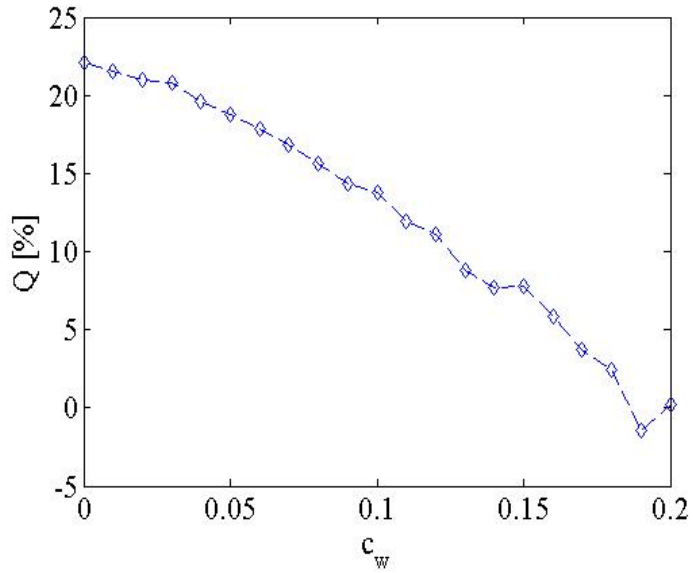

Figure 8.11 Fuel Improvement vs. Rate of Change of Wind Speed

Figure above shows the fuel saving Q with respect to the rate of change of the real wind speed. As the rate of change of real wind speed increases, the fuel savings decreases, i.e. if the real wind field changes so fast that the wind model cannot capture the wind properties timely, then the generated trajectory may not yield much fuel savings.

8.6 Wind Model with Imperfect Structure

In this section, it is assumed that the structure of the wind model does not match the structure of the real wind field. In other words, a linear wind model is used to approximate a nonlinear real wind field. The objective is to study the effects of wind model structure on fuel savings.

In this scenario, the real wind is simulated by the following nonlinear model:

$$W_x = \frac{W_0}{H_0}(A_w h + \frac{1 - A_w}{H_0} h^2) \sin \psi_w \tag{8.13}$$

$$W_y = \frac{W_0}{H_0}(A_w h + \frac{1 - A_w}{H_0} h^2) \cos \psi_w \tag{8.14}$$

$$W_h = 0 \tag{8.15}$$

where

$$A_w = 1 + A_1 t \tag{8.16}$$

In the above expression of A_w, if $A_1 = 0$, then the linear wind model matches the structure of the real wind field, otherwise, the real wind field has a nonlinear structure and time-varying.

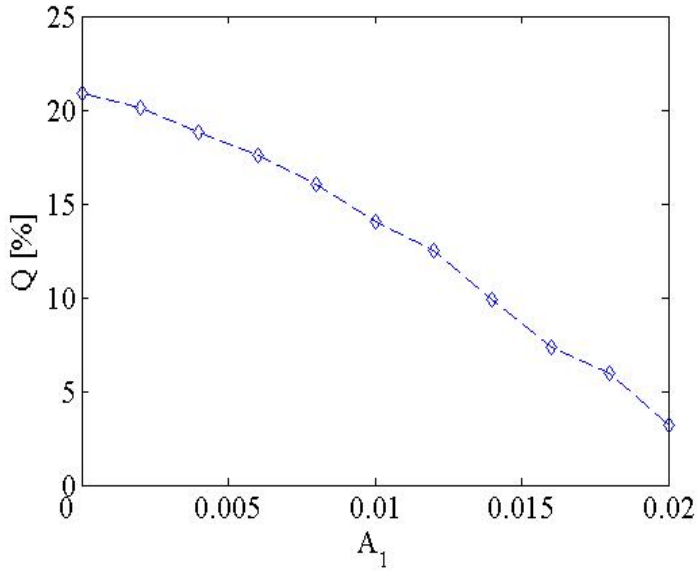

Figure 8.12 Fuel Improvement vs. Rate of Change of Wind Gradient Coefficient

Simulation results show that the fuel improvement decreases as A_1 increases, which indicates that the discrepancy between structures of the real wind field and wind model impacts potential fuel savings negatively.

Chapter 9

Conclusions and Future Work

9.1 Conclusions

This research studies the problem of utilizing wind energies to generate fuel-efficient trajectories and thus enhance the flight performance for a UAV in loiter missions. A solution strategy is proposed that in a loiter flight, a UAV can measure the wind velocity components along its flight path, then use this information to improve its flight efficiency for the next cycle. A model-based approach is used to estimate wind model and use the estimated model in successive trajectory planning and optimization between flight cycles. The simulation results show that the proposed successive trajectory improvement strategy works well if wind model structure matches that of the real wind field. The fuel savings achieved using this strategy are also affected by various errors in wind model estimation and real wind field changes.

This thesis presents a useful framework for online wind energy utilization in practical flights. It also demonstrates a reliable linearized solution approach for solving nonlinear optimal control problems.

9.2 Future Work

To further explore the practical onboard wind energy utilization and to study the reliable solution method to a nonlinear optimal control problem, the following topics need to be further studied:

1. Methods to directly incorporate state and/or control inequality constraints in the linear quadratic solution algorithms, including expansion of the state transition method, or to solve a parameterized linear quadratic problem that can explicitly handle inequality constraints

2. Comparison of the solution trajectories generated using successive linearization trajectory improvement methods and the solutions of off-line nonlinear optimization results.

3. Study of the effects of algorithm parameters on the resultant trajectories and their fuel efficiencies. The key algorithm parameters include step size on control update α_u, step size on final time update α_t, weighting matrix on state variation Q, and weighting matrix on control variation R.

4. Exploration of utilizing different wind model structures such as nonlinear wind gradient model in successive trajectory planning and optimization.

Appendix A

Derivation of Wind Model Parameter Estimation

Here we assume H_0 is a pre-defined characteristic constant of the atmosphere. In order to estimate the wind model parameters W_0, A_w, and ψ_w, we need to solve the following optimization problem:

$$\begin{aligned}\min_{p_1,\, p_2,\, A_w} I &= \sum_{k=1}^{N} \left\{ \left[W_x(h_k) - \hat{W}_{x_k} \right]^2 + \left[W_y(h_k) - \hat{W}_{y_k} \right]^2 \right\} \\ &= \sum_{k=1}^{N} \left[p_1 z_0(h_k) + A_w p_1 z_1(h_k) - \hat{W}_{x_k} \right]^2 + \\ &\quad + \sum_{k=1}^{N} \left[p_2 z_0(h_k) + A_w p_2 z_1(h_k) - \hat{W}_{y_k} \right]^2 \end{aligned} \tag{A.1}$$

where $\hat{W}_{x_k}$ and $\hat{W}_{y_k}$ are the wind velocity components measured at position (x_k, y_k, h_k), $k = 1, 2, ..., N$, i.e.

$$\hat{W}_{x_k} \triangleq \hat{W}_x(x_k, y_k, h_k)$$

$$\hat{W}_{y_k} \triangleq \hat{W}_y(x_k, y_k, h_k)$$

Define

$$z_{0_k} \triangleq z_0(h_k), \quad z_{1_k} \triangleq z_1(h_k) \tag{A.2}$$

then (A.1) becomes

$$\min_{p_1,\, p_2,\, A_w} I = \sum_{k=1}^{N} \left\{ \left[z_{0_k} p_1 + z_{1_k} p_1 A_w - \hat{W}_{x_k} \right]^2 + \left[z_{0_k} p_2 + z_{1_k} p_2 A_w - \hat{W}_{y_k} \right]^2 \right\} \tag{A.3}$$

The necessary conditions for this optimization problem are

$$\frac{\partial I}{\partial p_1} = \sum_{k=1}^{N} 2(z_{0_k}p_1 + z_{1_k}p_1A_w - \hat{W}_{x_k})(z_{0_k} + z_{1_k}A_w) = 0 \qquad (A.4)$$

$$\frac{\partial I}{\partial p_2} = \sum_{k=1}^{N} 2(z_{0_k}p_2 + z_{1_k}p_2A_w - \hat{W}_{y_k})(z_{0_k} + z_{1_k}A_w) = 0 \qquad (A.5)$$

$$\begin{aligned}\frac{\partial I}{\partial A_w} = &\sum_{k=1}^{N} 2(z_{0_k}p_1 + z_{1_k}p_1A_w - \hat{W}_{x_k})z_{1_k}p_1 + \\ &+ \sum_{k=1}^{N} 2(z_{0_k}p_2 + z_{1_k}p_2A_w - \hat{W}_{y_k})z_{1_k}p_2 = 0\end{aligned} \qquad (A.6)$$

Solving for p_1 and p_2 in (A.4) and (A.5), respectively, we obtain

$$p_1 = \frac{\sum_{k=1}^{N} \hat{W}_{x_k}z_{0_k} + A_w \sum_{k=1}^{N} \hat{W}_{x_k}z_{1_k}}{\sum_{k=1}^{N} z_{0_k}^2 + A_w \sum_{k=1}^{N} 2z_{0_k}z_{1_k} + A_w^2 \sum_{k=1}^{N} z_{1_k}^2} \qquad (A.7)$$

$$p_2 = \frac{\sum_{k=1}^{N} \hat{W}_{y_k}z_{0_k} + A_w \sum_{k=1}^{N} \hat{W}_{y_k}z_{1_k}}{\sum_{k=1}^{N} z_{0_k}^2 + A_w \sum_{k=1}^{N} 2z_{0_k}z_{1_k} + A_w^2 \sum_{k=1}^{N} z_{1_k}^2} \qquad (A.8)$$

Define

$$a_0 \triangleq \sum_{k=1}^{N} z_{0_k}^2, \quad a_1 \triangleq \sum_{k=1}^{N} 2z_{0_k}z_{1_k}, \quad a_2 \triangleq \sum_{k=1}^{N} z_{1_k}^2 \qquad (A.9)$$

$$b_{0_x} \triangleq \sum_{k=1}^{N} \hat{W}_{x_k}z_{0_k}, \quad b_{1_x} \triangleq \sum_{k=1}^{N} \hat{W}_{x_k}z_{1_k} \quad b_{0_y} \triangleq \sum_{k=1}^{N} \hat{W}_{y_k}z_{0_k}, \quad b_{1_y} \triangleq \sum_{k=1}^{N} \hat{W}_{y_k}z_{1_k} \qquad (A.10)$$

Substituting (A.9) and (A.10) into (A.7) and (A.8), we get

$$p_1 = \frac{b_{0_x} + b_{1_x}A_w}{a_0 + a_1A_w + a_2A_w^2} \qquad (A.11)$$

$$p_2 = \frac{b_{0_y} + b_{1_y}A_w}{a_0 + a_1A_w + a_2A_w^2} \qquad (A.12)$$

then

$$p_1^2 + p_2^2 = \frac{c_0 + c_1 A_w + c_2 A_w^2}{(a_0 + a_1 A_w + a_2 A_w^2)^2} \tag{A.13}$$

where

$$c_0 \triangleq b_{0_x}^2 + b_{0_y}^2 \tag{A.14}$$

$$c_1 \triangleq 2(b_{0_x} b_{1_x} + b_{0_y} b_{1_y}) \tag{A.15}$$

$$c_2 \triangleq b_{1_x}^2 + b_{1_y}^2 \tag{A.16}$$

From (A.6), we get

$$(p_1^2 + p_2^2)\left(\sum_{k=1}^{N} z_{0_k} z_{1_k} + A_w \sum_{k=1}^{N} z_{1_k}^2\right) = p_1 \sum_{k=1}^{N} \hat{W}_{x_k} z_{1_k} + p_2 \sum_{k=1}^{N} \hat{W}_{y_k} z_{1_k} \tag{A.17}$$

Substituting (A.9), (A.10), and (A.13) into (A.17) and re-arrange terms for A_w, we get

$$A_w^2(c_2 a_1 - c_1 a_2) + 2A_w(c_2 a_0 - c_0 a_2) + (c_1 a_0 - c_0 a_1) = 0 \tag{A.18}$$

Define

$$B_0 = c_1 a_0 - c_0 a_1 \tag{A.19}$$

$$B_1 = c_2 a_0 - c_0 a_2 \tag{A.20}$$

$$B_2 = c_2 a_1 - c_1 a_2 \tag{A.21}$$

then (A.18) becomes

$$B_2 A_w^2 + 2B_1 A_w + B_0 = 0 \tag{A.22}$$

Solving for A_w in the above equation subject to the constraint $0 < A_w < 2$, we obtain

$$A_w = \begin{cases} \dfrac{-B_1 + \sqrt{B_1^2 - B_0 B_2}}{B_2} & \text{if } B2 > 0,\ -4(B_1 + B_2) \leq B_0 \leq 0 \\ \dfrac{-B_1 - \sqrt{B_1^2 - B_0 B_2}}{B_2} & \text{if } B2 < 0,\ 0 \leq B_0 \leq -4(B_1 + B_2) \\ \dfrac{-B_0}{2B_1} & \text{if } B2 = 0,\ -4 \leq \frac{B_0}{B_1} \leq 0 \end{cases} \tag{A.23}$$

Substituting (A.23) into (3.14) and (3.15), we get

$$W_0 = H_0 \frac{\sqrt{c_0 + c_1 A_w + c_2 A_w^2}}{a_0 + a_1 A_w + a_2 A_w^2} \tag{A.24}$$

$$\tan \psi_w = \frac{b_{0_x} + b_{1_x} A_w}{b_{0_y} + b_{1_y} A_w} \tag{A.25}$$

Appendix B

Details of Linearization of Equations

B.1 Linearized Equations of Motion With Real Wind

We use $[\bar{\mathbf{x}}^{\mathbf{o}}(\bar{t}), \bar{\mathbf{u}}^{\mathbf{o}}(\bar{t})]$, $\bar{t}_0^o \leq \bar{t} \leq \bar{t}_f^o$, denote a normalized nominal trajectory that satisfies the normalized equations of motion

$$\dot{\bar{\mathbf{x}}} = \mathbf{f}(\bar{\mathbf{x}}, \bar{\mathbf{u}}, \bar{\mathbf{W}}(\bar{\mathbf{x}}, \bar{t}), \bar{t}) \tag{B.1}$$

Then the above equation may be linearized around the nominal trajectory as

$$\begin{aligned}\delta\dot{\bar{\mathbf{x}}} &= \mathbf{f}(\bar{\mathbf{x}}^o + \delta\bar{\mathbf{x}}, \bar{\mathbf{u}}^o + \delta\bar{\mathbf{u}}, \bar{\mathbf{W}}(\bar{\mathbf{x}}^o + \delta\bar{\mathbf{x}}, \bar{t}), \bar{t}) - \mathbf{f}(\bar{\mathbf{x}}^o, \bar{\mathbf{u}}^o, \bar{\mathbf{W}}(\bar{\mathbf{x}}^o, \bar{t}), \bar{t}) \\ &\triangleq A\delta\bar{\mathbf{x}} + B\delta\bar{\mathbf{u}}\end{aligned}$$

where

$$A(t) = \left(\frac{\partial \mathbf{f}}{\partial \bar{\mathbf{x}}} + \frac{\partial \mathbf{f}}{\partial \bar{\mathbf{W}}}\frac{\partial \bar{\mathbf{W}}}{\partial \bar{\mathbf{x}}}\right)_{\bar{\mathbf{x}}^o, \bar{\mathbf{u}}^o} \quad B(t) = \left(\frac{\partial \mathbf{f}}{\partial \bar{\mathbf{u}}}\right)_{\bar{\mathbf{x}}^o, \bar{\mathbf{u}}^o} \tag{B.2}$$

and

$$A = \left(\frac{\partial \mathbf{f}}{\partial \bar{\mathbf{x}}} + \frac{\partial \mathbf{f}}{\partial \bar{\mathbf{W}}}\frac{\partial \bar{\mathbf{W}}}{\partial \bar{\mathbf{x}}}\right)_{\bar{\mathbf{x}}^o, \bar{\mathbf{u}}^o} = \begin{bmatrix} \frac{\partial \bar{V}'}{\partial \bar{\mathbf{x}}} + \frac{\partial \bar{V}'}{\partial \bar{\mathbf{W}}}\frac{\partial \bar{\mathbf{W}}}{\partial \bar{\mathbf{x}}} \\ \frac{\partial \psi'}{\partial \bar{\mathbf{x}}} + \frac{\partial \psi'}{\partial \bar{\mathbf{W}}}\frac{\partial \bar{\mathbf{W}}}{\partial \bar{\mathbf{x}}} \\ \frac{\partial \gamma'}{\partial \bar{\mathbf{x}}} + \frac{\partial \gamma'}{\partial \bar{\mathbf{W}}}\frac{\partial \bar{\mathbf{W}}}{\partial \bar{\mathbf{x}}} \\ \frac{\partial \bar{x}'}{\partial \bar{\mathbf{x}}} + \frac{\partial \bar{x}'}{\partial \bar{\mathbf{W}}}\frac{\partial \bar{\mathbf{W}}}{\partial \bar{\mathbf{x}}} \\ \frac{\partial \bar{y}'}{\partial \bar{\mathbf{x}}} + \frac{\partial \bar{y}'}{\partial \bar{\mathbf{W}}}\frac{\partial \bar{\mathbf{W}}}{\partial \bar{\mathbf{x}}} \\ \frac{\partial \bar{h}'}{\partial \bar{\mathbf{x}}} + \frac{\partial \bar{h}'}{\partial \bar{\mathbf{W}}}\frac{\partial \bar{\mathbf{W}}}{\partial \bar{\mathbf{x}}} \end{bmatrix}_{\bar{\mathbf{x}}^o, \bar{\mathbf{u}}^o} \tag{B.3}$$

The partial derivatives of the normalized equations of motion (4.60) through (4.65) with respect to the states and controls are shown below.

True airspeed rate

$$\bar{V}' = \bar{T} - k_a \bar{\rho} \bar{V}^2 (C_{D_0} + K C_L^2) - \sin\gamma - \bar{W}_V' \tag{B.4}$$

Partial Derivatives of $\bar{V}'$ with respect to $\bar{\mathbf{x}}$

Define

$$\bar{V}_1' = \bar{T} - k_a \bar{\rho} \bar{V}^2 (C_{D_0} + K C_L^2) - \sin\gamma \tag{B.5}$$

then

$$\bar{V}' = \bar{V}_1' - \bar{W}_V' \tag{B.6}$$

$$\frac{\partial \bar{V}'}{\partial \bar{\mathbf{x}}} + \frac{\partial \bar{V}'}{\partial \bar{\mathbf{W}}} \frac{\partial \bar{\mathbf{W}}}{\partial \bar{\mathbf{x}}} = \frac{\partial \bar{V}_1'}{\partial \bar{\mathbf{x}}} - \frac{\partial \bar{W}_V'}{\partial \bar{\mathbf{x}}} \tag{B.7}$$

$$\begin{aligned} \frac{\partial \bar{V}_1'}{\partial \bar{\mathbf{x}}} &= \left[\frac{\partial \bar{V}_1'}{\partial \bar{V}} \quad \frac{\partial \bar{V}_1'}{\partial \psi} \quad \frac{\partial \bar{V}_1'}{\partial \gamma} \quad \frac{\partial \bar{V}_1'}{\partial \bar{x}} \quad \frac{\partial \bar{V}_1'}{\partial \bar{y}} \quad \frac{\partial \bar{V}_1'}{\partial \bar{h}} \right] \\ &= \left[-2k_a \bar{\rho} \bar{V} (C_{D_0} + K C_L^2) \quad 0 \quad -\cos\gamma \quad 0 \quad 0 \quad -k_a \bar{V}^2 (C_{D_0} + K C_L^2) \frac{\partial \bar{\rho}}{\partial \bar{h}} \right] \end{aligned} \tag{B.8}$$

and

$$\frac{\partial \bar{W}_V'}{\partial \bar{\mathbf{x}}} = \left[\frac{\partial \bar{W}_V'}{\partial \bar{V}} \quad \frac{\partial \bar{W}_V'}{\partial \psi} \quad \frac{\partial \bar{W}_V'}{\partial \gamma} \quad \frac{\partial \bar{W}_V'}{\partial \bar{x}} \quad \frac{\partial \bar{W}_V'}{\partial \bar{y}} \quad \frac{\partial \bar{W}_V'}{\partial \bar{h}} \right] \tag{B.9}$$

thus

$$\frac{\partial \bar{V}'}{\partial \bar{\mathbf{x}}} + \frac{\partial \bar{V}'}{\partial \bar{\mathbf{W}}} \frac{\partial \bar{\mathbf{W}}}{\partial \bar{\mathbf{x}}} = \begin{bmatrix} -2k_a\bar{\rho}\bar{V}(C_{D_0} + KC_L^2) - \frac{\partial \bar{W}'_V}{\partial \bar{V}} \\ -\frac{\partial \bar{W}'_V}{\partial \psi} \\ -\cos\gamma - \frac{\partial \bar{W}'_V}{\partial \gamma} \\ -\frac{\partial \bar{W}'_V}{\partial \bar{x}} \\ -\frac{\partial \bar{W}'_V}{\partial \bar{y}} \\ -k_a\bar{V}^2(C_{D_0} + KC_L^2)\frac{\partial \bar{\rho}}{\partial \bar{h}} - \frac{\partial \bar{W}'_V}{\partial \bar{h}} \end{bmatrix}^T \tag{B.10}$$

Since

$$\begin{aligned} \bar{W}'_V &= [\cos\gamma\sin\psi \quad \cos\gamma\cos\psi \quad \sin\gamma] \begin{bmatrix} \bar{W}'_x \\ \bar{W}'_y \\ \bar{W}'_h \end{bmatrix} \\ &= [\cos\gamma\sin\psi \quad \cos\gamma\cos\psi \quad \sin\gamma]\, \bar{M} \begin{bmatrix} 1 \\ \bar{V}\cos\gamma\sin\psi + \bar{W}_x \\ \bar{V}\cos\gamma\cos\psi + \bar{W}_y \\ \bar{V}\sin\gamma + \bar{W}_h \end{bmatrix} \end{aligned} \tag{B.11}$$

we get the following partial derivatives of $\bar{W}'_V$ with respective to $\bar{\mathbf{x}}$

$$\frac{\partial \bar{W}'_V}{\partial \bar{V}} = [\cos\gamma\sin\psi \quad \cos\gamma\cos\psi \quad \sin\gamma]\, \bar{M} \begin{bmatrix} 0 \\ \cos\gamma\sin\psi \\ \cos\gamma\cos\psi \\ \sin\gamma \end{bmatrix} \tag{B.12}$$

$$\begin{aligned} \frac{\partial \bar{W}'_V}{\partial \psi} &= [\cos\gamma\sin\psi \quad \cos\gamma\cos\psi \quad \sin\gamma]\, \bar{M} \begin{bmatrix} 0 \\ \bar{V}\cos\gamma\cos\psi \\ -\bar{V}\cos\gamma\sin\psi \\ 0 \end{bmatrix} + \\ &\quad + [\cos\gamma\cos\psi \quad -\cos\gamma\sin\psi \quad 0]\, \bar{M} \begin{bmatrix} 1 \\ \bar{V}\cos\gamma\sin\psi + \bar{W}_x \\ \bar{V}\cos\gamma\cos\psi + \bar{W}_y \\ \bar{V}\sin\gamma + \bar{W}_h \end{bmatrix} \end{aligned} \tag{B.13}$$

$$\frac{\partial \bar{W}'_V}{\partial \gamma} = [\cos\gamma\sin\psi \quad \cos\gamma\cos\psi \quad \sin\gamma]\, \bar{M} \begin{bmatrix} 0 \\ -\bar{V}\sin\gamma\sin\psi \\ -\bar{V}\sin\gamma\cos\psi \\ \bar{V}\cos\gamma \end{bmatrix} +$$

$$+\left[\begin{array}{ccc}-\sin\gamma\sin\psi & -\sin\gamma\cos\psi & \cos\gamma\end{array}\right]\bar{M}\begin{bmatrix}1\\ \bar{V}\cos\gamma\sin\psi+\bar{W}_x\\ \bar{V}\cos\gamma\cos\psi+\bar{W}_y\\ \bar{V}\sin\gamma+\bar{W}_h\end{bmatrix} \tag{B.14}$$

$$\frac{\partial\bar{W}'_V}{\partial\bar{x}}=\left[\begin{array}{ccc}\cos\gamma\sin\psi & \cos\gamma\cos\psi & \sin\gamma\end{array}\right]\bar{M}\begin{bmatrix}0\\ \frac{\partial\bar{W}_x}{\partial\bar{x}}\\ \frac{\partial\bar{W}_y}{\partial\bar{x}}\\ \frac{\partial\bar{W}_h}{\partial\bar{x}}\end{bmatrix}+$$
$$+\left[\begin{array}{ccc}\cos\gamma\sin\psi & \cos\gamma\cos\psi & \sin\gamma\end{array}\right]\frac{\partial\bar{M}}{\partial\bar{x}}\begin{bmatrix}1\\ \bar{V}\cos\gamma\sin\psi+\bar{W}_x\\ \bar{V}\cos\gamma\cos\psi+\bar{W}_y\\ \bar{V}\sin\gamma+\bar{W}_h\end{bmatrix} \tag{B.15}$$

$$\frac{\partial\bar{W}'_V}{\partial\bar{y}}=\left[\begin{array}{ccc}\cos\gamma\sin\psi & \cos\gamma\cos\psi & \sin\gamma\end{array}\right]\bar{M}\begin{bmatrix}0\\ \frac{\partial\bar{W}_x}{\partial\bar{y}}\\ \frac{\partial\bar{W}_y}{\partial\bar{y}}\\ \frac{\partial\bar{W}_h}{\partial\bar{y}}\end{bmatrix}+$$
$$+\left[\begin{array}{ccc}\cos\gamma\sin\psi & \cos\gamma\cos\psi & \sin\gamma\end{array}\right]\frac{\partial\bar{M}}{\partial\bar{y}}\begin{bmatrix}1\\ \bar{V}\cos\gamma\sin\psi+\bar{W}_x\\ \bar{V}\cos\gamma\cos\psi+\bar{W}_y\\ \bar{V}\sin\gamma+\bar{W}_h\end{bmatrix} \tag{B.16}$$

$$\frac{\partial\bar{W}'_V}{\partial\bar{h}}=\left[\begin{array}{ccc}\cos\gamma\sin\psi & \cos\gamma\cos\psi & \sin\gamma\end{array}\right]\bar{M}\begin{bmatrix}0\\ \frac{\partial\bar{W}_x}{\partial\bar{h}}\\ \frac{\partial\bar{W}_y}{\partial\bar{h}}\\ \frac{\partial\bar{W}_h}{\partial\bar{h}}\end{bmatrix}+$$

$$+\left[\cos\gamma\sin\psi \quad \cos\gamma\cos\psi \quad \sin\gamma\right]\frac{\partial\bar{M}}{\partial\bar{h}}\begin{bmatrix}1\\ \bar{V}\cos\gamma\sin\psi+\bar{W}_x\\ \bar{V}\cos\gamma\cos\psi+\bar{W}_y\\ \bar{V}\sin\gamma+\bar{W}_h\end{bmatrix} \tag{B.17}$$

Partial Derivatives of $\bar{V}'$ with respect to $\bar{\mathbf{u}}$

$$\frac{\partial\bar{V}'}{\partial\bar{T}}=1 \tag{B.18}$$

$$\frac{\partial\bar{V}'}{\partial C_L}=-2k_a\bar{\rho}\bar{V}^2KC_L \tag{B.19}$$

$$\frac{\partial\bar{V}'}{\partial\mu}=0 \tag{B.20}$$

Heading Angle Rate

$$\psi'=k_a\bar{\rho}\bar{V}C_L\frac{\sin\mu}{\cos\gamma}-\frac{1}{\bar{V}\cos\gamma}\bar{W}'_\psi \tag{B.21}$$

Partial Derivatives of ψ' with respect to $\bar{\mathbf{x}}$

Define

$$\psi'_1\triangleq k_a\bar{\rho}\bar{V}C_L\frac{\sin\mu}{\cos\gamma} \tag{B.22}$$

$$\bar{W}'_{\psi_1}\triangleq\frac{1}{\bar{V}\cos\gamma}\bar{W}'_\psi \tag{B.23}$$

then

$$\psi'=\psi'_1-\bar{W}'_{\psi_1} \tag{B.24}$$

$$\frac{\partial\psi'}{\partial\bar{\mathbf{x}}}+\frac{\partial\psi'}{\partial\bar{\mathbf{W}}}\frac{\partial\bar{\mathbf{W}}}{\partial\bar{\mathbf{x}}}=\frac{\partial\psi'_1}{\partial\bar{\mathbf{x}}}-\frac{\partial\bar{W}'_{\psi_1}}{\partial\bar{\mathbf{x}}} \tag{B.25}$$

where

$$\begin{aligned}\frac{\partial \psi_1'}{\partial \bar{\mathbf{x}}} &= \begin{bmatrix} \frac{\partial \psi_1'}{\partial \bar{V}} & \frac{\partial \psi_1'}{\partial \psi} & \frac{\partial \psi_1'}{\partial \gamma} & \frac{\partial \psi_1'}{\partial \bar{x}} & \frac{\partial \psi_1'}{\partial \bar{y}} & \frac{\partial \psi_1'}{\partial \bar{h}} \end{bmatrix} \\ &= \begin{bmatrix} k_a \bar{\rho} C_L \frac{\sin\mu}{\cos\gamma} & 0 & k_a \bar{\rho} \bar{V} C_L \frac{\sin\mu \sin\gamma}{\cos^2\gamma} & 0 & 0 & k_a \bar{V} C_L \frac{\sin\mu}{\cos\gamma} \frac{\partial \bar{\rho}}{\partial \bar{h}} \end{bmatrix}\end{aligned} \tag{B.26}$$

and

$$\frac{\partial \bar{W}_{\psi_1}'}{\partial \bar{\mathbf{x}}} = \begin{bmatrix} -\frac{1}{\bar{V}^2 \cos\gamma} \bar{W}_\psi' + \frac{1}{\bar{V}\cos\gamma} \frac{\partial \bar{W}_\psi'}{\partial \bar{V}} \\ \frac{1}{\bar{V}\cos\gamma} \frac{\partial \bar{W}_\psi'}{\partial \psi} \\ \frac{\sin\gamma}{\bar{V}\cos^2\gamma} \bar{W}_\psi' + \frac{1}{\bar{V}\cos\gamma} \frac{\partial \bar{W}_\psi'}{\partial \gamma} \\ \frac{1}{\bar{V}\cos\gamma} \frac{\partial \bar{W}_\psi'}{\partial \bar{x}} \\ \frac{1}{\bar{V}\cos\gamma} \frac{\partial \bar{W}_\psi'}{\partial \bar{y}} \\ \frac{1}{\bar{V}\cos\gamma} \frac{\partial \bar{W}_\psi'}{\partial \bar{h}} \end{bmatrix}^T \tag{B.27}$$

thus

$$\frac{\partial \psi'}{\partial \bar{\mathbf{x}}} + \frac{\partial \psi'}{\partial \bar{\mathbf{W}}} \frac{\partial \bar{\mathbf{W}}}{\partial \bar{\mathbf{x}}} = \begin{bmatrix} k_a \bar{\rho} C_L \frac{\sin\mu}{\cos\gamma} + \frac{1}{\bar{V}^2\cos\gamma} \bar{W}_\psi' - \frac{1}{\bar{V}\cos\gamma} \frac{\partial \bar{W}_\psi'}{\partial \bar{V}} \\ -\frac{1}{\bar{V}\cos\gamma} \frac{\partial \bar{W}_\psi'}{\partial \psi} \\ k_a \bar{\rho} \bar{V} C_L \frac{\sin\mu\sin\gamma}{\cos^2\gamma} - \frac{\sin\gamma}{\bar{V}\cos^2\gamma} \bar{W}_\psi' - \frac{1}{\bar{V}\cos\gamma} \frac{\partial \bar{W}_\psi'}{\partial \gamma} \\ -\frac{1}{\bar{V}\cos\gamma} \frac{\partial \bar{W}_\psi'}{\partial \bar{x}} \\ -\frac{1}{\bar{V}\cos\gamma} \frac{\partial \bar{W}_\psi'}{\partial \bar{y}} \\ k_a \bar{V} C_L \frac{\sin\mu}{\cos\gamma} \frac{\partial \bar{\rho}}{\partial \bar{h}} - \frac{1}{\bar{V}\cos\gamma} \frac{\partial \bar{W}_\psi'}{\partial \bar{h}} \end{bmatrix}^T \tag{B.28}$$

Since

$$\bar{W}_\psi' = \begin{bmatrix} \cos\psi & -\sin\psi & 0 \end{bmatrix} \begin{bmatrix} \bar{W}_x' \\ \bar{W}_y' \\ \bar{W}_h' \end{bmatrix}$$

$$= [\cos\psi \quad -\sin\psi \quad 0]\,\bar{M}\begin{bmatrix} 1 \\ \bar{V}\cos\gamma\sin\psi + \bar{W}_x \\ \bar{V}\cos\gamma\cos\psi + \bar{W}_y \\ \bar{V}\sin\gamma + \bar{W}_h \end{bmatrix} \tag{B.29}$$

we get the following partial derivatives of $\bar{W}'_\psi$ with respective to $\bar{\mathbf{x}}$

$$\frac{\partial \bar{W}'_\psi}{\partial \bar{V}} = [\cos\psi \quad -\sin\psi \quad 0]\,\bar{M}\begin{bmatrix} 0 \\ \cos\gamma\sin\psi \\ \cos\gamma\cos\psi \\ \sin\gamma \end{bmatrix} \tag{B.30}$$

$$\begin{aligned}\frac{\partial \bar{W}'_\psi}{\partial \psi} = {} & [\cos\psi \quad -\sin\psi \quad 0]\,\bar{M}\begin{bmatrix} 0 \\ \bar{V}\cos\gamma\cos\psi \\ -\bar{V}\cos\gamma\sin\psi \\ 0 \end{bmatrix} + \\ & + [-\sin\psi \quad -\cos\psi \quad 0]\,\bar{M}\begin{bmatrix} 1 \\ \bar{V}\cos\gamma\sin\psi + \bar{W}_x \\ \bar{V}\cos\gamma\cos\psi + \bar{W}_y \\ \bar{V}\sin\gamma + \bar{W}_h \end{bmatrix}\end{aligned} \tag{B.31}$$

$$\frac{\partial \bar{W}'_\psi}{\partial \gamma} = [\cos\psi \quad -\sin\psi \quad 0]\,\bar{M}\begin{bmatrix} 0 \\ -\bar{V}\sin\gamma\sin\psi \\ -\bar{V}\sin\gamma\cos\psi \\ \bar{V}\cos\gamma \end{bmatrix} \tag{B.32}$$

$$\begin{aligned}\frac{\partial \bar{W}'_\psi}{\partial \bar{x}} = {} & [\cos\psi \quad -\sin\psi \quad 0]\,\bar{M}\begin{bmatrix} 0 \\ \dfrac{\partial \bar{W}_x}{\partial \bar{x}} \\ \dfrac{\partial \bar{W}_y}{\partial \bar{x}} \\ \dfrac{\partial \bar{W}_h}{\partial \bar{x}} \end{bmatrix} + \\ & + [\cos\psi \quad -\sin\psi \quad 0]\,\frac{\partial \bar{M}}{\partial \bar{x}}\begin{bmatrix} 1 \\ \bar{V}\cos\gamma\sin\psi + \bar{W}_x \\ \bar{V}\cos\gamma\cos\psi + \bar{W}_y \\ \bar{V}\sin\gamma + \bar{W}_h \end{bmatrix}\end{aligned} \tag{B.33}$$

$$\frac{\partial \bar{W}'_\psi}{\partial \bar{y}} = [\cos\psi \quad -\sin\psi \quad 0]\,\bar{M}\begin{bmatrix} 0 \\ \dfrac{\partial \bar{W}_x}{\partial \bar{y}} \\ \dfrac{\partial \bar{W}_y}{\partial \bar{y}} \\ \dfrac{\partial \bar{W}_h}{\partial \bar{y}} \end{bmatrix} +$$

$$+ \left[\cos\psi \quad -\sin\psi \quad 0\right] \frac{\partial \bar{M}}{\partial \bar{y}} \begin{bmatrix} 1 \\ \bar{V}\cos\gamma\sin\psi + \bar{W}_x \\ \bar{V}\cos\gamma\cos\psi + \bar{W}_y \\ \bar{V}\sin\gamma + \bar{W}_h \end{bmatrix} \tag{B.34}$$

$$\frac{\partial \bar{W}'_\psi}{\partial \bar{h}} = \left[\cos\psi \quad -\sin\psi \quad 0\right] \bar{M} \begin{bmatrix} 0 \\ \dfrac{\partial \bar{W}_x}{\partial \bar{h}} \\ \dfrac{\partial \bar{W}_y}{\partial \bar{h}} \\ \dfrac{\partial \bar{W}_h}{\partial \bar{h}} \end{bmatrix} +$$

$$+ \left[\cos\psi \quad -\sin\psi \quad 0\right] \frac{\partial \bar{M}}{\partial \bar{h}} \begin{bmatrix} 1 \\ \bar{V}\cos\gamma\sin\psi + \bar{W}_x \\ \bar{V}\cos\gamma\cos\psi + \bar{W}_y \\ \bar{V}\sin\gamma + \bar{W}_h \end{bmatrix} \tag{B.35}$$

Partial Derivatives of ψ' with respect to $\bar{\mathbf{u}}$

$$\frac{\partial \psi'}{\partial \bar{T}} = 0 \tag{B.36}$$

$$\frac{\partial \psi'}{\partial C_L} = k_a \bar{\rho} \bar{V} \frac{\sin\mu}{\cos\gamma} \tag{B.37}$$

$$\frac{\partial \psi'}{\partial \mu} = k_a \bar{\rho} \bar{V} C_L \frac{\cos\mu}{\cos\gamma} \tag{B.38}$$

Flight Path Angle Rate

$$\gamma' = k_a \bar{\rho} \bar{V} C_L \cos\mu - \frac{1}{\bar{V}} \cos\gamma + \frac{1}{\bar{V}} \bar{W}'_\gamma \tag{B.39}$$

Partial Derivatives of γ' with respect to $\bar{\mathbf{x}}$

Define

$$\gamma'_1 \triangleq k_a \bar{\rho} \bar{V} C_L \cos\mu - \frac{1}{\bar{V}} \cos\gamma \tag{B.40}$$

$$\bar{W}'_{\gamma_1} \triangleq \frac{1}{\bar{V}} \bar{W}'_{\gamma} \tag{B.41}$$

then

$$\gamma' = \gamma'_1 + \bar{W}'_{\gamma_1} \tag{B.42}$$

$$\frac{\partial \gamma'}{\partial \bar{\mathbf{x}}} + \frac{\partial \gamma'}{\partial \bar{\mathbf{W}}} \frac{\partial \bar{\mathbf{W}}}{\partial \bar{\mathbf{x}}} = \frac{\partial \gamma'_1}{\partial \bar{\mathbf{x}}} + \frac{\partial \bar{W}'_{\gamma_1}}{\partial \bar{\mathbf{x}}} \tag{B.43}$$

where

$$\begin{aligned} \frac{\partial \gamma'_1}{\partial \bar{\mathbf{x}}} &= \left[\begin{array}{cccccc} \frac{\partial \gamma'_1}{\partial \bar{V}} & \frac{\partial \gamma'_1}{\partial \psi} & \frac{\partial \gamma'_1}{\partial \gamma} & \frac{\partial \gamma'_1}{\partial \bar{x}} & \frac{\partial \gamma'_1}{\partial \bar{y}} & \frac{\partial \gamma'_1}{\partial h} \end{array} \right] \\ &= \left[\begin{array}{cccccc} k_a \bar{\rho} C_L \cos\mu + \frac{1}{\bar{V}^2} \cos\gamma & 0 & \frac{1}{\bar{V}} \sin\gamma & 0 & 0 & k_a \bar{V} C_L \cos\mu \frac{\partial \bar{\rho}}{\partial h} \end{array} \right] \end{aligned} \tag{B.44}$$

and

$$\frac{\partial \bar{W}'_{\gamma_1}}{\partial \bar{\mathbf{x}}} = \left[\begin{array}{cccccc} -\frac{1}{\bar{V}^2} \bar{W}'_{\gamma} + \frac{1}{\bar{V}} \frac{\partial \bar{W}'_{\gamma}}{\partial \bar{V}} & \frac{1}{\bar{V}} \frac{\partial \bar{W}'_{\gamma}}{\partial \psi} & \frac{1}{\bar{V}} \frac{\partial \bar{W}'_{\gamma}}{\partial \gamma} & \frac{1}{\bar{V}} \frac{\partial \bar{W}'_{\gamma}}{\partial \bar{x}} & \frac{1}{\bar{V}} \frac{\partial \bar{W}'_{\gamma}}{\partial \bar{y}} & \frac{1}{\bar{V}} \frac{\partial \bar{W}'_{\gamma}}{\partial h} \end{array} \right] \tag{B.45}$$

thus

$$\frac{\partial \gamma'}{\partial \bar{\mathbf{x}}} + \frac{\partial \gamma'}{\partial \bar{\mathbf{W}}} \frac{\partial \bar{\mathbf{W}}}{\partial \bar{\mathbf{x}}} = \left[\begin{array}{c} k_a \bar{\rho} C_L \cos\mu + \frac{1}{\bar{V}^2} \cos\gamma - \frac{1}{\bar{V}^2} \bar{W}'_{\gamma} + \frac{1}{\bar{V}} \frac{\partial \bar{W}'_{\gamma}}{\partial \bar{V}} \\ \frac{1}{\bar{V}} \frac{\partial \bar{W}'_{\gamma}}{\partial \psi} \\ \frac{1}{\bar{V}} \sin\gamma + \frac{1}{\bar{V}} \frac{\partial \bar{W}'_{\gamma}}{\partial \gamma} \\ \frac{1}{\bar{V}} \frac{\partial \bar{W}'_{\gamma}}{\partial \bar{x}} \\ \frac{1}{\bar{V}} \frac{\partial \bar{W}'_{\gamma}}{\partial \bar{y}} \\ k_a \bar{V} C_L \cos\mu \frac{\partial \bar{\rho}}{\partial h} + \frac{1}{\bar{V}} \frac{\partial \bar{W}'_{\gamma}}{\partial h} \end{array} \right]^T \tag{B.46}$$

Since

$$\bar{W}'_{\gamma} = \left[\begin{array}{ccc} \sin\gamma \sin\psi & \sin\gamma \cos\psi & -\cos\gamma \end{array} \right] \left[\begin{array}{c} \bar{W}'_x \\ \bar{W}'_y \\ \bar{W}'_h \end{array} \right]$$

$$= [\sin\gamma\sin\psi \quad \sin\gamma\cos\psi \quad -\cos\gamma]\,\bar{M}\begin{bmatrix}1\\ \bar{V}\cos\gamma\sin\psi+\bar{W}_x\\ \bar{V}\cos\gamma\cos\psi+\bar{W}_y\\ \bar{V}\sin\gamma+\bar{W}_h\end{bmatrix} \tag{B.47}$$

we get the following partial derivatives of $\bar{W}'_\gamma$ with respective to $\bar{\mathbf{x}}$

$$\frac{\partial\bar{W}'_\gamma}{\partial\bar{V}} = [\sin\gamma\sin\psi \quad \sin\gamma\cos\psi \quad -\cos\gamma]\,\bar{M}\begin{bmatrix}0\\ \cos\gamma\sin\psi\\ \cos\gamma\cos\psi\\ \sin\gamma\end{bmatrix} \tag{B.48}$$

$$\begin{aligned}\frac{\partial\bar{W}'_\gamma}{\partial\psi} &= [\sin\gamma\sin\psi \quad \sin\gamma\cos\psi \quad -\cos\gamma]\,\bar{M}\begin{bmatrix}0\\ \bar{V}\cos\gamma\cos\psi\\ -\bar{V}\cos\gamma\sin\psi\\ 0\end{bmatrix}+\\ &+[\sin\gamma\cos\psi \quad -\sin\gamma\sin\psi \quad 0]\,\bar{M}\begin{bmatrix}1\\ \bar{V}\cos\gamma\sin\psi+\bar{W}_x\\ \bar{V}\cos\gamma\cos\psi+\bar{W}_y\\ \bar{V}\sin\gamma+\bar{W}_h\end{bmatrix}\end{aligned} \tag{B.49}$$

$$\begin{aligned}\frac{\partial\bar{W}'_\gamma}{\partial\gamma} &= [\sin\gamma\sin\psi \quad \sin\gamma\cos\psi \quad -\cos\gamma]\,\bar{M}\begin{bmatrix}0\\ -\bar{V}\sin\gamma\sin\psi\\ -\bar{V}\sin\gamma\cos\psi\\ \bar{V}\cos\gamma\end{bmatrix}+\\ &+[\cos\gamma\sin\psi \quad \cos\gamma\cos\psi \quad \sin\gamma]\,\bar{M}\begin{bmatrix}1\\ \bar{V}\cos\gamma\sin\psi+\bar{W}_x\\ \bar{V}\cos\gamma\cos\psi+\bar{W}_y\\ \bar{V}\sin\gamma+\bar{W}_h\end{bmatrix}\end{aligned} \tag{B.50}$$

$$\begin{aligned}\frac{\partial\bar{W}'_\gamma}{\partial\bar{x}} &= [\sin\gamma\sin\psi \quad \sin\gamma\cos\psi \quad -\cos\gamma]\,\bar{M}\begin{bmatrix}0\\ \frac{\partial\bar{W}_x}{\partial\bar{x}}\\ \frac{\partial\bar{W}_y}{\partial\bar{x}}\\ \frac{\partial\bar{W}_h}{\partial\bar{x}}\end{bmatrix}+\\ &+[\sin\gamma\sin\psi \quad \sin\gamma\cos\psi \quad -\cos\gamma]\,\frac{\partial\bar{M}}{\partial\bar{x}}\begin{bmatrix}1\\ \bar{V}\cos\gamma\sin\psi+\bar{W}_x\\ \bar{V}\cos\gamma\cos\psi+\bar{W}_y\\ \bar{V}\sin\gamma+\bar{W}_h\end{bmatrix}\end{aligned} \tag{B.51}$$

$$\frac{\partial \bar{W}'_\gamma}{\partial \bar{y}} = \begin{bmatrix} \sin\gamma\sin\psi & \sin\gamma\cos\psi & -\cos\gamma \end{bmatrix} \bar{M} \begin{bmatrix} 0 \\ \frac{\partial \bar{W}_x}{\partial \bar{y}} \\ \frac{\partial \bar{W}_y}{\partial \bar{y}} \\ \frac{\partial \bar{W}_h}{\partial \bar{y}} \end{bmatrix} + \\ + \begin{bmatrix} \sin\gamma\sin\psi & \sin\gamma\cos\psi & -\cos\gamma \end{bmatrix} \frac{\partial \bar{M}}{\partial \bar{y}} \begin{bmatrix} 1 \\ \bar{V}\cos\gamma\sin\psi + \bar{W}_x \\ \bar{V}\cos\gamma\cos\psi + \bar{W}_y \\ \bar{V}\sin\gamma + \bar{W}_h \end{bmatrix} \tag{B.52}$$

$$\frac{\partial \bar{W}'_\gamma}{\partial \bar{h}} = \begin{bmatrix} \sin\gamma\sin\psi & \sin\gamma\cos\psi & -\cos\gamma \end{bmatrix} \bar{M} \begin{bmatrix} 0 \\ \frac{\partial \bar{W}_x}{\partial \bar{h}} \\ \frac{\partial \bar{W}_y}{\partial \bar{h}} \\ \frac{\partial \bar{W}_h}{\partial \bar{h}} \end{bmatrix} + \\ + \begin{bmatrix} \sin\gamma\sin\psi & \sin\gamma\cos\psi & -\cos\gamma \end{bmatrix} \frac{\partial \bar{M}}{\partial \bar{h}} \begin{bmatrix} 1 \\ \bar{V}\cos\gamma\sin\psi + \bar{W}_x \\ \bar{V}\cos\gamma\cos\psi + \bar{W}_y \\ \bar{V}\sin\gamma + \bar{W}_h \end{bmatrix} \tag{B.53}$$

Partial Derivatives of γ' with respect to $\bar{\mathbf{u}}$

$$\frac{\partial \gamma'}{\partial \bar{T}} = 0 \tag{B.54}$$

$$\frac{\partial \gamma'}{\partial C_L} = k_a \bar{\rho} \bar{V} \cos\mu \tag{B.55}$$

$$\frac{\partial \gamma'}{\partial \mu} = -k_a \bar{\rho} \bar{V} C_L \sin\mu \tag{B.56}$$

East Position Rate

$$\bar{x}' = \bar{V}\cos\gamma\sin\psi + \bar{W}_x \tag{B.57}$$

Partial Derivatives of $\bar{x}'$ with respect to $\bar{\mathbf{x}}$

Define

$$\bar{x}'_1 \triangleq \bar{V}\cos\gamma\sin\psi \tag{B.58}$$

then

$$\bar{x}' = \bar{x}'_1 + \bar{W}_x \tag{B.59}$$

$$\frac{\partial \bar{x}'}{\partial \bar{\mathbf{x}}} + \frac{\partial \bar{x}'}{\partial \bar{\mathbf{W}}}\frac{\partial \bar{\mathbf{W}}}{\partial \bar{\mathbf{x}}} = \frac{\partial \bar{x}'_1}{\partial \bar{\mathbf{x}}} + \frac{\partial \bar{W}_x}{\partial \bar{\mathbf{x}}} \tag{B.60}$$

where

$$\frac{\partial \bar{x}'_1}{\partial \bar{\mathbf{x}}} = \begin{bmatrix} \cos\gamma\sin\psi & \bar{V}\cos\gamma\cos\psi & -\bar{V}\sin\gamma\sin\psi & 0 & 0 & 0 \end{bmatrix} \tag{B.61}$$

and

$$\frac{\partial \bar{W}_x}{\partial \bar{\mathbf{x}}} = \begin{bmatrix} 0 & 0 & 0 & \frac{\partial \bar{W}_x}{\partial \bar{x}} & \frac{\partial \bar{W}_x}{\partial \bar{y}} & \frac{\partial \bar{W}_x}{\partial \bar{h}} \end{bmatrix} \tag{B.62}$$

thus

$$\frac{\partial \bar{x}'}{\partial \bar{\mathbf{x}}} + \frac{\partial \bar{x}'}{\partial \bar{\mathbf{W}}}\frac{\partial \bar{\mathbf{W}}}{\partial \bar{\mathbf{x}}} = \begin{bmatrix} \cos\gamma\sin\psi & \bar{V}\cos\gamma\cos\psi & -\bar{V}\sin\gamma\sin\psi & \frac{\partial \bar{W}_x}{\partial \bar{x}} & \frac{\partial \bar{W}_x}{\partial \bar{y}} & \frac{\partial \bar{W}_x}{\partial \bar{h}} \end{bmatrix} \tag{B.63}$$

Partial Derivatives of $\bar{x}'$ with respect to $\bar{\mathbf{u}}$

$$\frac{\partial \bar{x}'}{\partial \bar{T}} = 0 \tag{B.64}$$

$$\frac{\partial \bar{x}'}{\partial C_L} = 0 \tag{B.65}$$

$$\frac{\partial \bar{x}'}{\partial \mu} = 0 \tag{B.66}$$

North Position Rate

$$\bar{y}' = \bar{V}\cos\gamma\cos\psi + \bar{W}_y \tag{B.67}$$

Partial Derivatives of $\bar{y}'$ with respect to $\bar{\mathbf{x}}$

Define

$$\bar{y}'_1 \triangleq \bar{V}\cos\gamma\cos\psi \tag{B.68}$$

then

$$\bar{y}' = \bar{y}'_1 + \bar{W}_y \tag{B.69}$$

$$\frac{\partial \bar{y}'}{\partial \bar{\mathbf{x}}} + \frac{\partial \bar{y}'}{\partial \bar{\mathbf{W}}}\frac{\partial \bar{\mathbf{W}}}{\partial \bar{\mathbf{x}}} = \frac{\partial \bar{y}'_1}{\partial \bar{\mathbf{x}}} + \frac{\partial \bar{W}_y}{\partial \bar{\mathbf{x}}} \tag{B.70}$$

where

$$\frac{\partial \bar{y}'_1}{\partial \bar{\mathbf{x}}} = \begin{bmatrix} \cos\gamma\cos\psi & -\bar{V}\cos\gamma\sin\psi & -\bar{V}\sin\gamma\cos\psi & 0 & 0 & 0 \end{bmatrix} \tag{B.71}$$

and

$$\frac{\partial \bar{W}_y}{\partial \bar{\mathbf{x}}} = \begin{bmatrix} 0 & 0 & 0 & \frac{\partial \bar{W}_y}{\partial \bar{x}} & \frac{\partial \bar{W}_y}{\partial \bar{y}} & \frac{\partial \bar{W}_y}{\partial \bar{h}} \end{bmatrix} \tag{B.72}$$

thus

$$\frac{\partial \bar{y}'}{\partial \bar{\mathbf{x}}} + \frac{\partial \bar{y}'}{\partial \bar{\mathbf{W}}}\frac{\partial \bar{\mathbf{W}}}{\partial \bar{\mathbf{x}}} = \begin{bmatrix} \cos\gamma\cos\psi & -\bar{V}\cos\gamma\sin\psi & -\bar{V}\sin\gamma\cos\psi & \frac{\partial \bar{W}_y}{\partial \bar{x}} & \frac{\partial \bar{W}_y}{\partial \bar{y}} & \frac{\partial \bar{W}_y}{\partial \bar{h}} \end{bmatrix} \tag{B.73}$$

Partial Derivatives of $\bar{y}'$ with respect to $\bar{\mathbf{u}}$

$$\frac{\partial \bar{y}'}{\partial \bar{T}} = 0 \tag{B.74}$$

$$\frac{\partial \bar{y}'}{\partial C_L} = 0 \tag{B.75}$$

$$\frac{\partial \bar{y}'}{\partial \mu} = 0 \tag{B.76}$$

Altitude Rate

$$\bar{h}' = \bar{V} \sin\gamma + \bar{W}_h \tag{B.77}$$

Partial Derivatives of $\bar{h}'$ with respect to $\bar{\mathbf{x}}$

Define

$$\bar{h}'_1 \triangleq \bar{V} \sin\gamma \tag{B.78}$$

then

$$\bar{h}' = \bar{h}'_1 + \bar{W}_h \tag{B.79}$$

$$\frac{\partial \bar{h}'}{\partial \bar{\mathbf{x}}} + \frac{\partial \bar{h}'}{\partial \bar{\mathbf{W}}} \frac{\partial \bar{\mathbf{W}}}{\partial \bar{\mathbf{x}}} = \frac{\partial \bar{h}'_1}{\partial \bar{x}} + \frac{\partial \bar{W}_h}{\partial \bar{\mathbf{x}}} \tag{B.80}$$

where

$$\frac{\partial \bar{h}'_1}{\partial \bar{\mathbf{x}}} = \begin{bmatrix} \sin\gamma & 0 & \bar{V}\cos\gamma & 0 & 0 & 0 \end{bmatrix} \tag{B.81}$$

and

$$\frac{\partial \bar{W}_h}{\partial \bar{\mathbf{x}}} = \begin{bmatrix} 0 & 0 & 0 & \frac{\partial \bar{W}_h}{\partial \bar{x}} & \frac{\partial \bar{W}_h}{\partial \bar{y}} & \frac{\partial \bar{W}_h}{\partial \bar{h}} \end{bmatrix} \tag{B.82}$$

thus

$$\frac{\partial \bar{h}'}{\partial \bar{\mathbf{x}}} + \frac{\partial \bar{h}'}{\partial \bar{\mathbf{W}}} \frac{\partial \bar{\mathbf{W}}}{\partial \bar{\mathbf{x}}} = \begin{bmatrix} \sin\gamma & 0 & \bar{V}\cos\gamma & \frac{\partial \bar{W}_h}{\partial \bar{x}} & \frac{\partial \bar{W}_h}{\partial \bar{y}} & \frac{\partial \bar{W}_h}{\partial \bar{h}} \end{bmatrix} \tag{B.83}$$

Partial Derivatives of $\bar{h}'$ with respect to $\bar{\mathbf{u}}$

$$\frac{\partial \bar{h}'}{\partial \bar{T}} = 0 \tag{B.84}$$

$$\frac{\partial \bar{h}'}{\partial C_L} = 0 \tag{B.85}$$

$$\frac{\partial \bar{h}'}{\partial \mu} = 0 \tag{B.86}$$

B.2 Linearized Equations of Motion With Modeled Wind

In the normalized equations of motion, if we assume the wind velocity components can be modeled by (4.51), (4.52), and (4.53), then the coefficient matrices A and B for the linearized equations of motion may be simplified.

First of all, (4.39) may be expressed as

$$\bar{M} = \begin{bmatrix} 0 & 0 & 0 & \bar{\beta}_w(A_w + 2\bar{B}_w\bar{h})\sin\psi_w \\ 0 & 0 & 0 & \bar{\beta}_w(A_w + 2\bar{B}_w\bar{h})\cos\psi_w \\ 0 & 0 & 0 & 0 \end{bmatrix} \tag{B.87}$$

The partial derivatives of $\bar{M}$ with respect to $\bar{x}$, $\bar{y}$, and $\bar{h}$ are

$$\frac{\partial \bar{M}}{\partial \bar{x}} = 0^{3\times 4} \tag{B.88}$$

$$\frac{\partial \bar{M}}{\partial \bar{y}} = 0^{3\times 4} \tag{B.89}$$

$$\frac{\partial \bar{M}}{\partial \bar{h}} = \begin{bmatrix} 0 & 0 & 0 & 2\bar{\beta}_w\bar{B}_w\sin\psi_w \\ 0 & 0 & 0 & 2\bar{\beta}_w\bar{B}_w\cos\psi_w \\ 0 & 0 & 0 & 0 \end{bmatrix} \tag{B.90}$$

Assume a random vector $\mathbf{b}$,

$$\mathbf{b} = \begin{bmatrix} b_1 \\ b_2 \\ b_3 \\ b_4 \end{bmatrix} \tag{B.91}$$

then the product of $\bar{M}$ and $\mathbf{b}$ is determined by

$$\begin{aligned} \bar{M}\mathbf{b} &= \begin{bmatrix} 0 & 0 & 0 & \bar{\beta}_w(A_w + 2\bar{B}_w\bar{h})\sin\psi_w \\ 0 & 0 & 0 & \bar{\beta}_w(A_w + 2\bar{B}_w\bar{h})\cos\psi_w \\ 0 & 0 & 0 & 0 \end{bmatrix} \begin{bmatrix} b_1 \\ b_2 \\ b_3 \\ b_4 \end{bmatrix} \\ &= \begin{bmatrix} b_4\bar{\beta}_w(A_w + 2\bar{B}_w\bar{h})\sin\psi_w \\ b_4\bar{\beta}_w(A_w + 2\bar{B}_w\bar{h})\cos\psi_w \\ 0 \end{bmatrix} \end{aligned} \tag{B.92}$$

The partial derivatives of the normalized equations of motion (4.60) through (4.65) with respect to the states and controls with modeled wind can be obtained by utilizing (B.87), (B.88), (B.89), (B.90), and (B.92).

True airspeed rate

$$\begin{aligned} \frac{\partial \bar{V}'}{\partial \bar{V}} &= -2k_a\bar{\rho}\bar{V}(C_{D,0} + KC_L^2) - \\ &\quad - \frac{1}{2}\sin 2\gamma\cos(\psi - \psi_w)\bar{\beta}_w(A_w + 2\bar{B}_w\bar{h}) && (B.93) \\ \frac{\partial \bar{V}'}{\partial \psi} &= \frac{1}{2}\bar{V}\sin 2\gamma\sin(\psi - \psi_w)\bar{\beta}_w(A_w + 2\bar{B}_w\bar{h}) && (B.94) \\ \frac{\partial \bar{V}'}{\partial \gamma} &= -\cos\gamma - \bar{V}\cos 2\gamma\cos(\psi - \psi_w)\bar{\beta}_w(A_w + 2\bar{B}_w\bar{h}) && (B.95) \\ \frac{\partial \bar{V}'}{\partial \bar{x}} &= 0 && (B.96) \\ \frac{\partial \bar{V}'}{\partial \bar{y}} &= 0 && (B.97) \\ \frac{\partial \bar{V}'}{\partial \bar{h}} &= -k_a\bar{V}^2(C_{D,0} + KC_L^2)\frac{\partial \bar{\rho}}{\partial \bar{h}} - \bar{V}\sin 2\gamma\cos(\psi - \psi_w)\bar{\beta}_w\bar{B}_w && (B.98) \\ \frac{\partial \bar{V}'}{\partial \bar{T}} &= 1 && (B.99) \\ \frac{\partial \bar{V}'}{\partial C_L} &= -2k_a\bar{\rho}\bar{V}^2KC_L && (B.100) \end{aligned}$$

$$\frac{\partial \bar{V}'}{\partial \mu} = 0 \tag{B.101}$$

Heading rate

$$\frac{\partial \psi'}{\partial \bar{V}} = k_a \bar{\rho} C_L \frac{\sin \mu}{\cos \gamma} \tag{B.102}$$

$$\frac{\partial \psi'}{\partial \psi} = \tan \gamma \cos(\psi - \psi_w) \bar{\beta}_w (A_w + 2\bar{B}_w \bar{h}) \tag{B.103}$$

$$\frac{\partial \psi'}{\partial \gamma} = k_a \bar{\rho} \bar{V} C_L \frac{\sin \mu \sin \gamma}{\cos^2 \gamma} + \frac{\sin(\psi - \psi_w)}{\cos^2 \gamma} \bar{\beta}_w (A_w + 2\bar{B}_w \bar{h}) \tag{B.104}$$

$$\frac{\partial \psi'}{\partial \bar{x}} = 0 \tag{B.105}$$

$$\frac{\partial \psi'}{\partial \bar{y}} = 0 \tag{B.106}$$

$$\frac{\partial \psi'}{\partial \bar{h}} = k_a \bar{V} C_L \frac{\sin \mu}{\cos \gamma} \frac{\partial \bar{\rho}}{\partial \bar{h}} + \sin(\psi - \psi_w) \tan \gamma 2 \bar{\beta}_w \bar{B}_w \tag{B.107}$$

$$\frac{\partial \psi'}{\partial \bar{T}} = 0 \tag{B.108}$$

$$\frac{\partial \psi'}{\partial C_L} = k_a \bar{\rho} \bar{V} \frac{\sin \mu}{\cos \gamma} \tag{B.109}$$

$$\frac{\partial \psi'}{\partial \mu} = k_a \bar{\rho} \bar{V} C_L \frac{\cos \mu}{\cos \gamma} \tag{B.110}$$

Flight path angle rate

$$\frac{\partial \gamma'}{\partial \bar{V}} = k_a \bar{\rho} C_L \cos \mu + \frac{\cos \gamma}{\bar{V}^2} \tag{B.111}$$

$$\frac{\partial \gamma'}{\partial \psi} = -\sin^2 \gamma \sin(\psi - \psi_w) \bar{\beta}_w (A_w + 2\bar{B}_w \bar{h}) \tag{B.112}$$

$$\frac{\partial \gamma'}{\partial \gamma} = \frac{1}{\bar{V}} \sin \gamma + \sin 2\gamma \cos(\psi - \psi_w) \bar{\beta}_w (A_w + 2\bar{B}_w \bar{h}) \tag{B.113}$$

$$\frac{\partial \gamma'}{\partial \bar{x}} = 0 \tag{B.114}$$

$$\frac{\partial \gamma'}{\partial \bar{y}} = 0 \tag{B.115}$$

$$\frac{\partial \gamma'}{\partial \bar{h}} = k_a \bar{V} C_L \cos \mu \frac{\partial \bar{\rho}}{\partial \bar{h}} + 2 \sin^2 \gamma \cos(\psi - \psi_w) \bar{\beta}_w \bar{B}_w \tag{B.116}$$

$$\frac{\partial \gamma'}{\partial \bar{T}} = 0 \tag{B.117}$$

$$\frac{\partial \gamma'}{\partial C_L} = k_a \bar{\rho} \bar{V} \cos \mu \tag{B.118}$$

$$\frac{\partial \gamma'}{\partial \mu} = -k_a \bar{\rho} \bar{V} C_L \sin \mu \tag{B.119}$$

East Position rate

$$\frac{\partial \bar{x}'}{\partial \bar{V}} = \cos \gamma \sin \psi \tag{B.120}$$

$$\frac{\partial \bar{x}'}{\partial \psi} = \bar{V} \cos \gamma \cos \psi \tag{B.121}$$

$$\frac{\partial \bar{x}'}{\partial \gamma} = -\bar{V} \sin \gamma \sin \psi \tag{B.122}$$

$$\frac{\partial \bar{x}'}{\partial \bar{x}} = 0 \tag{B.123}$$

$$\frac{\partial \bar{x}'}{\partial \bar{y}} = 0 \tag{B.124}$$

$$\frac{\partial \bar{x}'}{\partial \bar{h}} = \sin \psi_w \bar{\beta}_w (A_w + 2\bar{B}_w \bar{h}) \tag{B.125}$$

$$\frac{\partial \bar{x}'}{\partial \bar{T}} = 0 \tag{B.126}$$

$$\frac{\partial \bar{x}'}{\partial C_L} = 0 \tag{B.127}$$

$$\frac{\partial \bar{x}'}{\partial \mu} = 0 \tag{B.128}$$

North Position rate

$$\frac{\partial \bar{y}'}{\partial \bar{V}} = \cos \gamma \cos \psi \tag{B.129}$$

$$\frac{\partial \bar{y}'}{\partial \psi} = -\bar{V} \cos \gamma \sin \psi \tag{B.130}$$

$$\frac{\partial \bar{y}'}{\partial \gamma} = -\bar{V} \sin \gamma \cos \psi \tag{B.131}$$

$$\frac{\partial \bar{y}'}{\partial \bar{x}} = 0 \tag{B.132}$$

$$\frac{\partial \bar{y}'}{\partial \bar{y}} = 0 \tag{B.133}$$

$$\frac{\partial \bar{y}'}{\partial \bar{h}} = \cos \psi_w \bar{\beta}_w (A_w + 2\bar{B}_w \bar{h}) \tag{B.134}$$

$$\frac{\partial \bar{y}'}{\partial \bar{T}} = 0 \tag{B.135}$$

$$\frac{\partial \bar{y}'}{\partial C_L} = 0 \tag{B.136}$$

$$\frac{\partial \bar{y}'}{\partial \mu} = 0 \tag{B.137}$$

Altitude rate

$$\frac{\partial \bar{h}'}{\partial \bar{V}} = \sin\gamma \tag{B.138}$$

$$\frac{\partial \bar{h}'}{\partial \psi} = 0 \tag{B.139}$$

$$\frac{\partial \bar{h}'}{\partial \gamma} = \bar{V}\cos\gamma \tag{B.140}$$

$$\frac{\partial \bar{h}'}{\partial \bar{x}} = 0 \tag{B.141}$$

$$\frac{\partial \bar{h}'}{\partial \bar{y}} = 0 \tag{B.142}$$

$$\frac{\partial \bar{h}'}{\partial \bar{h}} = 0 \tag{B.143}$$

$$\frac{\partial \bar{h}'}{\partial \bar{T}} = 0 \tag{B.144}$$

$$\frac{\partial \bar{h}'}{\partial C_L} = 0 \tag{B.145}$$

$$\frac{\partial \bar{h}'}{\partial \mu} = 0 \tag{B.146}$$

Appendix C

Derivation of Feedback Control

Normalized 3-D point-mass equations of motion of an aircraft with wind component

$$\bar{V}' = \bar{T} - k_a \bar{\rho} \bar{V}^2 (C_{D_0} + K C_L^2) - \sin\gamma - \bar{W}_V' \tag{C.1}$$

$$\psi' = k_a \bar{\rho} \bar{V} C_L \frac{\sin\mu}{\cos\gamma} - \frac{1}{\bar{V}\cos\gamma} \bar{W}_\psi' \tag{C.2}$$

$$\gamma' = k_a \bar{\rho} \bar{V} C_L \cos\mu - \frac{1}{\bar{V}} \cos\gamma + \frac{1}{\bar{V}} \bar{W}_\gamma' \tag{C.3}$$

$$\bar{x}' = \bar{V} \cos\gamma \sin\psi + \bar{W}_x \tag{C.4}$$

$$\bar{y}' = \bar{V} \cos\gamma \cos\psi + \bar{W}_y \tag{C.5}$$

$$\bar{h}' = \bar{V} \sin\gamma + \bar{W}_h \tag{C.6}$$

where

$$k_a \triangleq \frac{\rho_C V_C^2}{2(mg/S)} \tag{C.7}$$

$$K = \frac{1}{4E_{\max}^2 C_{D_0}} \tag{C.8}$$

Define

$$\bar{V}' = \bar{T} + a_1 C_L^2 + b_1 \tag{C.9}$$

$$\psi' = a_2 C_L \sin\mu + b_2 \tag{C.10}$$

$$\gamma' = a_3 C_L \cos\mu + b_3 \tag{C.11}$$

where

$$a_1 \triangleq -k_a \bar{\rho} \bar{V}^2 K \tag{C.12}$$

$$b_1 \triangleq -k_a \bar{\rho} \bar{V}^2 C_{D_0} - \sin\gamma - \bar{W}'_V \tag{C.13}$$

$$a_2 \triangleq k_a \bar{\rho} \bar{V} \frac{1}{\cos\gamma} \tag{C.14}$$

$$b_2 \triangleq -\frac{1}{\bar{V}\cos\gamma} \bar{W}'_\psi \tag{C.15}$$

$$a_3 \triangleq k_a \bar{\rho} \bar{V} \tag{C.16}$$

$$b_3 \triangleq -\frac{1}{\bar{V}} \cos\gamma + \frac{1}{\bar{V}} \bar{W}'_\gamma \tag{C.17}$$

Take the time derivatives of $\bar{x}'$, $\bar{y}'$, and $\bar{h}'$ in (C.4), (C.5), and (C.6), we obtain

$$\bar{x}'' = \bar{V}' \cos\gamma \sin\psi - \bar{V}\gamma' \sin\gamma \sin\psi + \bar{V}\psi' \cos\gamma \cos\psi + \bar{W}'_x \tag{C.18}$$

$$\bar{y}'' = \bar{V}' \cos\gamma \cos\psi - \bar{V}\gamma' \sin\gamma \cos\psi - \bar{V}\psi' \cos\gamma \sin\psi + \bar{W}'_y \tag{C.19}$$

$$\bar{h}'' = \bar{V}' \sin\gamma + \bar{V}\gamma' \cos\gamma + \bar{W}'_h \tag{C.20}$$

At any time t, $\bar{V}(t)'$, $\psi(t)'$, and $\gamma(t)'$ can be obtained by solving the following equations:

$$\begin{bmatrix} \cos\gamma\sin\psi & \bar{V}\cos\gamma\cos\psi & -\bar{V}\sin\gamma\sin\psi \\ \cos\gamma\cos\psi & -\bar{V}\cos\gamma\sin\psi & -\bar{V}\sin\gamma\cos\psi \\ \sin\gamma & 0 & \bar{V}\cos\gamma \end{bmatrix} \begin{bmatrix} \bar{V}' \\ \psi' \\ \gamma' \end{bmatrix} = \begin{bmatrix} \bar{x}'' - \bar{W}'_x \\ \bar{y}'' - \bar{W}'_y \\ \bar{h}'' - \bar{W}'_h \end{bmatrix} \tag{C.21}$$

Denote the desired trajectory as $[\bar{x}_d(t), \bar{y}_d(t), \bar{h}_d(t)]^T$ for $t \in [0, t_{f_d}]$. Since $\bar{x}$, $\bar{y}$, and $\bar{h}$ are second-order states, the desired trajectory tracking error dynamics are

$$(\bar{x} - \bar{x}_d)'' + 2\xi_x \omega_x (\bar{x} - \bar{x}_d)' + \omega_x^2 (\bar{x} - \bar{x}_d) = 0 \tag{C.22}$$

$$(\bar{y} - \bar{y}_d)'' + 2\xi_y\omega_y(\bar{y} - \bar{y}_d)' + \omega_y^2(\bar{y} - \bar{y}_d) = 0 \tag{C.23}$$

$$(\bar{h} - \bar{h}_d)'' + 2\xi_h\omega_h(\bar{h} - \bar{h}_d)' + \omega_h^2(\bar{h} - \bar{h}_d) = 0 \tag{C.24}$$

Then

$$\bar{x}'' = \bar{x}_d'' + 2\xi_x\omega_x(\bar{x}_d - \bar{x})' + \omega_x^2(\bar{x}_d - \bar{x}) \tag{C.25}$$

$$\bar{y}'' = \bar{y}_d'' + 2\xi_y\omega_y(\bar{y}_d - \bar{y})' + \omega_y^2(\bar{y}_d - \bar{y}) \tag{C.26}$$

$$\bar{h}_d'' = \bar{h}_d'' + 2\xi_h\omega_h(\bar{h}_d - \bar{h})' + \omega_h^2(\bar{h}_d - \bar{h}) \tag{C.27}$$

where $\bar{x}'$, $\bar{y}'$, and $\bar{h}'$ can be calculated using (C.4), (C.5), and (C.6).

Once $\bar{V}(t)'$, $\psi(t)'$, and $\gamma(t)'$ are obtained using (C.21), the control $\bar{T}$, μ, and C_L can be solved in the following equations:

$$\bar{T} + a_1C_L^2 + b_1 = \bar{V}' \tag{C.28}$$

$$a_2C_L\sin\mu + b_2 = \psi' \tag{C.29}$$

$$a_3C_L\cos\mu + b_3 = \gamma' \tag{C.30}$$

Then

$$C_L\sin\mu = \frac{\psi' - b_2}{a_2} \tag{C.31}$$

$$C_L\cos\mu = \frac{\gamma' - b_3}{a_3} \tag{C.32}$$

and

$$\tan\mu = \frac{a_3(\psi' - b_2)}{a_2(\gamma' - b_3)} \tag{C.33}$$

$$C_L^2 = (\frac{\psi' - b_2}{a_2})^2 + (\frac{\gamma' - b_3}{a_3})^2 \tag{C.34}$$

$$\bar{T} = \bar{V}' - a_1C_L^2 - b_1 \tag{C.35}$$

Bibliography

[1] Derek Piggott. *The Principles of Soaring Flight*, chapter 3. Adam and Charles Black, London, 1977.

[2] Y. J. Zhao and Y. C. Qi. Minimum fuel powered dynamic soaring of unmanned aerial vehicles utilizing wind gradient. *Optimal Control Application and Methods*, pages 211–233, 2004.

[3] Y. Qi. *Optimal Flights of Unmanned Aerial Vehicles Utilizing Wind Energy*. PhD thesis, University of Minnesota, May 2007.

[4] J. D. Anderson. *Introduction to Flight*. McGraw-Hill, 5th edition, 2004.

[5] M. B. E. Boslough. Autonomous dynamic soaring platform for distributed mobile sensor arrays. Technical Report Sand Report: SAND2002-1896, Sandia National Laboratories, June 2002.

[6] P. D. Bridges. Alternative solution to optimum gliding velocity in a steady head wind to tail wind. *Journal of Aircraft*, 27(7), 1990.

[7] A. E. Bryson. Jr. *Applied Linear Optimal Control: Examples and Algorithms*. Cambridge University Press, 2002.

[8] A. E. Bryson. Jr. *Dynamic Optimization*, chapter 5, pages 201–260. Addison Wesley, 1999.

[9] C. D. Cone. The soaring flight of birds. *Scientific American*, April 1962.

[10] L. J. Genalo and B. L. Pierson. A singular-arc approximation to a dynamic sailplane flight path optimization problem. *Engineering Optimization*, 3(4):175–182, 1978.

[11] P. E. Gill, W. Murray, M. A. Saunders, and M. H. Wright. User's guide for npsol (version 4.0): A fortran package for nonlinear programming. Technical Report SOL 86-2, 1986.

[12] F. Hendricks. *Dynamic Soaring*. PhD thesis, University of California - Los Angeles, 1972.

[13] D. Hull. Conversion of optimal control problems into parameter optimization problems. *Journal of Guidance, Control, and Dynamics*, 20(1):57–60, 1997.

[14] M. R. Jackson, Y. J. Zhao, and R. A. Slattery. Sensitivity of trajectory prediction in air traffic management. *Journal of Guidance, Control, and Dynamics*, 22(2):219–228, March-April 1999.

[15] S. A. Jenkins and J. Wasyl. Optimization of glides for constant wind fields and course headings. *Journal of Aircraft*, 27(7), 1990.

[16] J. L. de Jong. The "convex-combination approach," a geometric approach to the optimization of sailplane trajectories. *Technical Soaring*, 8(3), 1983.

[17] J. L. de Jong. Instationary dolphin flight: The optimal energy exchange between a sailplane and vertical currents in the atmosphere. *Optimal Control Application and Methods*, 6:113–124, 1985.

[18] J. C. Kaimal and J. J. Finnigan. *Atmospheric Boundary Layer Flows: Their Structure and Measurement*, chapter 1. Oxford University Press, 1994.

[19] H. Kawabe and N. Goto. Modified direct optimization method for optimal control problems. *Theoretical and Applied Mechanics*, 48:225–234, 1999.

[20] T. T. Lankford. *Aviation Weather Handbook*. McGraw-Hill, 2001.

[21] F. X. Litt and G. Sander. Optimal flight strategy in a given space distribution of lifts with minimum and maximal altitude constraints. *Technical Soaring*, 6(2), 1981.

[22] J. Lorenz. Numerical solution of the minimum-time flight of a glider through a thermal by use of multiple shooting methods. *Optimal Control Application and Methods*, 6:125–140, 1985.

[23] D. E. Metzger and J. K. Hedrick. Optimal flight paths for soaring flight. *Journal of Aircraft*, 12(11):867–871, November 1975.

[24] J. M. Moran and M. D. Morgan. *Meteorology, The Atmosphere and the Science of Weather*. Prentice Hall, 5th edition, 1997.

[25] E. C. Pielou. *The Energy of Nature*, chapter 4-5. The University of Chicago Press, 2001. ISBN 0-226-66806-1. QC73.P54 2001.

[26] B. L. Pierson and J. L. de Jong. Cross-country sailplane flight as a dynamic optimization problem. *International Journal for Numerical Methods in Engineering*, 12:1743–1759, 1978.

[27] B. L. Pierson. Maximum altitude sailplane winch launch trajectories. *Aeronautical Quarterly*, 28:75–81, 1977.

[28] B. L. Pierson and I. Chen. Minimum altitude-loss soaring in a sinusoidal vertical wind distribution. *Optimal Control Application and Methods*, 1(3):205–215, 1980.

[29] B. L. Pierson and I. Chen. Minimum landing-approach distance for a sailplane. *Journal of Aircraft*, 16:287–288, 1979.

[30] B. L. Pierson and I. Chen. Minimum-time soaring through a specified vertical wind distribution. *Control and Information Sciences*, 22:350–357, 1980.

[31] Lord Rayleigh. The soaring of birds. *Nature*, 27:534–535, 1883.

[32] G. Sachs, A. Knoll, and K. Lesch. Optimal utilization of wind energy for dynamic soaring. *Technical Soaring*, 15(2), 1991.

[33] R. B. Stull. *An Introduction to Boundary Layer Meteorology*, chapter 1. Kluwer Academic Publishers, P. O. Box 17, 3300 AA Dordrecht, The Netherlands, 1988.

[34] Y. J. Zhao. Optimal patterns of glider dynamic soaring. *Optimal Control Application and Methods*, 25:67–89, 2004.